Geoscientific Research

and the

Global Positioning System

Recent Developments and Future Prospects

A Report of the

University Navstar Consortium

Summer, 1994

Contents

1 Overview

The Global Positioning System (GPS), a now fully operational 26-satellite constellation, represents one of those rare technological developments which suddenly opens up whole new opportunities for scientific advance, with broad influence on commerce and society at large. It was put in place by the U.S. Department of Defense primarily to provide accurate geographic position location and navigation for a wide variety of military purposes, through distance ranging to the satellites. In designing the system, DoD adopted an enlightened dual-use policy, providing for civilian use of the system for positioning at a limited level of accuracy (about 100 meters), but one adequate for many applications.

The tremendous boom in civilian use of GPS in recent years for a multitude of purposes—ship and private boat navigation, vehicle fleet location, emergency vehicle location, aircraft and spacecraft guidance, and commercial surveying, to name a few—reveals the dual-use policy to have been remarkably foresightful. A large and rapidly growing commercial industry has come into existence because of GPS, both within the U.S. and abroad. Yet the designers of the system could hardly have foreseen the scientific bonanza of GPS applications that came about through the discovery that by carefully measuring the phase of the radio signals from the GPS satellites, as well as the ranges to them, it is possible in principle to determine positions with an accuracy to five orders of magnitude better than the system was designed for. That is, using radio transmissions received from satellites 20,000 kilometers up, it is now possible to determine relative positions at or above the Earth's surface to better than 1 centimeter.

That this discovery originated in the space geodetic community was a natural consequence of the intensive effort over many years, under the sponsorship of NASA's Crustal Dynamics Project, to develop the technologies for applying Very Long Baseline Interferometry (VLBI) and Satellite Laser Ranging (SLR) to the direct measurement of the relative velocities of the Earth's great tectonic plates on a global scale. Thus, the original geoscientific applications of GPS had the same focus, but it was soon realized that the potential applications extend far beyond plate tectonics.

Realization of the scientific potential of GPS has produced a tremendous sense of excitement across the geosciences—Earth science, atmospheric science, oceanography, polar science, and geospace physics—and a strong new sense of interdisciplinary community has developed. Much of the effort of the past decade has been focused on eliminating sources of error that limit accuracy, and with such an intensity that the accuracy goals which seemed only a distant possibility just a few years ago have already been exceeded. We are just now in a period in which investigations in all areas of the geosciences are beginning to bear fruit, and are proving successful beyond expectations. Scientific output is on an upward curve which parallels the rapid improvement in measurement accuracy and a decline in hardware costs (Figure 1).

The decade to come promises a proliferation of scientific applications of GPS which will parallel and be closely connected with a proliferation in commercial and civil applications. The intent of this report is to give an overview of developments in geoscientific applications of GPS of recent years and an indication of things to come. What is already clear is that there will be a continuum of diverse scientific applications of GPS from fundamental investigations into how the Earth

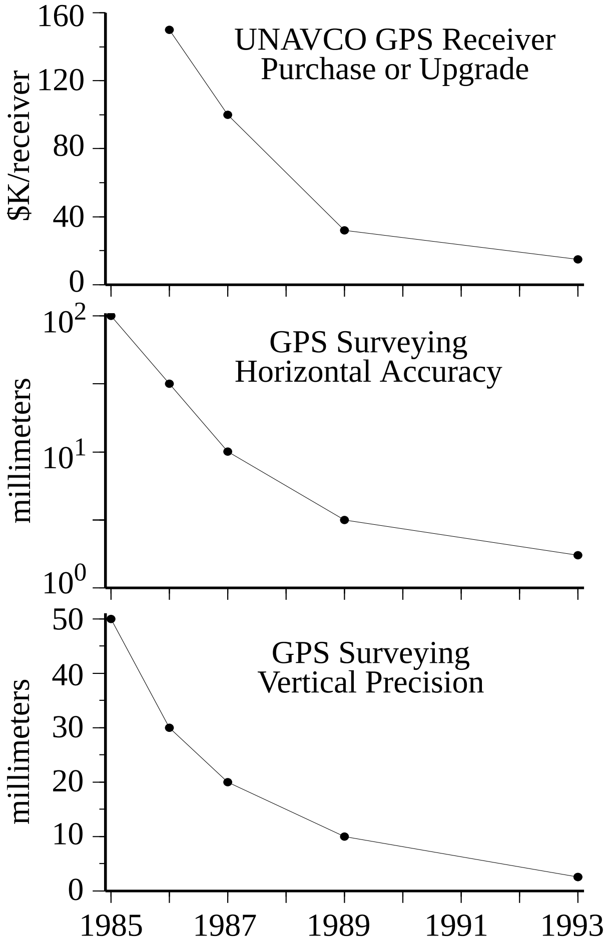

Figure 1. Trends in receiver cost, horizontal accuracy, and vertical precision for GPS scientific applications (Ware).

works to highly applied investigations with immediate focus on diverse matters of public safety, such as earthquake hazard, movement of landslides, climate change, sea level rise, coastal erosion, volcanic eruptions, land subsidence, and the integrity of dams and other man-made structures. But the distinction between basic and applied science in the GPS realm is not meaningful, and across the board GPS will play an important part in organized national and international programs such as the Earthquake Hazard Reduction Program and the International Decade of Natural Hazard Reduction. In this arena, the scientific community and the civil and commercial sectors already form an interdependent and mutually supporting network.

Below are given some highlights of recent developments in the application of GPS to geoscientific research, followed by a look to the future, recognizing that the whole field is developing with breathtaking speed, and that much of what is today could not have been foreseen only a few years ago.

1.1 State of the Art

1.1.1 Complex Deformation in Plate Boundary Zones

In contrast with predecessor technologies, GPS receivers are highly mobile and relatively cheap. This means in principle that large numbers of them can be deployed anywhere on Earth that benchmarks can be emplaced. Thus, the deformation patterns of active regions of the Earth's surface can be observed to the detail required to adequately describe them. Then dynamic models can be built around these observations, through which we can infer the real physical processes within the Earth and what causes them. This will be especially important in the boundary zones where tectonic plates interact, for example that between the Pacific and North American plates in California (Figure 2), which, far from being knife-sharp, are broad deforming regions with complex networks of active faults and intervening blocks which interact and evolve with time.

1.1.2 Capturing Earthquakes

The University Navstar Consortium (UNAVCO) now provides equipment and technical and logistical support for scores of GPS field projects worldwide (Figure 3), and most of these involve investigations of the tectonics

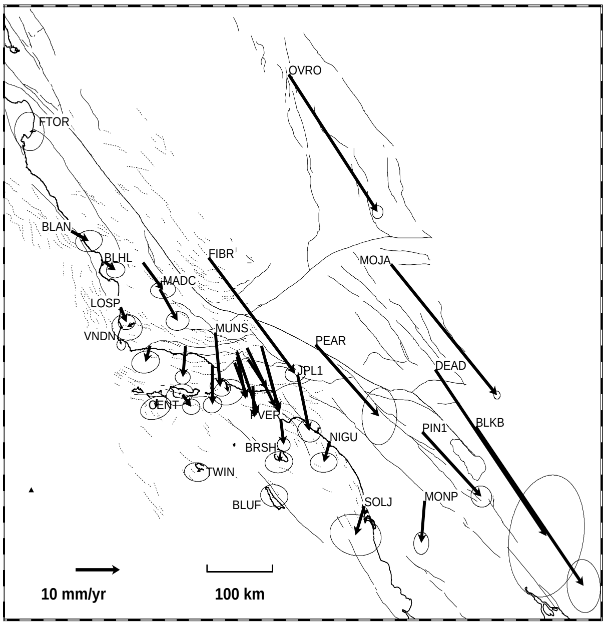

Figure 2. Observed velocity vectors and 95% confidence ellipses for the combined GPS and VLBI data in southern California (Feigl et al., 1993). Velocities are referenced to the Pacific Plate.

of plate boundary zones. For a large number of these regions, repeated GPS surveys of geodetic networks spanning active fault zones have made it possible to "capture" earthquakes—that is, determine the deformation field over a wide area surrounding the locus of fault slippage. Rapid deployment of GPS receivers following the several large earthquakes of recent years in California have measured the post-seismic deformations, which decay over long time periods. Such measurements complement information from seismographs concerning the depth, orientation, and amount of fault slippage.

In tandem, geodesy and seismology are telling us much about the mechanics of earthquake-generating fault motions and the larger tectonic framework which produces the stresses which cause them. The magnitude 6.6 Northridge earthquake of 1994, which devastated large sections of Los Angeles, was determined, by

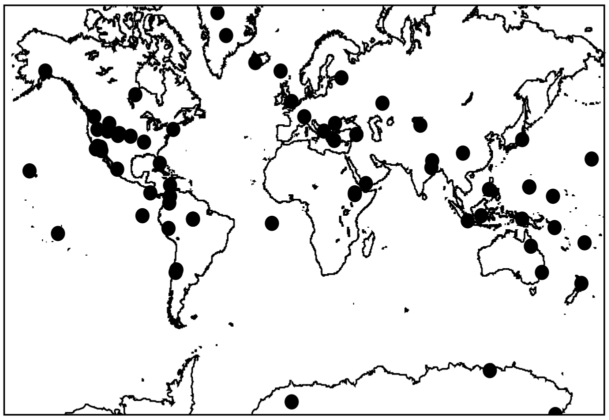

Figure 3. Locations of UNAVCO-supported GPS surveying projects.

combined analysis of GPS and seismology data, to be the result of a previously unknown "blind" thrust fault at depth in the Los Angeles Basin (Figure 4). But the regional pattern of deformation of which that fault was a part, not directly related to the San Andreas system, had already started to emerge from repeated GPS

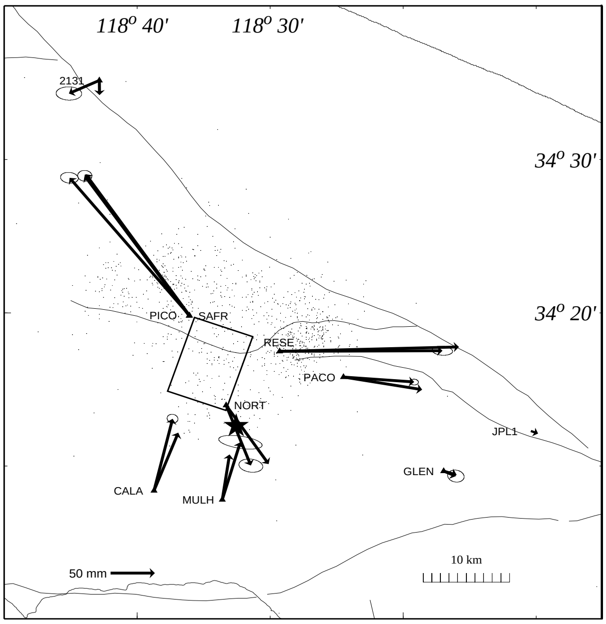

Figure 4. Northridge GPS displacements and modeling of slip zone at depth from surface deformation (Hudnut and Murray, January 25, 1994).

surveys of the Los Angeles and Ventura Basins just in recent years (Figure 5).

1.1.3 Continuously Operating GPS Networks

Within plate boundary zones, the relative movement of the adjoining plates causes stress to accumulate, which is relieved by slip on faults by elastic strain. For an extended period thereafter, anelastic deformation continues at a decaying rate, as stresses again build, until slip recurs; this is the earthquake cycle. As is only too well known, such fault slip usually is associated with earthquakes. Analysis of the time and space variation in deformation during and after fault movements using GPS, as well as traditional geodetic tools, tells us much about the rheology of the crust and underlying mantle and the tectonic processes at work, and may shed light on the frequency and amount of future fault slip.

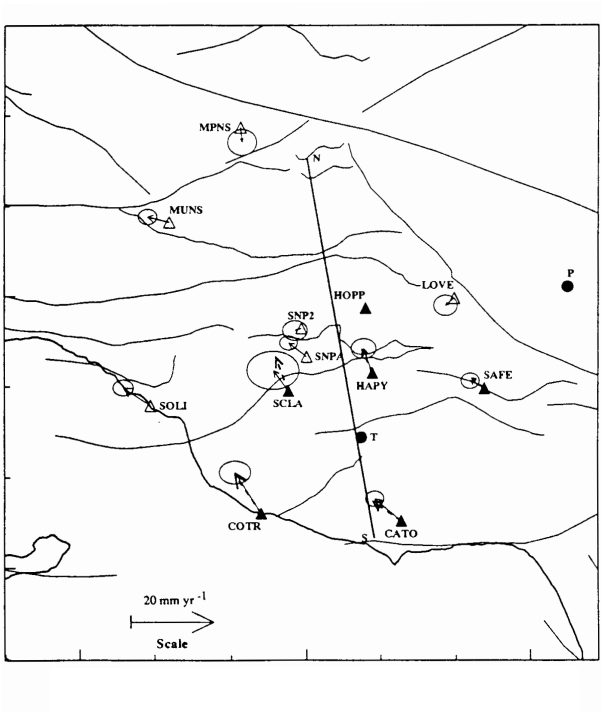

Figure 5. Relative velocities of sites in the Ventura Basin region, California (Donnellan et al., 1993). The error ellipses represent 95% confidence.

The 15-station Permanent GPS Geodetic Array (PGGA) (Figure 6), a recently established network of continuously recording GPS receivers in southern California, operated by the Scripps Institution of Oceanography, captured the Northridge earthquake, as it has other recent earthquakes, such as the magnitude 7.4 Landers earthquake of 1992 (Figure 7). The virtues of having fixed instruments which continuously monitor networks of baselines in order to observe patterns of movement of the Earth after, during, and (perhaps in the future) before an earthquake is evident. A similar network is operational in Japan, and these networks are forerunners of much more extensive networks in the future.

1.1.4 Volcano Monitoring

The success of detailed earthquake monitoring in predicting the recent eruptions of Mt. Pinatubo in the Philippines and Mt. Redoubt in Alaska saved thousands of lives and points out the use of geophysical tools to forecast eminent eruptions. As in earthquake research, the GPS receiver has become complementary to the seismograph for scientific investigations of active volcanos, while at the same time

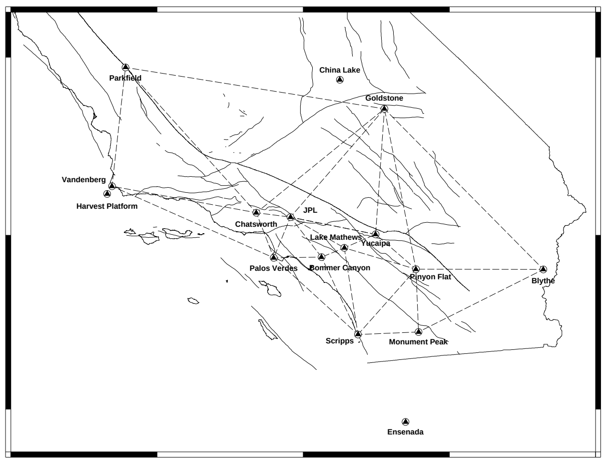

Figure 6. Permanent GPS geodetic array (PGGA), southern California (Bock).

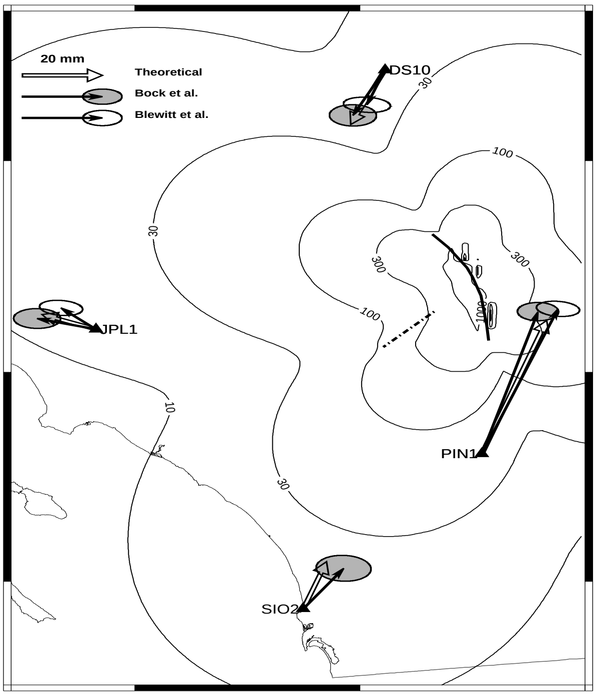

Figure 7. Observed versus *modeled displacements from the PGGA tracking network for the Landers earthquake (Bock et al., 1993). The contours show displacement magnitude in millimeters for the elastic dislocation model.*

providing an important new tool for volcano hazard assessment and eruption warning.

In recent years, GPS networks have been established in numerous areas of active volcanism—for example Hawaii, Alaska, Yellowstone, Iceland, New Zealand, and Italy—and as noted in this report are already providing scientific insight into complex volcanic processes. GPS can give three-dimensional views of the movement of volcano surfaces in response to seismic or aseismic activity; this has provided a new means for inferring the volume and movement of magma at depth.

1.1.5 Post-Glacial Rebound

Large parts of the Earth's surface which were depressed under the weight of huge continental ice sheets during the last glaciation are still slowly rebounding at rates measurable by GPS. From rates of post-glacial rebound, inferences can be made about the rheological properties of the Earth's mantle. Such information is of crucial importance to modeling the slow convective circulation of the mantle, which ultimately drives plate tectonics.

Previous studies were limited to estimating vertical rates from inferred ancient shorelines; GPS, on the other hand, can directly measure both vertical and horizontal motions anywhere a benchmark can be emplaced. The horizontal rate is much more sensitive to the vertical variation of mantle viscoelastic properties and to the ice loading history than the vertical rate. GPS measurements should make it possible to distinguish between competing models of mantle rheology within a decade.

The problem is complicated for glaciated areas near plate boundaries, where multiple deformations may superimpose; in coastal areas, both effects need to be distinguished from real eustatic sea level rise. This requires well-distributed, high-accuracy GPS measurements combined with geologic observations and models. The Pacific Northwest is a good example of where this is important: inferences may be possible about whether the region is in danger of a great earthquake, provided the tectonic signal due to subduction of the Juan de Fuca plate beneath North America can be distinguished from that due to post-glacial rebound and real changes in sea level.

1.1.6 Global Climate Change

A plausible result of anthropogenic warming of the atmosphere through addition of greenhouse gasses would be melting of the Earth's ice sheets and mountain glaciers. This would lead to a rise in sea level which could have very serious consequences for low-lying coastal population centers in terms of inundation, coastal erosion, and salt encroachment in aquifers. On the other hand, it is also plausible that atmospheric warming could lead to increases in precipitation which could cause at least some ice masses to grow.

Although some mountain glaciers do seem to be shrinking, at present it is not at all clear whether the polar ice caps are shrinking or growing. The problem is lack of data. There is some consensus, based on tide gauge data, that sea level has risen on the average of about 2 mm/year over the last several decades, but measurement of sea level change is exceedingly difficult due to the superposition of innumerable effects. GPS is being applied to the climatic temperature question in a number of new ways which are likely to produce some rapid advances.

The topographic profile of mountain glaciers are being measured remotely from aircraft positioned by GPS with a view toward detecting temporal changes. The same is being applied to the Antarctic ice sheets and rapidly moving ice streams, along with direct measurements of the ice surface using GPS. These observations will complement developing techniques for measuring changes in ice topography from spacecraft.

Tide gauge sites have begun to be tied to GPS networks; ultimately, tying a global network of tide gauges to a common GPS-based reference frame will greatly facilitate the determination of absolute sea level changes.

Warming of the oceans will accompany warming of the atmosphere. An experiment has been carried out to measure the time of transmission of acoustic waves through the surface layers of the ocean along very long oceanic paths. Accurate distance measurements were achieved with GPS. Repeat measurements will look for changes in average transmission velocity due to warming of the ocean.

1.1.7 Ocean Circulation

GPS is providing unprecedented orbit accuracy for the TOPEX/Poseidon spacecraft, which is measuring ocean topography in conjunction with the World Ocean Circulation Experiment (WOCE). Ocean topography is the basis for inferring large-scale circulation of ocean currents. Improved orbits lead to improved determination of ocean circulation on all scales for both time variable and time average motions, which in turn leads to improvement in climate models. Small geographically correlated orbit errors make possible the determination of absolute geostrophic circulation (net flow through the full water column), which cannot be determined globally otherwise. GPS is providing a reference frame for acoustic Doppler current profilers, which measure the current profiles in the upper few hundred meters of the ocean from ships by providing accurate ship speed and heading. By a quite different approach, deep ocean current velocities are being measured by use of GPS receivers on a surface ship and buoy, while tracking via sonar a probe drifting in a deep current.

1.1.8 Atmospheric Sensing

Water vapor plays a crucial role in atmospheric processes acting over a wide range of temporal and spacial scales. Knowledge of the variability of water vapor is central to understanding weather phenomena and, over the long term, climate. Water vapor variations cause changes in velocity, and thus refraction, of the GPS signals passing through the atmosphere. It was thought early on that errors in GPS positioning due to water vapor could well limit the ultimate utility of GPS for scientific uses. But quite the opposite occurred: methods were developed, not only to correct for path delays, but to turn the problem around and use the delays as a tool to remotely sense variations in atmospheric water vapor.

GPS-based meteorology has thus become an extremely valuable new tool for the atmospheric sciences. The method relies on the use of networks of continuously operating GPS receivers simultaneously observing multiple GPS satellites. Recently developed water vapor radiometers which are highly accurate and portable can be used as a companion tool to fix biases in small-aperture arrays. The method has been shown to be highly successful in tests involving placement of GPS receivers at the NOAA Wind Profiler sites in the U.S. midcontinent.

1.1.9 Space-Based GPS Meteorology

This approach takes the well-known radio occultation methodologies for studying planetary atmospheres and applies it to the Earth. Observations of signal delays along successive paths to rising or setting GPS satellites, as observed by a small satellite in low-Earth orbit (LEO), can be inverted to a vertical profile of refractivity through the atmosphere. Refractivity is a function of temperature and water vapor.

Thus, in principle, if the temperature distribution is known or can be modeled, the vertical distribution of water vapor can be inferred, or vice versa. The method provides a high degree of vertical resolution, but low resolution horizontally. Because ground-based GPS meteorology involves high resolution laterally, but low resolution vertically, the methods are highly complementary. A similar statement can be made about space-based GPS meteorology in comparison with the imaging radiometers used in the familiar NOAA weather satellites. A demonstration experiment is under way to collect occultation data from a GPS receiver accompanying a commercial LEO satellite. The single receiver should be able to record more than 500 occultations per day with nearly global coverage.

1.1.10 Probing the Ionosphere

This ionized part of the Earth's atmosphere affects the GPS signals dispersively—that is, the delay experienced by a signal is a function of its frequency. Dual frequency receivers can correct for this effect, and in the process determine the degree of ionization of the ionosphere along the path of the radio signals. Precise dual frequency measurements by ground and space-based receivers will probe the ionosphere along many paths. Measurement of total electron content along these paths will be assembled into high-resolution 3-D electron distribution maps by computerized tomography to study irregular and transient mesoscale structures, such as equatorial bubbles and the mid-latitude trough. Study of the ionosphere with GPS signals will lead to a better understanding of communication problems associated with ionospheric disturbances.

1.2 The Future

Based on the experience of the last several years, it is quite likely that many new applications of GPS in all areas of the geosciences will emerge over the next several years which we cannot now foresee. On the other hand, we can identify certain things which, if adequately nurtured, have a reasonable expectation of reaching fruition within the next 5–10 years.

1.2.1 Permanently Operating Networks

Permanently operating GPS networks are likely to proliferate in the future in earthquake-prone regions with the continuing decline in receiver costs, expansion of data storage and networking capability, and increasing numbers of people trained in GPS technology, both within the U.S. and abroad. Such networks will complement seismic networks already established in many such regions. Because of the same factors, regional GPS networks in many areas of the world will be outfitted with permanent receivers, which will have significant logistical advantages over the current mode involving massive shipments from the U.S. or Europe and the necessity of coordinating large, complex field campaigns. Such networks will provide frameworks for local scientific or civil surveys. Along the same lines, there is likely to be a strong movement to establish continuously monitoring GPS networks on active volcanoes worldwide.

1.2.2 Multipurpose National Network

Several government agencies intend to establish GPS networks within the U.S. for a wide variety of applications. A significant opportunity exists for coordinating these efforts toward the establishment of a dense, high-quality national GPS network which could serve many purposes—scientific, civil, and commercial—while providing significant cost leveraging for all parties concerned. Of central importance is the deployment of high-quality GPS receivers which would satisfy all requirements.

Such a network would simultaneously serve the FAA's program for instrumenting airports; NOAA's programs in meteorology, sea level, and geodetic networks; the DOE ARM program in water vapor climatology; the Coast Guard's program to provide differential GPS (DGPS) service in coastal areas; and NSF and NASA programs in active tectonics and satellite tracking.

At the same time, the DGPS capability would be available to a wider community of users, such as transportation companies, emergency services, commercial surveyors, and schools. It could be used by the space physics community to study ionospheric effects which have a major impact on commercial and government communications systems. Such a system would be a case of technology transfer of genuinely high value on a large scale.

1.2.3 Global Change Research

Continuing reduction in errors in orbits of satellites measuring ocean topography through GPS tracking will lead to much better determination of ocean circulation. This could lead to the computation of flux divergences of heat to and from the atmosphere from the ocean at a level of accuracy required to infer directly a greenhouse warming.

A network of continuously operating GPS stations at coastal tide gauges, tied to a global reference frame, will allow much better determination of absolute sea level trends, while providing input to models of isostatic readjustments and shifts in the Earth's center of mass due to redistributions of water between the ice caps and the oceans. A network of GPS stations will be established around the Antarctic to monitor elastic crustal strains due to ice addition or subtraction from its ice caps.

Extensive GPS networks established on ice caps and glaciers will be used to monitor ice flow, in an effort to determine long-term patterns of accumulation or wastage.

An oceanographic experiment to look for secular trends in long range acoustic travel times between fixed sites positioned by GPS will be complemented by similar experiments involving drifting buoys, also positioned by GPS. Such experiments should be able to detect a greenhouse warming signal within a decade.

There is much potential for using DGPS and kinematic surveying to map coastal zones in detail sufficient to study erosion rates, storm damage, and ecosystem modification.

1.2.4 Space-Based Meteorology

Following demonstration phases for using GPS occultation measurements from LEO satellites to determine vertical refractivity profiles in the atmosphere, a significant opportunity exists for expanding the effort significantly.

If provision could be made for outfitting the hundreds of LEO communications satellites planned for the next decade with suitable GPS receivers, occultation measurements could be made with a density adequate for providing valuable input to daily meteorological forecast models on the mesoscale globally. Further, over the longer term such measurements will provide important input to climate models.

Simulations suggest that changes in the temperature profile of the atmosphere due to greenhouse warming should be detectable in a matter of years (Figure 8). The potential benefits of such a program, resulting from a partnership of the academic, government, and commercial sectors, clearly are great.

2 Contributors to This Report

UNAVCO convened a two-day workshop in September, 1993, at which the participants crafted the framework for this report. Other individuals subsequently contributed substantively to the report. The work of all the contributors, who are named below, is very much appreciated.

John Beavan, *Lamont-Doherty Earth Observatory*

Robin Bell, *Lamont-Doherty Earth Observatory*

Michael Bevis, *University of Hawaii*

Roger Bilham, *University of Colorado*

Yehuda Bock, *Scripps Institution of Oceanography*

George Born, *University of Colorado*

George Davis, *University of Arizona*

Roy Dokka, *Louisiana State University*

Michael Exner, *University Corporation for Atmospheric Research*

Thomas Herring, *Massachusetts Institute of Technology*

Michael Jackson, *University of Colorado*

Myron McCallum, *UNAVCO*

Marcia McNutt, *Massachusetts Institute of Technology*

William Melbourne, *Jet Propulsion Laboratory*

Charles Meertens, *UNAVCO and University of Utah*

Richard O'Connell, *Harvard University*

John Orcutt, *Scripps Institution of Oceanography*

Robert Reilinger, *Massachusetts Institute of Technology*

Christian Rocken, *UNAVCO*

Leigh Royden, *Massachusetts Institute of Technology*

John Rundle, *University of Colorado*

Robert Schutz, *University of Texas*

David Simpson, *Incorporated Research Institutions for Seismology*

Robert Smith, *University of Utah*

Wayne Thatcher, *U.S. Geological Survey*

Randolph Ware, *UNAVCO*

3 UNAVCO

The University Navstar Consortium (UNAVCO) provides information and

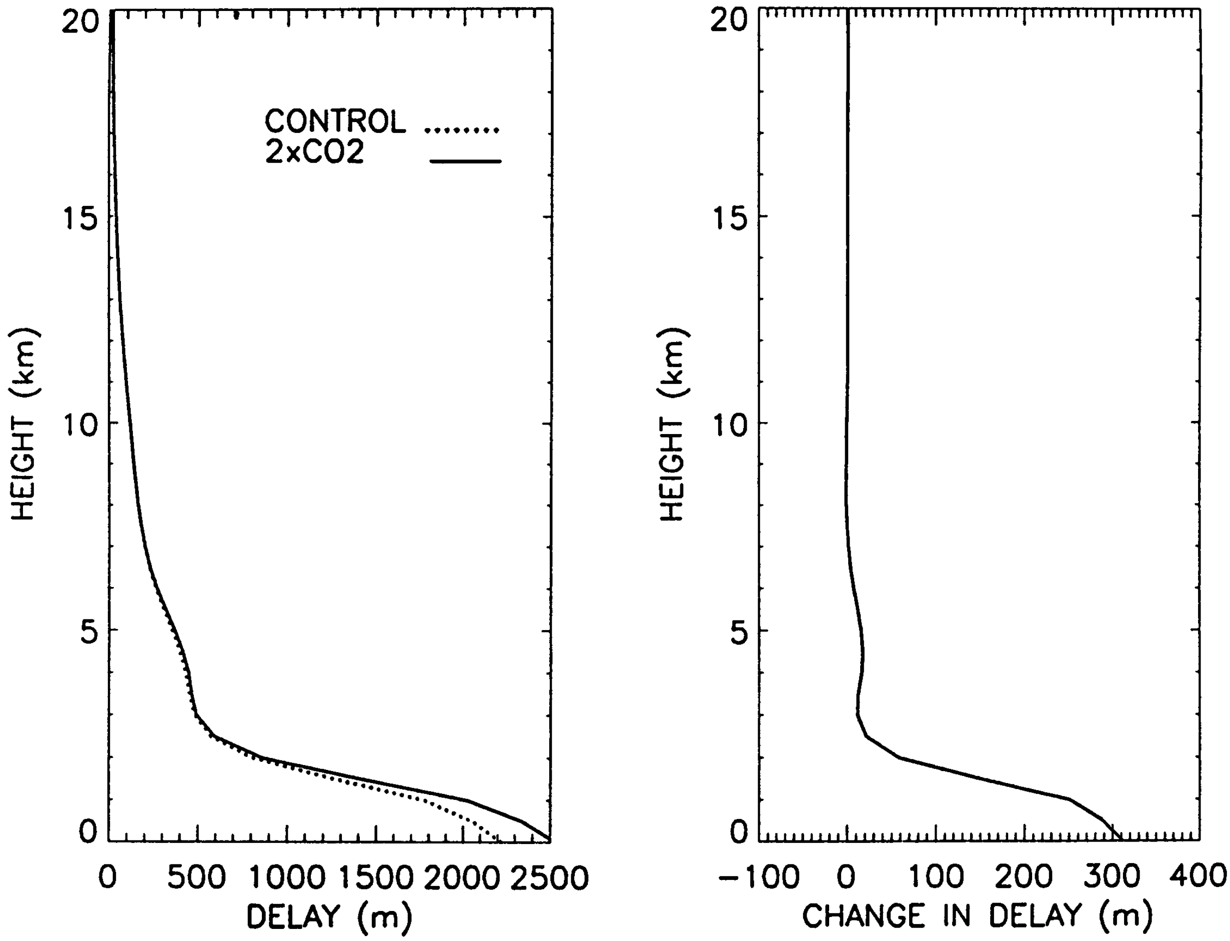

Figure 8. Phase delay versus *altitude in the tropics for a model atmosphere, for current and doubled CO_2 (Yuan et al., 1993).*

scientific infrastructure to investigators making use of the GPS satellites for Earth science and related research. University investigators assisted by UNAVCO are conducting research that is important to the nation and its citizens. Topics include earthquake, volcano, sea level, polar ice dynamic, weather forecasting, global climate, and natural resource exploration research.

UNAVCO's charter, defined by its Steering Committee, follows:

UNAVCO is a national program, governed by universities and funded by NSF to provide GPS equipment and technical support to university-based investigators in the geosciences, and to pursue a research program that complements and enhances the programs of universities. The aim of UNAVCO is to extend the capabilities of the university community, nationally and internationally, to better understand the behavior of the Earth and the global environment; and to foster the transfer of knowledge and technology for the betterment of life on Earth.

In pursuit of this charter, UNAVCO plans to continue its primary role in supporting research conducted by NSF-supported Earth science investigators. During the past 10 years, remarkable progress in the understanding of important Earth science problems has been achieved by this community, with assistance from the UNAVCO facility. The facility provides investigators with a standardized GPS equipment pool, assistance in planning and execution of high-accuracy GPS surveying projects, technical support, data analysis, and data archiving.

During the past decade, regional GPS geodesy campaigns of growing size were conducted to establish epoch and re-survey measurements. Large, coordinated projects demanded high levels of equipment and facility staff resources. New procedures, including multi-modal occupation strategies, and rapid surveying, are now under development. We anticipate that these procedures will lead to large increases in scientific productivity, and significant changes in the facility as it works with the community to develop and support these new procedures.

In addition, the UNAVCO community will continue to encourage and support the use of GPS technology in other geoscience areas. The facility plans to provide the GPS-related information and scientific infrastructure needed by geoscience researchers as they address national problems, and to identify and exploit synergies between the various geoscience disciplines.

4 Scientific Opportunities

From the beginning, the space geodetic community realized that in principle it is possible to achieve accuracies in GPS positioning several orders of magnitude better than that specified by the system design for civilian use, provided that significant sources of error could be managed. As a result of intensive research by many groups, accuracies have increased rapidly and dramatically. Applications to complexities of deformation in tectonic plate boundary zones, active volcanic regions, whole-Earth dynamics, and other fields of research have mushroomed. Atmospheric scientists have learned to use the GPS signals to probe the atmosphere through which the signals pass, opening vast potential for understanding and forecasting weather, climatic trends, and ionospheric fluctuations. GPS can accurately track or navigate any sort of instrumented platform: ship or buoy, airplane, snowmobile, or spacecraft. Thus, GPS has opened up a huge variety of scientific applications encompassing the whole of the geosciences. This section provides a perspective on these applications, today and in the future.

4.1 Deformation of the Earth's Lithosphere

Plate tectonics has provided a unifying theory for understanding the kinematics of global-scale plate motions for large regions of the Earth that behave in a rigid framework. A central achievement of the Crustal Dynamics Project was the direct measurement of rates of plate motion on a global scale using the techniques of Very Long Baseline Interferometry (VLBI) and Satellite Laser Ranging (SLR). Now, GPS has brought about a new era. The very rapid improvements in position accuracy have made it possible to measure baselines on the large scale as well as VLBI and SLR. More importantly, the high degree of portability and relatively low cost of GPS receivers means that a far greater number and density of measurements are possible, so that active geologic processes can be observed down to the local scale.

Thus, we are now in a position to directly observe how plates deform internally within non-rigid tectonic regimes and across regions of rapid and complex tectonism. This information is crucial to understanding the dynamics of Earth processes, including the distribution of displacements and finite strain, parameters leading to understanding the stresses responsible for Earth processes. Inferences about lateral and vertical partitioning of displacements across plate boundaries, as well as intraplate regions of active seismicity and Quaternary tectonism, are needed to determine rates of tectonic deformation and earthquake occurrence. Understanding the vertical distribution of strain and how it is partitioned between surface deformation and that inferred from observations such as heat flow and earthquake data is critical to understanding the role of coupling between the mantle and the lower crust and to how rheology controls tectonic processes.

Real-time and periodic monitoring of earthquake zones and regions of active volcanism offers new information on the long- and short-term rates of deformation accompanying these processes. This information may be the key metric in accurate prediction of earthquakes and volcanoes, a broad societal goal of the Earth science community. These problems can for the first time be addressed by systematic GPS measurements, coupled with realistic three-dimensional models of these active processes, and integrated with other geological and geodetic information.

4.1.1 Plate Boundary Processes

Local and regional departures from rigid plate behavior occur along interplate boundaries and within domains of intraplate deformation. Where plate boundary deformation involves continental lithosphere, it is commonly distributed over complex networks of faults and folds up to several thousand kilometers wide, with zones of intense deformation along the margins of less deformed crustal fragments of dimensions from ten to hundreds of kilometers. This spatial complexity is demonstrably tied to temporal variations in the pattern of motions. In contrast to global plate motions, the complex history of deformation within regions of plate boundary interaction and intraplate deformation is known in most areas only at the crudest level of detail.

Actively deforming subregions are complex laboratories that evolve over time and involve a multitude of interrelated physical and chemical processes. Thus, tectonic analysis of actively deforming subregions requires an integrated approach involving the use and appreciation of diverse data sets. It requires a comprehensive understanding of the nature and distribution of rock units and structures within the crust and lithosphere, an appreciation of the relationship of the subregional tectonic framework to the regional and plate tectonic framework, and finally an understanding of the geological history.

Because it offers the unparalleled means to measure the subregional contemporary strain and rates of deformation as it occurs, GPS can play a major role in the study of contemporary deformation. These include: (1) establishing the recent and present-day displacement field by tracking the changes of position of ground points through time, (2) establishing rates of contemporary vertical and lateral deformation, (3) interpreting how the displacements are partitioned with respect to slip of surface faults, rigid-body rotation, permanent strains, and volumetric strains, (4) interpreting the mechanisms by which the regional deformation is accomplished, (5) tracking how the deformation accrues through time, (6) defining how surface deformation relates to the overall crustal structure, and (7) assessing regions of seismic *versus* aseismic (dormant) regions of expected earthquakes. Thus, the significant opportunity is to define comprehensively the displacement field(s) through time, including vertical changes, tilts, translations, rotations, and wholesale strains.

Ultimately the "paths" of displacements, viewed collectively, will permit investigators to distinguish among models of crustal/ lithospheric deformation. Understanding plate boundary deformation is particularly important because these zones host most of the world's catastrophic earthquakes and volcanoes (Alpine/Himalayan and Pacific Rim). Moreover, the boundaries of plates, if properly understood, are the only locations that can provide us with information on crust-mantle interaction and also provide some of the best insights into lithospheric rheology.

Problems in plate boundary deformation need to be addressed simultaneously at several different levels. First, one needs to map the active strain field within the global plate boundary system, by use of measurements on baselines of perhaps 100 km. Second, one needs to understand how strain is partitioned, in space and time, along zones of high strain that separate less deformed crustal blocks within plate boundaries, and how these high strain zones are expressed geologically. The latter need not, and probably should not, be carried out on a global scale, but may be undertaken in selected regions that are logistically accessible and geologically well expressed. Some examples of outstanding problems in each of these areas might be as follows:

1. Where are the regions undergoing rapid rates of lithospheric strain adjacent to and within the relatively rigid plates? What is the width of these zones of distributed deformation, and how is deformation partitioned within them?

2. How is slip partitioned between multiple faults within a plate boundary? How do fault zones develop and evolve through time? How are fault zones localized within the crust (for example by pre-existing crustal structures)? What conditions lead to the abandonment of existing fault systems and the development of new ones?

3. How is the deformation observed in the upper layers of the Earth expressed at deeper levels in flow of the lower crust and upper mantle? How are vertical axis rotations accommodated at depth?

4. How do strain measurements from geodetic observations compare with long-term geologic estimates of deformation? How much plate boundary slip occurs aseismically? How much deformation is not accommodated by slip on faults? How do geodetically determined rates compare to rates of deformation deduced from summation of moments of contemporary seismicity?

The contribution of GPS to each of these sets of questions is obvious. However, GPS can provide only a snapshot of 2-D motions at the Earth's surface. Our ultimate goal is to understand how the current deformation at the Earth's surface is the expression of 3-D dynamic systems that operate over time scales of perhaps tens of millions of years.

Thus the greatest long-term challenge in studies of regional plate boundary deformation is the successful merging of precise geodetic data with other geophysical data and careful geologic mapping to provide the most complete description of how these complex deformation systems reflect motions occurring at depth within the lower crust and mantle, and how they have evolved through time.

Ultimately, we must seek to understand the dynamic processes that drive surface deformation within zones of plate boundary deformation. Thus GPS will provide a more complete foundation to address even more fundamental questions such as:

1. What are the driving mechanisms for deformation within a plate boundary, such as boundary conditions imposed by the relative velocities of adjacent plates, potential energy from excess topography and subsurface loads, contributions from local dynamic systems within a plate boundary (e.g. localized subduction boundaries, back-arc systems), and influence of processes in the asthenosphere?

2. How are motions in the upper crust coupled to motions in the uppermost mantle? Over what time-scale and length-scale are these motions coupled? How does this reflect the rheology of the lithosphere?

Examples of tectonic processes are discussed below.

4.1.1.1 Mantle Dynamics and Tibet

At present, techniques for measuring flow within the mantle of a regional scale are not available, but recent work that combines crustal kinematics, gravity data, velocity structure, and theoretical models for fluid convection show promise for the future. The implications for our understanding of mantle dynamics are enormous, as can be illustrated by considering some basic questions about the deformation history of Tibet (Figure 9).

A number of studies suggest that deformation within Tibet involves movement of crustal fragments, with dimensions of tens to hundreds of kilometers, in directions oblique or even orthogonal to the overall direction of convergence between India and Asia. Data from northeastern Tibet show that, on a length scale of tens of kilometers, major deformation has switched from one system of faults to another and from one type of deformation to another over time intervals of less than a million years. If mantle flow beneath Tibet can be linked spatially to the active movements of sizable crustal fragments, then the spatial variability of mantle flow must correspond to the motions of individual crustal fragments (which can be measured using space-positioning techniques), whereas the temporal variability of mantle flow must occur over the same time scale as changes in the direction and rate of movements within the crust (which can be dated using traditional geological techniques and remote sensing data). Alternatively, if mantle flow can be shown to be related to crustal motion only at the scale of the entire plate boundary, then one might suspect that the temporal variability of flow in the mantle corresponds to that of the entire plate boundary zone.

4.1.1.2 The Pacific-North American Transform Boundary

The plate tectonics paradigm has provided Earth scientists with the conceptual framework with which to understand the kinematic history of and strain rates along plate boundaries such as the Pacific-North American transform. Instead of a single break, the transform is several hundred kilometers wide and composed of hundreds of fault-bounded slivers that have translated, rotated, and deformed over time. Plate circuit reconstructions provide a quantitative upper limit on integrated, long-term shear across this broad transform zone, but provide no details on where and how shear is partitioned across this complex boundary. For example, in southern California the boundary consists of the San Andreas fault system and the newly recognized eastern California shear zone (ECSZ) (Figure 10).

Comparison of the integrated net slip along the ECSZ with motion values across the entire transform boundary indicate that between 9% and 23% of the total relative plate motion has occurred and continues to occur along the ECSZ since its inception in late Miocene time. In this setting, GPS offers the unparalleled opportunity to track the lateral motions of the myriad of fault-bounded blocks that comprise the plate boundary. This powerful tool can also be used to examine the build-up of strain prior to and following major earthquakes, thus providing critical data relating to the formation of earthquakes.

4.1.1.3 Complexity of Continental Convergence in the Eastern Mediterranean

The Mediterranean region is one of the best documented examples of the spatial complexity found in zones of plate boundary deformation (Figure 11). At the largest scale this region comprises a zone of continental convergence and collision between the slowly

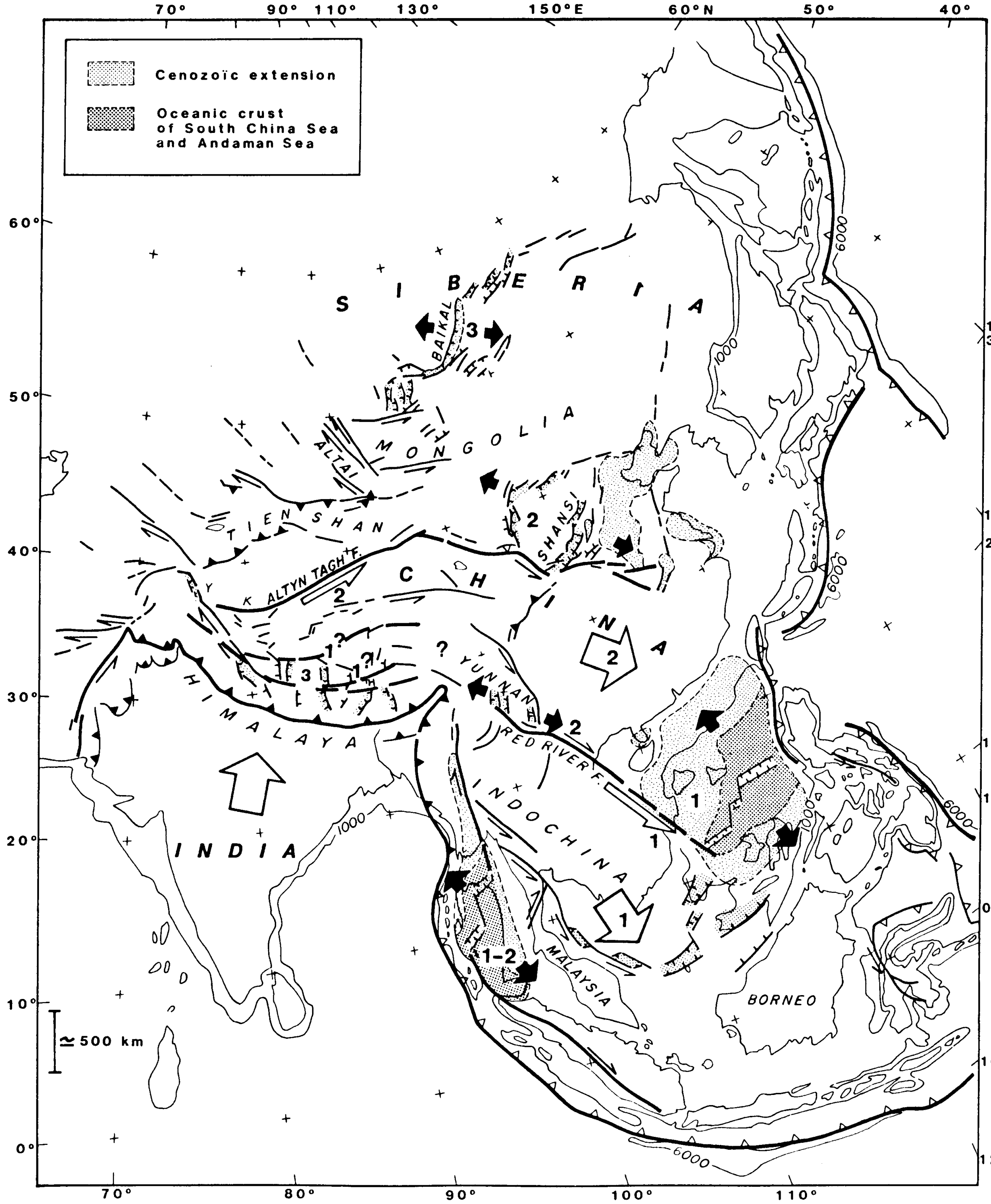

Figure 9. Schematic map of Cenozoic tectonics in eastern Asia (from Tapponnier et al., 1982). Heavy lines are major faults, thin lines are less important faults. Open barbs indicate subduction, solid barbs indicate intra-continental thrust faults.

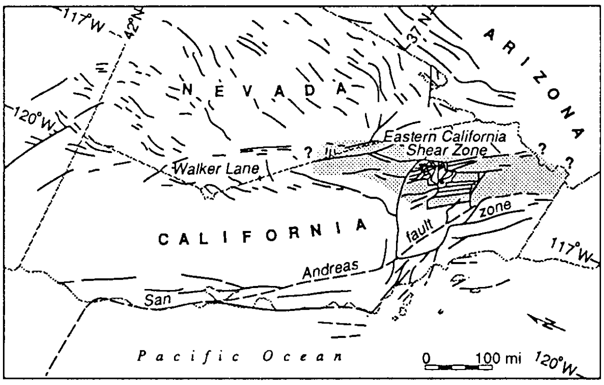

Figure 10. The Pacific-North American transform boundary in the western U.S., highlighting the location of the eastern California shear zone (modified from Dokka and Travis, 1990).

moving European and African continents. At every smaller scale, tectonic systems within this broad region exhibit convergent, divergent and strike-slip motions in a large number of different directions.

It is not uncommon for very different types of crustal motion and deformation to exist adjacent to one another, such as occurs in the Aegean-Hellenic subduction system in the Eastern Mediterranean where an area of active back-arc extension beneath the Aegean Sea exists adjacent to a zone of shortening and convergence along the Hellenic trench. Geological constraints on the timing and magnitude of extension and thrusting show that there is a close connection between thrusting and extension in space and time, but the detailed kinematic and dynamic relationships between thrusting, extension, and subduction remains poorly understood phenomena.

Figure 11. Late Cenozoic examples of thrust belts associated with coeval back arc extensional systems in the Mediterranean region (from Royden, 1988).

In the complex zone of interaction between the Eurasian, Arabian, and African plates, there is continent-continent collision in eastern Turkey and subduction of the leading edge of the African plate beneath Eurasia along the Hellenic and possibly the Cyprus arcs. GPS observations indicate that western, central, and east-central Turkey is de-coupled from the Eurasian plate and is moving as a more or less coherent unit about an Euler pole located north of the Sinai peninsula (Figure 12). Other space-based measurements of crustal motion in Greece and along the Hellenic arc suggest that this coherent motion includes southern Greece and the south-central Aegean Sea.

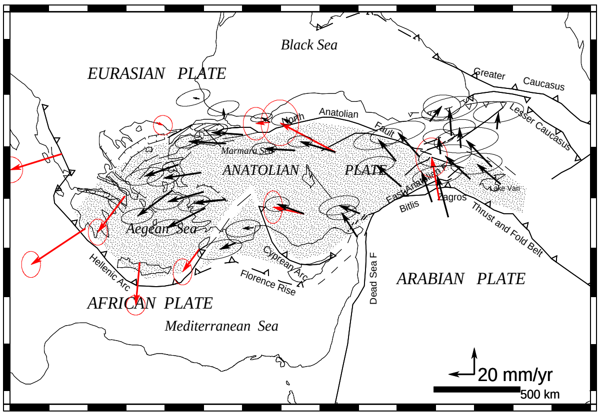

Figure 12. Velocities for GPS and SLR sites in a Europe-fixed reference frame, and their 95% confidence ellipses (Oral, 1994). Note the abrupt drop in the magnitude of velocities for sites north of the North Anatolian Fault and the change in orientation in northeastern Turkey

4.1.1.4 Southeast Asia and Indonesia Tectonics

In southeast Asia, four major tectonic plates (Australia, Eurasia, Pacific, and Philippine Sea) interact with each other, mostly along subduction zones (Figure 13). Their present-day kinematics is derived from inversion of earthquake slip vectors along their boundaries as well as transform fault azimuths and ocean floor magnetic anomalies. Within the kinematic frame defined by these four major plates, a broad zone of active crustal deformation covers central and southeast Asia. It extends from the Baikal rift in the north to the Indonesian subduction arc in the south where most of the stress induced by plate motions is released.

The present-day deformation pattern in southeast Asia combines the effects of the Java, Sumatra, Mariana, and Philippines subductions, as well as the effects of the India-Eurasia (Himalaya-Tibet), Australia-Asia (Banda arc), and Australia-Pacific (New Guinea) collisions. It has been imaged by geological and seismological studies but no direct measurements of the velocity field over the whole area has been proposed so far. GPS is the only existing tool that offers the opportunity to directly measure a regional velocity field for southeast Asia. This result is a critical basis for testing current geophysical models at different spatial and temporal scales, from plate kinematics to intracontinental deformation (Central Asia), plate boundary zone deformation (Indonesian arc), and co-seismic deformation.

In particular, the Indonesian archipelago has many active tectonic processes that result in phenomena such as mountain building, continental accretion, destruction of continents, emplacement of ophiolites, development of subduction zones, arc polarity reversal, and basin closure. Sumatra has been cited as a classic example of oblique plate convergence.

Eastern Indonesia is a region of broad deformation where the continental margins of Australia and Southeast Asia and the oceanic plates of the Pacific and Philippine Sea are coming together at rates of 80 to 110 mm/yr. Plate tectonic concepts do not explain the evolution of Indonesia because deformation is not confined to the edges of well-defined, rigid plates. Eastern Indonesia is at the stage of

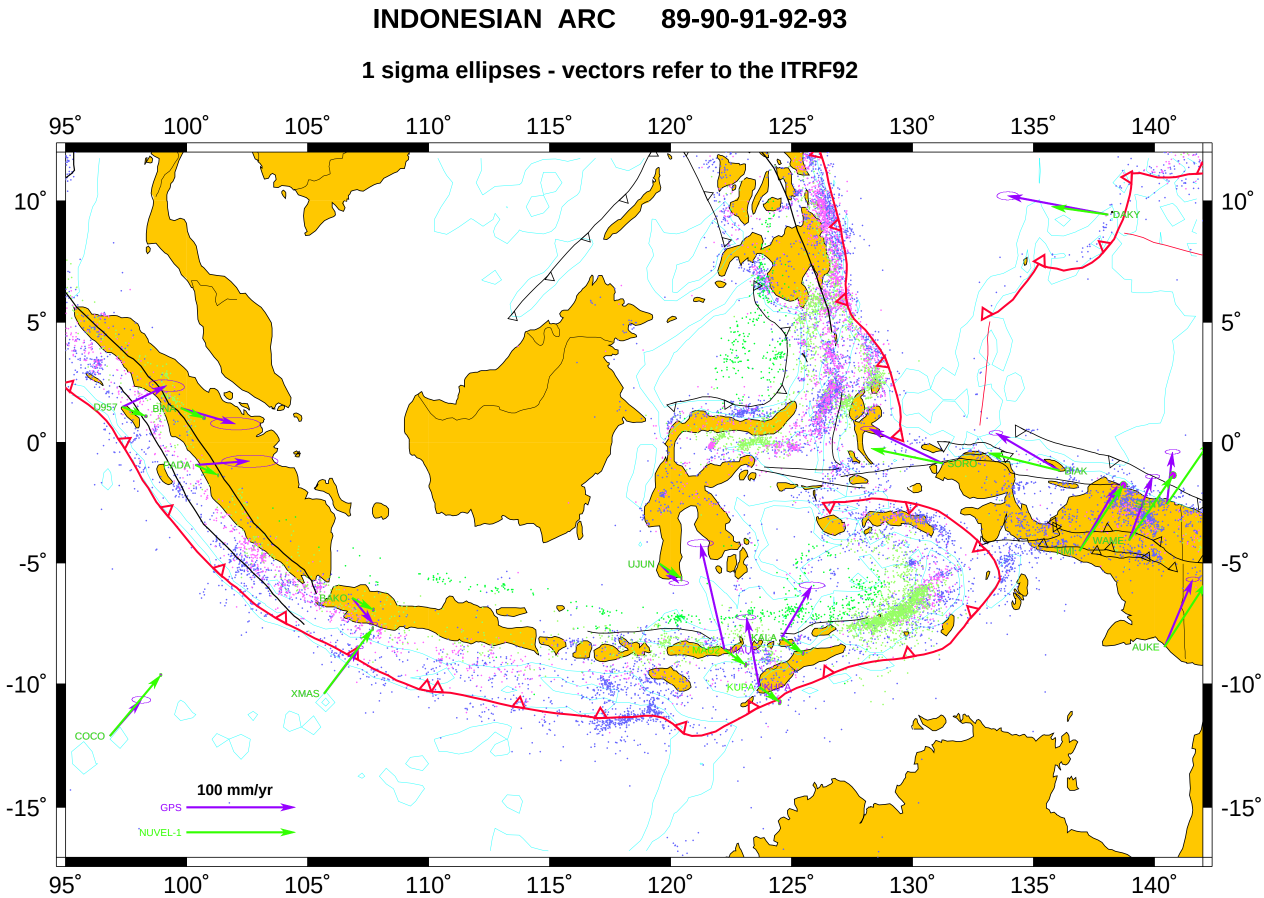

Figure 13. Plate boundaries, seismicity, and relative velocities determined by GPS for the Indonesian arc and adjacent regions (Calais, 1994).

assembly of crustal elements, both continental and oceanic, that will eventually form a complex mountain belt. The strain field within such deforming regions is a first-order observation that can constrain ideas about the behavior of the crust and upper mantle in mountain building.

Of particular interest is whether the brittle, shallow portion of the lithosphere, which is broken into fault-bounded blocks and produces most of the directly observable effects of tectonics, offers significant resistance to plate motions, or if it merely responds to horizontal shear stresses from a strong, ductile upper mantle. If the latter case holds, then the large-scale deformation of the lithosphere can be represented by a continuum, and the surface faulting has little to do with plate dynamics except in an average sense. An important geological consequence of this view is that the juxtaposition of rock types in mountain belts may be as much a consequence of small local mechanical and geometric irregularities as it is a consequence of plate motions.

4.1.1.5 The Interior Western U.S. and the Transition to the Stable Plate Interior

Much interest has been focused on the mechanism and mode of Late Cenozoic lithospheric extension of the western U.S. Cordillera encompassing the Basin and Range province, the world's largest region of intraplate continental extension (Figure 14). Tectonic process of the Basin-Range are generally thought to be locally driven, including crust-mantle coupled volcanism; “soft” shear coupling between the stable interior, the San Andreas transform fault, and the Cascadia subduction zone; localized topographic load-induced stresses; and coupling of quasi-plastic flow in the lower crust with surface deformation. Active tectonism of the Basin-Range is directly manifest by extensive earthquakes and large Quaternary fault scarps which occur primarily along its margins. Historically eight large earthquakes, dominated by normal- to oblique-slip, reflect ongoing tectonism that is measurable with GPS.

Measurements of contemporary tectonism in the Basin-Range are limited to a few VLBI/ SLR ~1000 km baselines which reveal ~1.0 cm/yr of east-west extension. These rates agree remarkably well with displacement rates deduced from summations of seismic moments of historic earthquakes of ~1 cm/yr as well as rates deduced from models of intraplate deformation tied to a fixed mantle framework, and suggest that the brittle mode of deformation accompanying earthquakes accounts for ongoing tectonism. However, little is known of how deformation is distributed across this wide region of extension or of the mechanisms responsible for this unusual style of intraplate deformation.

On a regional scale, VLBI measurements from a single baseline across the Basin-Range transition to the Stable Plate interior compared to the stable U.S. interior give a clue to the lateral distribution of intraplate strain release across the transition between the Basin-Range and stable interior of ~5 mm/yr east-west extension. This rate is remarkably similar to the first GPS measurements against historic trilateration/ triangulation data, as well as an annual resurvey of a GPS network across the Wasatch fault,

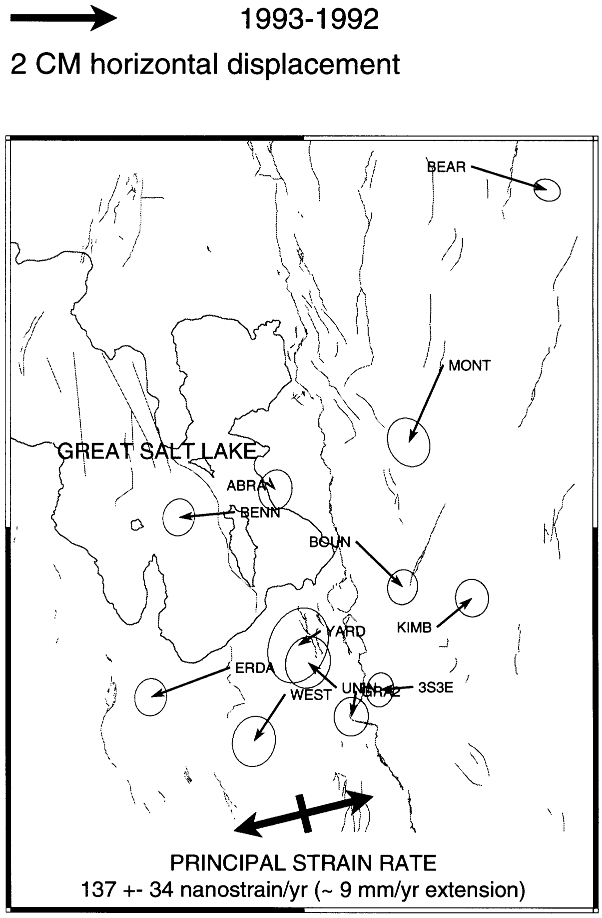

Figure 14. Horizontal strain and displacement from 1993 to 1992 GPS surveys on the central Wasatch fault (Smith, 1994). Error ellipse corresponds to one standard error.

Utah, which revealed 5 to 9 mm/yr northeast extension. This rate notably exceeds the inferred long term ~1 mm/yr rate deduced from Holocene slip determined from paleoseismic measurements. One interpretation of these data is that the now dormant Wasatch fault is storing strain energy at high rate preceding a future earthquake, which has important societal ramifications. However, without further analyses, additional GPS observations, and comparison with older geodetic data these high rates can not be verified.

These observations point out an important problem that can be addressed by GPS: How do rates of contemporary deformation compare with Holocene geologically deduced rates, and do deviations of these contemporary rates indicate short-term processes such as rapid strain accumulation preceding large earthquakes? This question has major implications for the occurrence of earthquakes on known or hidden faults. Low-angle listric and basal detachment faults were first observed in the Basin and Range based upon geologic mapping and seismic reflection data. These observations suggest an important paradox in tectonics, namely the occurrence low-angle normal faults at relatively shallow crustal depths, despite the lack of unequivocal evidence for low-angle faulting from earthquake data. This an important problem which can be addressed using an integrated approach of fault studies, earthquake monitoring, and high-precision GPS measurements.

The widespread seismicity, well-preserved Quaternary faults, and active extension of the Basin and Range thus provide excellent opportunities to evaluate rates of deformation using GPS and such processes questions as “characteristic” earthquakes, space-time clustering of earthquakes and stress coupling between the lower and upper crust, and topographically driven deformation. It is a particularly well-suited region for studying active continental extensional mechanisms with GPS.

4.1.2 Volcanic Processes

Geologic and historical records show that over 500 of the world’s volcanoes can be considered to be “active” or capable of producing an eruption. The vast majority of these volcanoes are associated with subduction-zone plate boundaries. Although constituting only about 15% of the annual global magma production, subduction-zone volcanoes can be explosive and have dramatic effects on human populations. In contrast, most magma is generated at plate spreading centers at remote mid-ocean ridges. The remainder of volcanic activity is located along mantle hotspot tracks.

Current geologic and geophysical volcano research investigations are examining the origins of magma, the physical and chemical properties of magmas, hydrothermal fluids and gasses, the structure of volcanoes and volcano plumbing, the mechanism of magma transport, and the relationships of volcanoes to tectonic boundaries and earthquakes. GPS measurements of crustal deformation are at the forefront of new techniques for studying these volcanic processes. A better understanding of these processes is contributing to improved volcano hazard assessments and volcano eruption predictions.

Surface deformation measurements offer only the means of constraining the volume and geometry of subsurface crustal magma sources. Traditionally done with trilateration and leveling, precision GPS surveys of ground motion now offer unprecedented simultaneous three-dimensional views of volcano deformation on scales of hundreds of meters to tens of kilometers, and can operate in remote regions not requiring line of sight to observation points. When tied to regional GPS survey networks, a direct measure of the relationship of the volcanic and tectonic framework can also be obtained. Examples of this application are studies of rifting and volcanism in Iceland, investigations of deformation of the Yellowstone caldera and its relationship to a large continental hotspot, and extensive USGS efforts to monitor such active features as Kilauea volcano, Hawaii, and some threatening Alaskan and Cascades volcanoes.

In general, volcano deformation can be separated into two types: that due to roughly equi-dimensional magma chambers and that due to rifting or dike intrusion. From the study of some basaltic shield volcanoes, notably in Hawaii and Iceland, we know that as magma rises from the mantle it collects in shallow magma chambers. As the magma chamber fills, the Earth's surface uplifts and stretches. These inflationary periods are interrupted by eruptions or intrusions into flanking rifts, which cause withdrawal of magma from the chamber and attendant subsidence and contraction.

The earliest models of the inflation-deflation cycle used point centers of dilatation (the so called Mogi source). The surface displacements produced by a Mogi source are nearly indistinguishable from that produced by a spherical magma chamber, and similar to that generated by other equi-dimensional models. It turns out that given only vertical displacement data it is nearly impossible to determine the shape of the magma chamber. Horizontal and vertical data together provide much tighter constraints on source models. One of the benefits of GPS over traditional methods (leveling and trilateration) is that GPS determines all three components of station displacement. Much of the same arguments hold true of rifting. Rifting can occur episodically, accompanied by extensive ground cracking and swarms of shallow earthquakes that migrate downrift at velocities of a few tens of centimeters per second. Examples of volcanic processes are discussed in the following sections.

Interpretations of the crustal deformation data obtained in volcanic studies, such as the studies presented in the following sections, are most meaningful when combined with other geophysical and geologic data. For example, seismicity patterns can be used to locate and identify potential faults related to magma pathways, whereas GPS measures both aseismic and seismic deformation associated with magmatic activity. Combined with precise gravity measurements, GPS and vertical motion observations can also be used to distinguish between changes in elevation due to tectonic strain and changes due to magma flux.

Hazards from volcanic events range from local phreatic (hot water and steam) blasts and lava flows to large catastrophic ash flows and air falls. Volcanic eruptions also produce secondary flooding and landslides. The long-term effects of volcanic eruptions are well known to effect globe-scale weather changes resulting from ash particulates deposited in the atmosphere. The primary goal of volcanic risk research, however, is to specify the timing and locations of potential volcanic eruptions. The location and long-term history of volcanoes are generally known from geologic and historical records. However, it is difficult to determine the short-term timing, style, and volume of an eruption at times scales of a few minutes to hours.

The success of detailed earthquake monitoring in predicting the recent eruptions of Mt. Pinatubo, Philippines, and Mt. Redoubt, Alaska, saved thousands of lives and points out the use of geophysical tools to forecast eminent eruptions. This class of research will benefit by parallel efforts in deformation monitoring for inflation and deflation of the surface which are associated with magma or hydrothermal fluid movements, to constrain the geometry and volume of magma chambers, plumbing of conduits, dikes and sills and associated faulting, and to assess incipient earthquake triggering.

Repeated GPS surveys taken over months and years give insight into the long-term deformation signal associated with volcanic processes. High precision static GPS surveys can be used where deformation rates may only be mm/year. In many cases however, the sequence of eruptive activity can take only hours to days and rates accompanying deformation are cm/hour. Deformation can be continuously monitored with GPS receivers deployed at remote sites and with data transmitted to a central recording site where processing can be done in near real-time kinematic differential modes.

Orbit information broadcast directly from the GPS satellites are sufficient for analyzing short baselines (~10 km), but where receivers are separated by large distances (>10 km), more precise satellite orbits are required for real-time processing. The U.S. Geological Survey is currently operating a small continuous tracking GPS network on St. Augustine volcano in Alaska and will install a network in Hawaii. Monitoring is more effective where augmented with repeated static surveys which can cover additional sites over a larger area and which can be used to determine spatial coherence of the deformation signal over longer time intervals.

New techniques are being developed to make remote sensing measurements of deformation using aircraft. For example, in an experiment at the Long Valley caldera in California, repeated aerial laser altimeter measurements are being made which will be used to produce an image of ground motion. Kinematic GPS is used for precise, centimeter-level positioning of the aircraft. Radar interferometry can detect map surface displacements at the centimeter level of horizontal accuracy, but requires GPS to control the coordinates of satellite images. Similarly, radar interferometry from space is likely to have much potential in observing deformations associated with volcanic activity, but likewise will require GPS calibration on the ground. These remote sensing methods not only have the potential to cover large and possibly remote areas, but also do not require observers to be physically located on a potentially hazardous volcano.

4.1.2.1 Kilauea

Geodetic and seismic data have been used to model the geometry and depth of rift zone intrusions. Kilauea is a case in point. On Kilauea, these models indicate that the dikes are steeply dipping bladelike structures a few meters thick, typically at depths of between 2 and 4 km. Less is known about the deeper part of the rift system and the long-term deformation accompanying intrusion within plate-boundary rift zones.

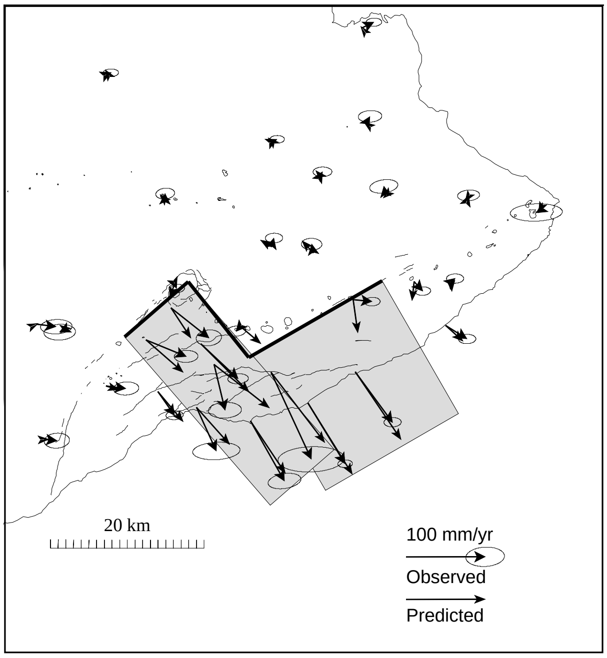

Figure 15. Displacements near the Kilauea rift zone determined by GPS compared with model displacements (Owen et al., 1994).

Deformation and seismicity data demonstrate that magmatic activity and slip on Kilauea’s fault systems, including the subhorizontal faults that generated the magnitude 7.2 1975 Kalapana earthquake, are coupled. Yet the subsurface geometry of these faults and the deep structure of Kilauea’s rift zones are poorly understood. Figure 15 shows the average station velocities for the three-year period with respect to a point on the northwestern side of the island of Hawaii. Stations on the central south flank of Kilauea moved SSE, away from the rift zones, at rates of up to 10 cm/yr. In contrast, stations north of the rift zone, only 6 or 7 km from the rift, are not moving within measurement errors.

Velocities also decrease dramatically to zero toward the more distal ends of the east and southwest rift zones. There seems to be a zone that is actively displacing seaward. Lateral gradients in velocity (strain-rates) are very large. In fact, these strain-rates are at least an order of magnitude greater than those across the San Andreas fault! The rapidly displacing section of the south flank coincides roughly with the source region of the 1975 earthquake, and the seismically active portion of the south flank.

The steep gradients in the surface velocity field show intriguing relationships to structural elements of the volcano as expressed in the topography and bathymetry. The rapidly displacing zone corresponds quite well to the extent of the Hilina fault system. The bathymetry off the south flank contains features indicative of gravitationally driven slumping. A series of topographic basins offshore of the rapidly displacing south flank block must be geologically active, since the high sediment flux off Kilauea would quickly fill any depression.

The western extent of the rapidly displacing zone may correspond to a prominent linear feature in the bathymetry, once referred to as the Papau Seamount, now interpreted by some to be the boundary of the Hilina mega-landslide system. However, there is no evidence for lateral “tear” faults at either the eastern or western edges of the rapidly deforming zones.

4.1.2.2 The Yellowstone Caldera

A GPS survey in 1987 established a dense network of 60 stations planned to measure crustal deformation of the active Yellowstone caldera and adjacent Hebgen Lake and Teton normal fault zones. Comparisons of data from a 1993 survey with GPS surveys in 1989 and 1991 show significant crustal deformation which is characterized by subsidence and contraction over the 60 km-long Yellowstone caldera superimposed upon a regional tectonic strain field. The principle components of the regional strain rate tensor, estimated using a method of simultaneous reduction after excluding data for stations outside the caldera, are 1.1±0.2 x 10^{-7}/yr of northwest contraction and 0.6±0.2 x 10^{-7}/yr of northeast extension. After removing the regional strain components from the observed GPS field, the residuals of the inner-caldera sites revealed up to 20±7 mm of horizontal displacement, directed radially toward the center of the caldera, and up to 70±20 mm of caldera-wide subsidence. This corresponds to an average subsidence rate of 17 mm/yr.

Forward models made with a 3-D boundary element technique can explain the caldera deformation with a shallow NE-elongate shaped, sill-like body beneath the caldera at depths of 3 km to 6 km (Figure 16) which lost volume at a rate of 0.02 km^3/yr, similar to rates independently estimated for magmatic fluid release. This deflationary model was confirmed with a 3-D volumetric source model derived by simultaneous inversion of the horizontal and the vertical GPS displacement data. The inverse model indicates that the largest deflation is quite shallow, between the surface and 3 km depth, in the depth range of extensive hydrothermal fluids and possible magmatic fluids in Yellowstone.

It is evident from the regional GPS observations that the extent of the current Yellowstone GPS network is insufficient to measure crustal deformation associated with the long-wavelength signature of the Yellowstone hotspot. For example, topographic and geoid data suggest that the influence of the hotspot extends up to 500 km from the caldera. To examine these large-scale effects of the hotspot signature, the new Yellowstone GPS surveys are designed to reobserve much of the existing network and to make ties to the high-

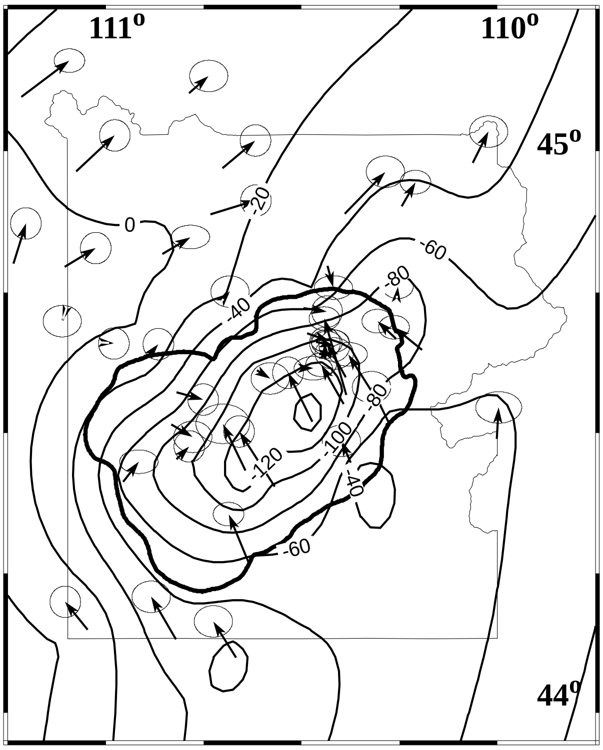

Figure 16. Three-dimensional deformation of the Yellowstone caldera showing subsidence, contraction, and regional strain (Meertens and Smith, 1994).

accuracy GPS networks of surrounding states which have approximately 100 km spacing.

4.2 The Earthquake Cycle

It has recently been estimated that within 50 years more thana third of the world's population will live in seismically and volcanically active zones. As a result, the international community is attempting to devise means to reduce and mitigate the occurrence of these devastating natural hazards. The International Council of Scientific Unions, together with UNESCO, the World Bank and a number of U.S. agencies including—NSF, the DOE, the USGS and NOAA—have endorsed the 1990s as the International Decade of Natural Disaster Reduction (IDNDR). These organizations are planning a variety of scientific programs in an attempt to understand how such natural disasters might be predicted, or at least mitigated.

Because both earthquakes and volcanoes are so strongly associated with significant crustal deformation, it is expected that GPS measurements will play a central role in many of these scientific projects. Virtually all of these projects will include GPS field observation, and in addition will use numerical models to interpret and understand the measurements; thus, modeling occupies a central focus in these integrated studies of earthquakes.

It is generally recognized that observations lead to the definition of distinct intervals during the more-or-less repetitive earthquake cycle, referred to as "coseismic," "postseismic," and "interseismic." The coseismic period is identified as the short (approximately minutes) interval associated with the earthquake itself, when the majority of the slip occurs and elastic and inertial effects dominate.

The postseismic interval is a somewhat loosely defined period comprising days to perhaps a decade in which further non-inertial slip (aseismic slip or creep) takes place, together with the surface deformation related to inelastic stress relaxation within the upper part of the asthenosphere. Both of these effects yield surface deformation that decays approximately exponentially. The interseismic interval comprises most of the long period between earthquakes, during which plate motion reloads the plate boundary, and which can be represented to a reasonable approximation by simple rigid plate motion. There are as yet no indisputable geodetic indications of a "preseismic" process interval, in which changes of an as-yet unobserved type might occur prior to the earthquake.

Resolution requirements for the various intervals depend to a certain extent on the nature of what space-time frame features of the event are of interest. For example, if details of the coseismic slip distribution are needed, then accuracy of better than 100 mm over time periods of days and spacial scales 1–100 km or larger are required. On the other hand, delineation of the physics of postseismic deformation requires accuracy of 10–100 mm over time scales of hours and spacial scales of again 1–100 km. The interseismic phase is obviously characterized by the same time-space scales that characterize plate tectonic motion. The only factor known about requirements for preseismic deformation is that the space-time accuracy and resolution currently available is not sufficient to resolve indisputable precursors.

In order to understand the physical meaning of the processes operating during each interval, models must be used to interpret the data. There are two broad categories of earthquake models: "kinematic" and "dynamic." Although recognizing the complexities of crustal deformation, most models have attacked the problem of strain accumulation and release on a single prescribed fault.

Models that prescribe the slip on the fault and then calculate the resulting surface deformation by numerically evaluating the appropriate Green's function are called kinematic models. Using these Green's functions, calculations have been carried out in which a series of earthquake slips are specified on fault planes in time and space. Together with relative path velocities, which are known from rigid plate motion models, the surface deformation can then be calculated at any time or location on the surface on the model Earth. Self-consistent kinematic models of earthquake cycle can be developed in which a history of earthquakes is prescribed. In these models, both the slip distribution along the fault as well as the time slip are given, and the resulting surface deformation is calculated. Models of this kind have been constructed for both purely elastic and layered viscoelastic-gravitational media.

The other kind of models are those in which the slip itself during a series of earthquakes is calculated as a consequence of a given set of dynamical governing equations, boundary conditions, and frictional properties on the fault. Once the earthquake history on the model fault has been computed, together with the slip in each event, the entire history of time-dependent deformation of the free surface can be calculated. Using this approach, earthquake researchers have begun to focus on the dynamics of interacting fault systems, and a series of fascinating new possibilities have emerged that define many new directions and lines of research.

For example, these models, which are fundamentally nonlinear in character due to the nonlinear frictional forces acting on the fault surface, have been shown to produce a full range of rich, complex dynamical behavior including limit cycles as well as chaotic behavior. Thus, at the same time that our ability to accurately observe crustal deformation has blossomed with the advent of GPS technology, dramatic improvements have developed our ability to realistically simulate the physics of an earthquake source process, and as a consequence predict the surface deformation that can be measured by space geodetic observations. It is therefore reasonable to expect that it may shortly be possible to critically test models for competing ideas of the physics of earthquake nucleation using space geodetic data.

A substantial and growing database of centimeter-level accuracy geodetic observations of deformation along active fault zones now exists. Important regions covered include those parts of California through which the San Andreas fault passes; the tectonically active Owens and Chalfant valleys and Long Valley caldera; the Wasatch range; Yellowstone; the

Delani, Totschunda, and Fairweather faults; as well as several islands sensitive to deformation along the Aleutian trench in Alaska; many parts of Japan; the Alpine fault in New Zealand; the Anatolian fault in Turkey; and the Pozzuloi-Campi Flegrei caldera in Italy, to name just a subset. A critical issue is how to make best use of these data. Many of the previous efforts have been devoted to verification of the predictions of regional and global kinematic plate motion models. A most challenging problem is that of using precise geodetic data to search for precursors to major earthquakes on these faults.

There are only three possible alternatives that can explain the lack of observations of precursors to date. The first is that there exist no precursors to observe at the precision that we have available to us with our current measurement techniques. If this is the case, one would like to prove it theoretically so that no more money is spent on fruitless searches. The second is that the space-time coverage of the effected region is inadequate. If this is the case, one would like to determine, using theory, what constitutes adequate coverage. The third alternative is that the precursory signals are presently there in the data, but we do not know how to recognize them. This alternative implies that theoretical models for the earthquake nucleation processes must be constructed to provide predictions of the corresponding geodetic signature. Observational techniques must then be devised to optimize chances for detection of these signals.

4.2.1 Loma Prieta

An opportunity to model the phases of the earthquake cycle was provided by the magnitude 7.1 Loma Prieta earthquake of October 17, 1989. This event was the largest earthquake in California in 40 years, and the largest earthquake in the San Francisco Bay Area since 1906. Following the earthquake, a GPS network in the Santa Cruz–Watsonville area that had been surveyed by the California Department of Transportation (Caltrans) in the year prior to the earthquake was remeasured. While the Caltrans measurements were made with single frequency receivers, it was found that day-to-day repeatability of the baseline vectors was 0.5–1.0 cm in the horizontal components and 3.0–3.5 cm in the vertical.

The GPS baseline vectors were combined with other data—Electronic Distance Measurements (EDM), Very Long Baseline Interferometry (VLBI), and spirit leveling—to obtain a complete picture of the three-dimensional coseismic deformation field. An iterative quasi-Newton method was used to find the dislocation geometry that best fits all of the available geodetic observations. When weighted properly, all of the data can be accounted for by a single dislocation surface that is consistent with the aftershock distribution. The strike and dip of the best-fitting dislocation is consistent with moment tensor solutions.

GPS has been the principal tool used in studying postseismic deformation following the Loma Prieta earthquake. Strain diffusion away from the epicentral region is predicted by theoretical models of viscoelastic relaxation below the seismogenic crust, and has been suggested as a mechanism to explain sequential rupturing along a fault system. Transient postseismic deformation has generally been explained either by viscous relaxation of a ductile (asthenospheric) layer underlying an elastic (lithospheric) plate, or by downward propagation of aseismic slip along an extension of the fault zone into the lower crust. The horizontal deformation field in the epicentral region prior to the 1989 earthquake was already well-established on the basis of 20 years of geodolite measurements and several years of GPS measurements.

Following the 1989 earthquake two arrays crossing the San Andreas in the epicentral region and northwest of the rupture zone were established and surveyed multiple times. Because of the extensive pre-earthquake monitoring, it is possible to identify features in the present-day deformation field that are attributable to the earthquake. The postseismic velocity field in the epicentral region of the Loma Prieta earthquake (Figure 17) differs significantly from displacement rates measured in the two decades preceding the event. The post-earthquake displacement rates along the Black Mountain profile, which crosses the San Andreas fault 44 km northwest of the Loma Prieta epicenter, do not differ significantly from those determined from 20 years of trilateration measurements. However, station velocities along the Loma Prieta profile, which passes through the epicentral region, significantly exceed pre-earthquake rates within 20 km of the Loma Prieta rupture.

There is also significant San Andreas normal shortening centered near Loma Prieta. Contrary to expectation, the post-Loma Prieta GPS data cannot be fit with slip on a single fault plane, or by distributed down-dip deformation following the earthquake. The data can be fit, however, with slip on two fault planes: strike-slip on a fault coincident with the rupture plane, and reverse-slip on a fault within the Foothills thrust belt more or less coincident with the Berrocal fault. Slip within the Foothills thrust belt appears to have been triggered by the stressing during the Loma Prieta mainshock.

4.3 Deep Earth and Whole Earth Applications

4.3.1 Earth Rotation

Geodetic techniques are able to sense the response of the mantle to internally and externally applied torque. With currently available systems and a data set which now spans over a decade, deviations of the Earth's motion from that predicted by geophysical theories with amplitude of 0.3 mm can now be measured, for signals that are coherent with the major tidal forcing signals. Results of this accuracy have been used to infer the flattening of the core-mantle boundary, to bound the anelastic properties of the mantle in the diurnal

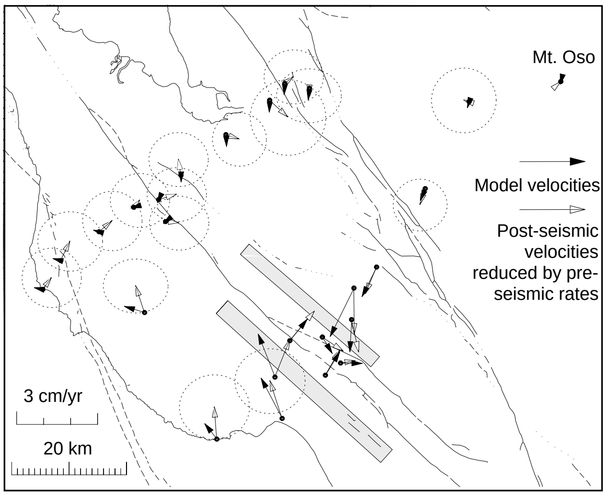

Figure 17. Excess postseismic station velocities (secular displacement rates subtracted from postseismic rates) assuming the velocity of Mt. Oso was unaffected by the earthquake (Bürgmann et al., 1994). Error ellipses (3 sigma) for the sites near Loma Prieta are not shown for clarity. They are the same order of magnitude as the error ellipses at other sites. Also shown are the velocities (filled arrows) computed from a dislocation model involving slip on two faults; strike slip on the Loma Prieta fault and thrusting on a reverse fault in the Foothills thrust system. The two shaded rectangles show the projections of the faults used to compute the modeled station displacements. The first fault lies in the Loma Prieta aftershock zone, from 6 to 17 km depth, dipping 70° SW, with a strike-slip displacement rate of 0.10 m/yr. The second fault slips 0.12 m/yr on a reverse fault dipping 47° SW, striking subparallel to the San Andreas, from 1.4 to 5.8 km depth.

frequency band, to detect the influence of the solid inner core on the rotational dynamics of the mantle, and to place upper bounds on conductivity at the base of the mantle and the strengths of the magnetic field near the core-mantle boundary. The effects of the oceans have also been detected, and the influence of the Earth's atmosphere are also now becoming evident.

The applications of geodetic systems, including GPS, cover all time scales from the diurnal and semidiurnal bands of the major tidal forces being applied to the Earth to decade duration variations whose study is limited only by the duration of the geodetic data themselves. In the former of these time scales, the forcing functions are well known and the geodetic systems can measure the response of the Earth to these forces. In the latter of these time scales, the forces themselves are not well understood and geodetic systems provide information about convolution of the forcing function with the response of the Earth. For very long-term measurements, GPS must rely on VLBI measurements to provide a link between long-term variations in the Earth's rotation and an inertial reference frame.

For deep Earth studies, geodetic measurements can provide accurate information about the dynamical interactions of the fluid core and mantle. Much of this information arises from a resonance in the rotation of the Earth due to the differential rotation of the core and mantle. The torques applied to the mantle by the core are sensitive measures of the flattening of the core-mantle boundary and deformation of the mantle arising from the pressure at the core-mantle boundary as the elliptical core rotates differentially with respect to the mantle. Since the frequencies of these torques are in the nearly diurnal band, the measurements of the nutations of the Earth and the associated surface deformations provide unique measures of the dynamical mantle properties in this frequency regime.

For example, competing models for the frequency dependence of the shear-strain Q of the mantle predict anelastic effects on the rotation whose amplitudes at the surface differ by a few millimeters. While these values are small, they are detectable with current data sets. Similarly, magnetic coupling between the core and mantle could also produce few millimeter deviations which are currently detectable.

The major differences between a geophysical theory for the motion of the Earth's body axis in space and those observed by VLBI are shown in Figure 18. The large annual signature (amplitude 2 mas) is interpreted as being due to a deviation of the core-mantle boundary from its hydrostatic shape by about 4.5%. The long period variations reflect deviations in the 18.6 year nutation whose accurate determination is currently limited by the duration of high quality VLBI data.

Not so evident in the figure is a semi-annual signal (amplitude 0.5 mas) which arises partly from the excess flattening of the core mantle boundary (0.3 mas), partly from ocean tides (0.6 mas), partly from the anelasticity of the mantle (0.3 mas), and partly from the deviation of the ellipticity of the whole Earth from that computed assuming hydrostatic equilibrium and geophysical models of the density distribution of the Earth. Although non-hydrostatic models of the Earth derived from seismic tomography have been available for a number of years, a rotational dynamic model for the Earth has yet to be constructed with such data. When such a consistent model is determined the anomalies due to the ellipticity of the whole Earth and fluid core should be eliminated.

Because the forcing functions are known for the nutations, both the in-phase and out-of-phase components of the response of the Earth

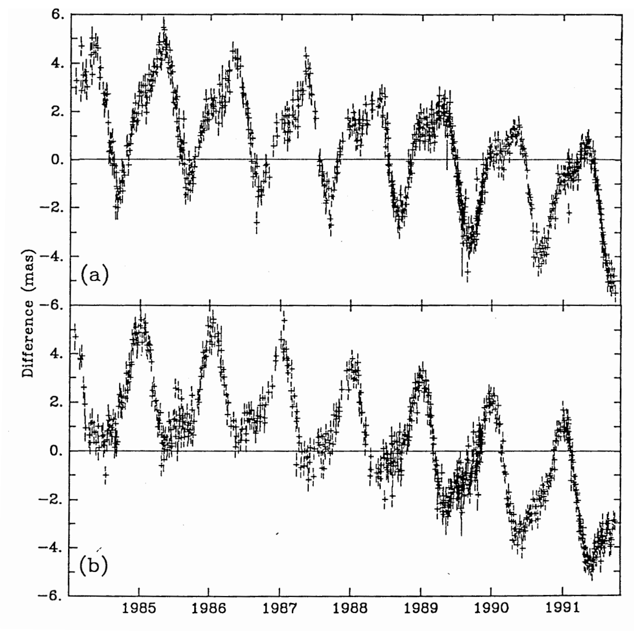

Figure 18. Differences between positions of an axis attached to the mean mantle of the Earth (body axis) in inertial space and that predicted by the IAU 1980 nutation series and observed with very long baseline interferometry (VLBI). The positions are expressed as two angles: (a) nutation in longitude and (b) nutation in obliquity. One milliarcsecond (mas) is equivalent to 30-mm displacement at the surface of the Earth (courtesy Herring, 1993).

can be determined, with the latter interpreted as arising from dissipative processes in the Earth. For example, 0.4 mas of the annual signal is out of phase and thought to arise from magnetic coupling between the core and mantle, while other out of phase components are consistent with anelasticity of the mantle.

The accuracy of these nutation results, along with other rotational components such as diurnal and semidiurnal variations in the rotation rate, is now so high that deficiencies in the accepted tidal displacement models also need to be examined, particularly in the light of the effects of mantle inhomogeneities and anelasticity. Although these effects are expected to be less than 1 mm of surface displacement, they are within the realm of detectability with the current systems and data sets.

Global geodetic networks also allow the motion of the rotation axis to be accurately determined. Much of the free nutation, or Chandler wobble, has been shown to correlate with variations in atmospheric mass distributions. However, it is likely that a part of the wobble is excited by large earthquakes and relatively rapid tectonic motions (that have been termed "silent earthquakes"). At the present, large earthquakes account for only a fraction of the relative motions of plates at convergent zones, and for even less at strike slip plate boundaries.

The detection of aseismic motions on plate boundaries would add greatly to our understanding of plate motions, and would contribute to understanding the development of large scale strain fields associated with large earthquakes on plate boundaries. Continued global monitoring of Earth rotation should allow the detection of changes in the rotation axis associated with such motions.

The establishment of global GPS networks will permit more precise determination of the rotation of the whole Earth and its relation to the transfers of mass and momentum between various parts. More importantly, it will allow the determination of the spatial structure of the whole Earth deformation field, and allow the nature of the loading and momentum transfer to be better determined.

4.4 Interaction of Mantle Convection and Tectonics

4.4.1 Vertical Motions

The Earth's surface adjusts vertically in response to temporal changes in the forces applied at the base of the lithosphere, such as might be caused by changes in temperature, mineral phase, or pattern of convection. For most processes, the predicted vertical motions are too slow to be detected by GPS instrumentation at present, or even with likely improvements in the next 10 years, with two possible exceptions. The first is the possibility that broad continental plateaus, such as Tibet and the Altiplano, might experience rapid uplift as the result of delamination of the dense lower lithosphere that becomes convectively unstable on account of over-thickening of the lithosphere at continental convergence zones.

For example, it has been proposed that 8 million years ago the Tibet Plateau abruptly rose by 1 to 3 km within the span of a million years on account of delamination of its cold, thickened lithospheric root. The rise of this abrupt and massive continental feature had a major influence on climate in southern Asia by triggering the onset of the monsoons. At rates of a few millimeters per year, vertical uplift in response to convective destabilization of the lower lithosphere could be measured and used to understand how the dynamics of the lower lithosphere affects continental tectonics.

The second example is the uplift of the Earth's surface as the lithosphere rides over mantle hot spots. From analysis of depth anomalies in the ocean basins, it is clear that the uplift is of the order of a kilometer or two, and it reaches its full height within a few million years. Investigation of the rate and pattern of uplift provides important information on the thermal and dynamic properties of hot spots and how they interact with the lower lithospheric boundary layer. Nothing is known about this process for hot spots underlying continental lithosphere, such as Yellowstone (Figure 19) and the many African hot spots, because we lack a vertical reference for measuring uplift associated with the passage of the lithosphere over these hot spots. GPS provides the only hope of recording this process of hot spot-continental lithosphere interaction, but detecting this small signal will require improvements in the vertical accuracy.

4.4.2 Horizontal Motions

Although it is generally acknowledged that lithospheric plate motions are driven by deeper seated convective flows, the exact nature of the coupling is not known. Recent comparisons of plate motions derived from geologic data over a few million years with geodetic measurements over a few years indicate that the plate motions are the same over both time scales. Yet we know that the motion at plate boundaries is not continuous, but is accomplished in large part by episodic earthquakes.

There is also evidence that the seismic (and subseismic) motions on plate boundaries may follow larger scale spatial and temporal patterns; there may be an alternation of earthquakes on convergent and transform plate boundaries on a time scale of decades. Deciphering such patterns and processes is clearly important for understanding the development of stress and strain along plate boundaries, and relating the earthquake cycle to plate motions.

Geodetic networks on the scale of hundreds of kilometers should be able to measure the displacements associated with major slip at plate boundaries, and detect its evolution with time as it diffuses away from the plate boundary into the interior of a plate, where the motion becomes more uniform. Such data will directly bear on the nature of the coupling between the plates and the underlying mantle, and will allow the determination of the upper mantle rheology that controls the coupling.

Such measurements will also address another central problem. To first order, lithospheric

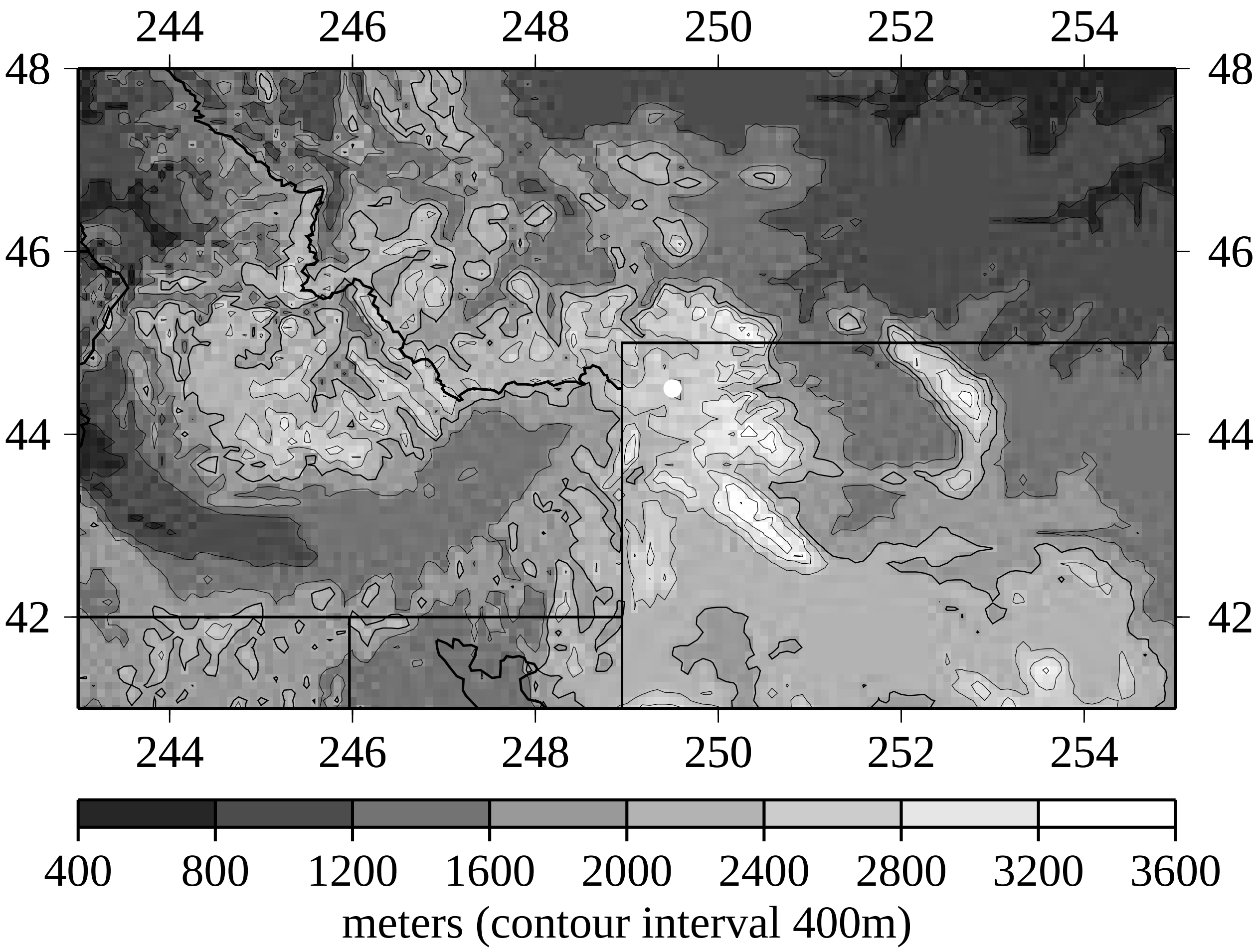

Figure 19. The Yellowstone hot spot swell (Waschbusch and McNutt, 1993). Based on the observed elevation of the topography and the predicted rate of motion of the North American plate relative to the hot spot framework, the rate of uplift of the eastern side of the swell is approximately 0.1 to 1 mm/year, but it is difficult to extract the long-wavelength signal of the swell from topographic noise created by older Cenozoic tectonics in the western U.S. Direct observations of the rate of uplift would improve our understanding of the hot spot phenomenon.

plates behave as rigid bodies; this is a central premise of plate tectonics. Nevertheless, plates do deform, and measuring the deformation is central to determining the limits of simple plate tectonic descriptions of surface motions, and to understanding processes that may ultimately lead to the formation of new plate boundaries. This is apparent in the case of continental portions of plates, which are not rigid and in which incipient rifts form. The extent of deformation in oceanic plates is not known at present, and measurements of whether any large scale deformation is occurring is of considerable interest.

4.4.3 Post-Glacial Rebound

To date, the principal constraints on the rebound of the Earth's surface in response to the glacial unloading have come from geologic observations of the vertical position with respect to present-day sea level of former shorelines with ages less than 18,000 years.

This approach is limited because the rebound signal can only be measured where the land surface intersects the sea and only the vertical component of the surface readjustment can be estimated.

Furthermore, the vertical datum, present-day sea level, has been continually changing position over the past 18,000 years on account of the draining of the glaciers into the ocean and changes in the geoid due to mass redistribution accompanying melting and rebound. GPS measurements promise to provide a much richer data set to solve for the Earth's response to unloading in several ways:

1. GPS measures horizontal, as well as vertical motions. Horizontal motions are much more sensitive to radial variations in viscosity than are vertical motions. And they are also sensitive to variations in models of the ice loading history. Differences among predictions from currently viable models exceed 2 mm/yr. Within 5-10 years, GPS observations will resolve much of the current debate about mantle viscosity structure.

2. GPS observations can provide data anywhere a receiver can be located, not just at a coastline. A wider geographical distribution of displacement data will make it possible to separate out the "noise" of local deformation due to other causes. In order to investigate the regional differences in rebound caused by lateral variations in mantle viscosity, we can study the desiccation of inland seas like the Aral and Caspian Seas using local GPS surveys to measure the rebound and periodic aero-gravity surveys to measure the rate of desiccation. These aero-gravity surveys will require precise navigation by GPS in order to separate gravitational from inertial accelerations of the moving platform.

3. Understanding the contribution of post-glacial rebound to contemporary deformations is critical for effectively monitoring present-day sea level rise and for properly interpreting possible tectonic deformations. For example, recent models of present-day post-glacial rebound predict onshore uplift and offshore subsidence at rates of a few mm/yr along the Pacific Northwest coast of the U.S. and Canada. This is similar to rates reported from repeated leveling and tide gauge measurements and interpreted to reflect on-going subduction of the Juan de Fuca plate beneath North America. On the basis of contemporary deformation, paleoseismic studies, and comparison to similar plate boundary settings, it has been suggested that this region could be vulnerable to extremely large (> magnitude 9) subduction earthquakes. GPS can contribute to our understanding of ongoing processes by providing 3-D estimates of contemporary deformation which should help separate contributions from tectonic and post-glacial mechanisms. This example illustrates the importance of improving the vertical resolution of GPS, integrating geologic and geodetic observations, and developing theoretical models to understand causative processes.

4. The rebound of the Earth's surface from glacial unloading at the longest wavelength can be inferred from temporal variations in the degree 2 gravity field as detected by monitoring variations in the precession of satellite orbits. The precision of such estimates can be improved with better tracking of satellites and by instrumenting satellites with GPS receivers.

Like the withdrawal of Quaternary glaciers, the drying-up of Quaternary lakes, and the associated lithospheric unloading, provides a means for estimating upper mantle viscosity. The Basin-Range intraplate regime represents a large 800-km wide area of active extension associated with dominant normal faulting. However, a more important signature of the extensional process is the relatively high topography of this region—that is, a 1200-meter central topographic high surrounded by large depressions on the province boundaries marked by the presence of large, but now desiccated, Quaternary lakes: Lake Lahanton on the west and Lake Bonneville on the east. The excess 250 m high of the central uplift has been attributed to mantle flow upwelling in the center of the Basin-Range, actively extending the lithosphere in a general east-west direction, opening at least 100% over its 20-million year history. Province-wide measurement by GPS of the topographic high compared to the surrounding lows can provide important constraints on processes such as mantle flow, viscosity and ultimately on how the Basin-Range works.

Furthermore, the upper mantle beneath Lake Bonneville reflects a recognized region of crustal rebound of more than 300 m in the past 10,000 years, attributed to a low-viscosity upper mantle of 1019 mPa. This value is well below the viscosity of the surrounding continental mantle of 1021 mPa, and is hypothesized to be reflective of a mobile mantle. GPS measurements of these large Quaternary lake shorelines can provide an additional dimension and greatly add to the detail of contemporary deformation of this region, which is postulated to materially effect the capability of nearby faults, such as the Wasatch fault.

4.5 Ice Dynamics and Sea Level

The world's oceans and the major ice sheets form a linked system which drive much of the world's climate change. The oceans are dominated by circulation systems which transport heat and material from the equators to the poles and back. This heat transport subsequently drives much of the local climatic systems. Ice sheets, as slow moving and isolated as they appear to be, have tremendous potential for modifying the ocean circulation system. Recent evidence indicates that collapsing ice sheets not only cause sea level rises but also rapid changes in climate. Thus deciphering the dynamics of the oceans and dynamics of major ice sheets both are critical targets in the ongoing effort to understand the record of past climate changes and predict future climate change.

4.5.1 Ice Dynamics

Over the last 20,000 years, the marine ice sheets of the Northern Hemisphere and Antarctica have been the largest contributors to sea level change. Evidence is building that rapid sea level rise results from an extreme non-linear response of these ice sheets to long-term climate change. Two approaches can be taken to understanding the link to sea level rise and the major ice sheets. One is to gauge the present mass balance of the remaining ice sheets of East and West Antarctica and Greenland, while the second is to understand the processes which control the rapid collapse of major ice sheets. Both these problems require the precise positioning available from GPS.

4.5.1.1 Mass Balance

The present mass balance estimates of the major ice sheets is based on limited poorly positioned data. These results to date are unsatisfactory. Changes in the surface provides insight into the total flux of material into and out of the ice sheet. Tracking these changes in surface elevation to better than 1 cm may be necessary to identify the changes.

The ideal approach would be to map the surface remotely or from aircraft. A number of space missions have attempted this—i.e., Geosat, Seasat, and ERS-1—but the results continue to be as ambiguous both due to the difficulty in recovering accurate results from steeply sloping regions, ambiguities in the orbits, and the lack of full coverage of the East and West Antarctic ice sheets. Future missions are targeted at this problem.

Aircraft are also capable of recovering accurate ice surface elevation over a wide region. Surface-based work provides the highest accuracy measurements, but continues to be plagued by uncertainties in location of the stations, as well as the difficulty of installing ground locations. It has been proposed that the mountain glaciers in temperate climates may be a significant contributor to short-term climate change. Monitoring the surface of the mountain glaciers to better than 1 cm may provide important insights into their contribution to the present rise in sea level.

A more direct determination of the mass balance of ice sheets can be made by taking advantage of the well-understood elastic response of the solid Earth to changes in surface loads. That is, to use the Earth as a spring balance to weigh the changes in ice sheet masses. For example, a continent-wide (~ 2100 km radius) uniform change in thickness of the Antarctic ice sheet sufficient to change sea level by 1 cm would lead to a vertical motion of the rock at the edge of the ice sheet of 4 mm and a horizontal displacement across the continent of 2 mm. For a given change in sea level (ice mass), the displacements scale inversely with the width of the ice sheet. Thus a uniform change in the thickness of the West Antarctic ice sheet (~ 700 km radius) sufficient to cause a 1 cm change in sea level would triple these displacements, giving elastic displacements comparable to the accompanying change in sea level.

A change in mass balance on the scale of an ice stream (~ 70 km) would lead to decimeter level elastic displacements for cm level changes in sea level. Since changes in sea level of meters are envisioned to accompany global change, the resulting deformation of the elastic Earth should be diagnostic of the change in ice sheet mass.

4.5.1.2 Ice Sheet Dynamics

To understand the entire ocean-ice sheet system it is important to examine how ice sheets collapse. Studies of both the climate record and the remaining ice sheets indicates that the collapse of an ice sheet may be a non-linear response to climate change. This non-linear response may be attributed to the bimodal dynamics now recognized for marine ice sheets.

One mode is represented by interior ice which is fixed to the bed and moves primarily by internal deformation with surface velocities of a few tens of meters per year. The “classic” parabolic ice sheet profile is indicative of this interior ice reservoir.

The second mode is characterized by ice gliding over its bed which is channeled into ice streams up to 100 kilometers in width and several hundred kilometers in length, with speeds of hundreds to thousands of meters per year. These ice streams, which have very low surface profiles, are the conduits that drain the interior ice reservoir.

Most of the potential sea level increase is locked within the interior ice reservoir. A migrating ice stream system may reduce the size of an interior ice reservoir at rates much faster than predicted by steady-state ice sheet models where the size of the reservoir changes only in response to changes in precipitation.

The end result of this migration is a rapid sea level rise. This migration of the interior-ice/ice-stream boundary, frequently called the onset of ice streaming, may be governed only by long-term climate change and the sub-glacial conditions which control ice streaming. In other words, rapid sea level rise caused by marine ice sheets may be largely independent of short-term changes in temperature and precipitation.

4.5.2 Sea Level: The Link Between Ice Dynamics and Tectonics

Mean global sea level rose at an average rate of 1.8 mm/year for the past 80 years. At this rate it will rise 2 cm in the next dozen years. This forecast based on 8 decades of data, is accurate to only 30%. If we are to forecast future sea level trends to, say, 20% for the next few decades, we should need to measure sea level to an accuracy of approximately 1 mm/year. This accuracy is almost an order of magnitude beyond what has been achieved in the past.

In measuring sea surface elevation directly we need to take account of the effects of thermal variations in the ocean that are an indirect consequence of global change, and which modify our interpretation of the significance of a sea level rise. The TOPEX mission will contribute substantially to our understanding of ocean dynamics, but with a 3 cm accuracy or better will contribute little to forecasting future trends in sea level *at yearly periods* unless the rate of rise increases by an order of magnitude.

The direct measurement of sea level at a continental coastal site often provides a noisy estimate of global sea level. Island sites are preferable. The precision of tide gauges is typically of the order of 1 mm but seasonal signals local to the tide gauge are generated by local wind stress, onshore currents, temperature and salinity variations. Some of these error signals perturb sea level in a random sense (e.g. residual errors in estimating local salinity or temperature). However, others may introduce systematic departures from sea level, as do, for example, long period fluctuations in onshore current direction which invite the development of trapped waves and onshore sea-surface slope.

In experiments designed to monitor differential tectonic vertical motions, tide gauges indicate that sea level can vary by up to 1 cm/year over distances less than 20 km even though long period energy may be coherent over many hundreds of km. This suggests that sub-cm residual errors in tide gauge measurements may be removed only by averaging a dense network.

The potential accuracy of the new VLBI/SLR global vertical datum is approximately 3 mm. Seven-mm vertical accuracy from a global network of continuously operating GPS receivers based on weekly averages has been reported. Recent developments in the application of radiometer corrections to GPS data suggest that GPS vertical repeatabilities of 2-3 mm may be achievable. Further work is needed to demonstrate whether these results are uncontaminated by systematic corrections, and if so, GPS measurements near tide gauges have the potential to provide an adequate vertical measure of tide gauge elevation.

It is envisaged that GPS can contribute in three ways to monitoring sea level: (1) links between VLBI sites (i.e. the international vertical datum) and coastal sites; (2) continuous measurements at selected tide gauges (a GPS vertical datum); and (3) measurements between shoreline and offshore buoys. The first two of these measurements would be applied to the GLOSS network (global sea level system), and a start on this has already been made.

In addition to the GLOSS sites, measurements to tide gauges on tectonically unstable coastlines yield both the tectonic signal and the sea level signal when they are related to the VLBI datum. Absolute-g and space geodesy deliver comparable vertical measurement precision. Combinations of absolute-g and space geodesy, with their similar error budgets (but different systematic sources of error) are likely to provide important tests of system accuracy.

4.6 Precise Mapping and Navigation in Oceanography

GPS technology can advance the study of the ocean dynamics problems by means analogous to those for ice dynamics. Unlike land based operations where locating point measurements is the dominant mode of operations, the ocean and ice issues are best addressed by remote sensing tools. These tools include buoys, aircraft, ships and satellites.

The crucial contribution of GPS is to accurately position these instruments, which then makes possible a wide variety of measurements, such as Doppler velocity measurements of the water column and precise measurements of the ocean or ice surface from an aircraft or satellite. The buoys must be positioned to 100 m, the aircraft to better than 1 m, the satellite to several centimeters and the ship to several meters.

Traditionally, oceanographers have relied upon point measurements of ocean currents using moored mechanical and electromagnetic current meters. However, during the past decade it has been possible to measure sea surface height to high accuracy with satellite-borne radar altimeters.

Because the large scale flow of ocean currents control sea level height, with contributions from essentially static variations in gravity in the underlying solid Earth, it has become common practice to infer currents globally and to repeat the measurements frequently. The importance of accurate positioning at sea has been well understood since the Renaissance. However, improvements in navigation have been largely incremental during the past several centuries. Precise positioning at sea has been extremely expensive, requiring specialized equipment and highly trained personnel. The advent of GPS has changed this picture completely; positioning with accuracies of 10 m is essentially instantaneous and inexpensive. Though time consuming, precise positioning to centimeter levels at sea is now possible.

4.6.1 Mapping of Global Sea Height

The TOPEX/Poseidon spacecraft is currently mapping sea surface height in coordination with the World Ocean Circulation Experiment (WOCE). The spacecraft is the only instrument being applied in WOCE to provide global coverage of ocean circulation. The spacecraft itself is tracked by a variety of methods including laser and ground-based techniques (SLR/DORIS) and the payload includes a GPS receiver. The baseline SLR/DORIS orbits are estimated to have an rms accuracy of 5–6 cm. The SLR/DORIS orbits are now limited by modeling errors that will be difficult to reduce further.

In contrast, the GPS-based orbits for TOPEX/Poseidon now have an accuracy approaching 2 cm, which represents an extraordinary increase in accuracy. Moreover, the accuracy of the GPS-based orbit solutions is much less sensitive to the accuracy of models of gravitational and non-gravitational forces on the satellite than the SLR/DORIS solutions and the GPS orbits have the smallest geographically correlated orbit errors. This feature makes the GPS-based orbit solutions uniquely suited for determining the absolute geostrophic circulation (the net flow through the full water column), a quantity that oceanographers have no other means for determining globally.

The GPS-based orbits for the TOPEX/Poseidon spacecraft have the potential to be improved to the 2 cm or better range in the radial direction. Any improvement in the accuracy of the orbits translates directly into much reduced uncertainty of the ocean circulation on all scales for both time variable and time average motions. Reduced uncertainty in estimates of the circulation in turn translates directly into improved model initialization and, therefore, smaller errors in forecasts of future climate states.

If 2 cm rms errors can be achieved, the orbit uncertainty will no longer be the dominant error source, as it is now over much of the Earth. Such accuracies could, for example, permit the computation of the flux divergences of heat to and from the atmosphere by the ocean at a level of accuracy approaching that required to infer directly a greenhouse warming.

4.6.2 Acoustic Doppler Current Profiling

Oceanographers have recently developed acoustic Doppler current profilers (ADCP) which are capable of measuring current profiles in the upper several hundred meters of ocean from moving ships. Such currents include the important western boundary currents such as the Gulf Stream. The principle of operation involves the measurement of the Doppler shift in acoustic energy back scattered by heterogeneities in the water column. This new tool permits the routine measurement of important shallow currents when the ship is underway between stations or accomplishing scientific tasks of an entirely unrelated nature.

GPS provides a reference frame for the measurement of shallow currents using the ADCP. The ship's heading must be known to high accuracy. Lack of knowledge of heading generates an enormous error in the inferred currents. Fortunately, the measurement of the attitude of a moving platform, including its heading, can be measured using several GPS antennae located around the ship using phase differences between broadcast signals. While such measurements on oceanographic ships is certainly not yet routine, GPS provides an elegant solution to this technical problem. The remaining unknown in the system is the ship's speed which, again, can be inferred by a judicious averaging of velocity determinations from GPS position, velocity, and time (PVT) measurements. The more accurate and frequent the PVT measurements, the more accurate the inferred shallow currents.

4.6.3 Ocean Warming

An international effort is underway to measure the temperature of the oceans and to determine if any secular change may be related directly to greenhouse warming. The idea is quite simple; the warmer the ocean, the faster the sound speed, and the shorter the acoustic travel time between a source and a receiver. Mesoscale variability, longer term variations such as El Niño, and seasonal variations lead to significant variations in temperature, but adequate averaging in time over large spatial scales (4–10 mm) can isolate the effects of warming.

An experiment recently conducted using a Navy-leased ship, the M/V Cory Chouest and a Navy source array to transmit coded sound successfully demonstrated the practicality of transmitting acoustic energy globally (Figure 20). The ship was positioned near Heard Island in the southern Indian Ocean and the signals were received along the east and west coasts of the U.S. as well as at other stations including an array at Ascension. The Gulf War had just begun and AS had been turned off to facilitate fixing in the battlefield. Figure 21 plots GPS determined position along a ray connecting to Ascension with the position integrated from the Doppler measurements at Ascension, 10,000 km away. The two positions agree extraordinarily well.

The object of the long-term measurement (Acoustic Thermometry of Ocean Climate, ATOC), however, is to fix the source and receiver and measure the travel times over a long period of time. In an associated experiment (GAMOT) the investigators plan to augment the permanent array with floating hydrophone buoys. The buoys will float freely through the world's oceans recording the transmitted signals every few hours. The position of the buoy is to be determined using GPS. Because the Precise Positioning Service

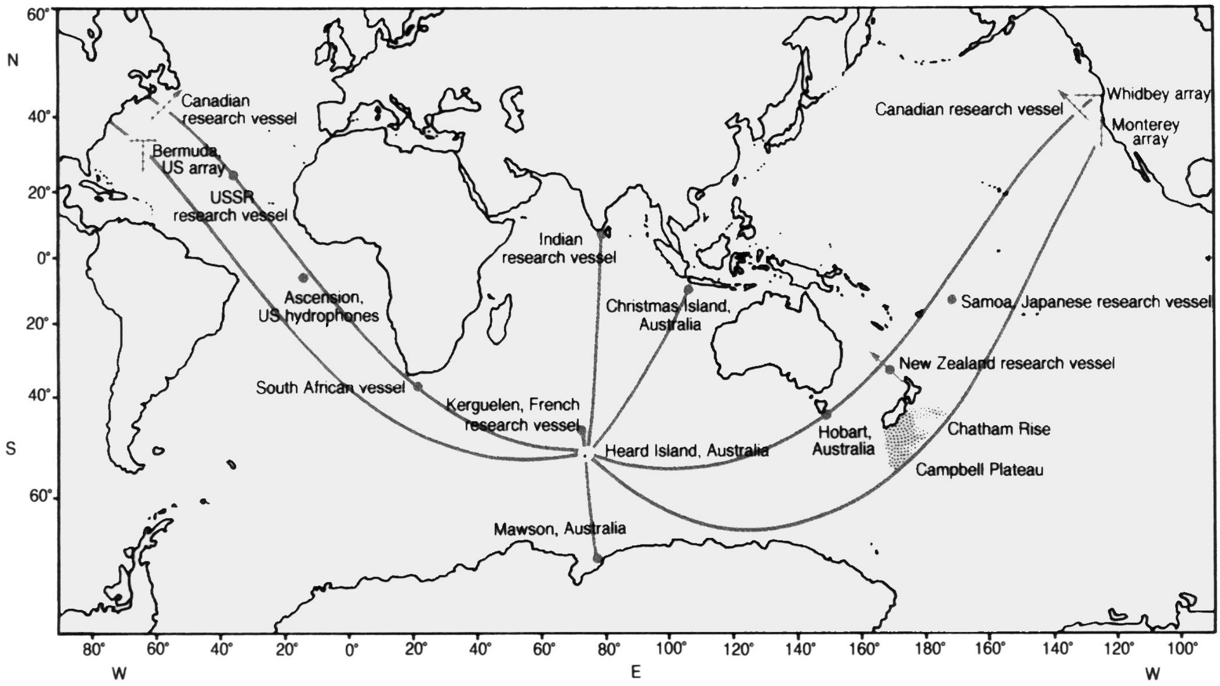

Figure 20. Paths taken by sound in the Heard Island feasibility test (Baggeroer, 1992).

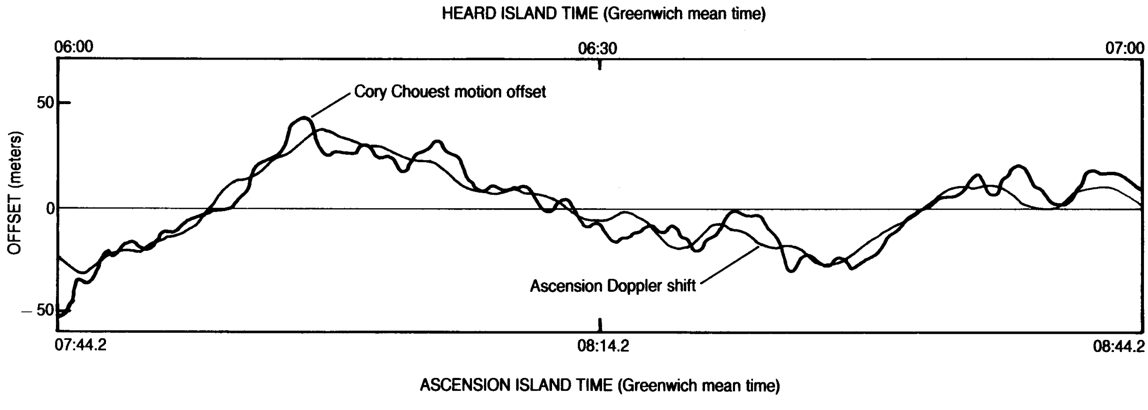

Figure 21. Observed and GPS phases (Baggeroer, 1992). The thick line shows the R/V Cory Chouest's departure from uniform motion along a course of 267° toward Ascension Island on 26 January 1991, as determined by GPS. The thin line is the detected phase of the signal at Ascension Island. The source-receiver separation is approximately 9000 km, yet the relative distance between them is tracked to within 10 m.

(PPS) cannot be installed on an unattended buoy, the on-board receiver will have access to only C/A code with an accuracy on the order of 100 m.

The investigators have determined that a 40 m accuracy is the minimum acceptable. In order to correct the positions, the buoy PVT data will be compressed and transmitted via the ARGOS (French) satellite to a classified Data Correction Facility (DCF) at Pennsylvania State University. The DCF will calculate corrected positions and these will subsequently be used for data analysis. The combination of these two acoustic systems, one of which relies entirely upon the GPS, should be capable of isolating a greenhouse warming signal in a decade's time.

4.6.4 Seafloor Mapping

Many important discoveries were made in the oceans during the 1960s and 1970s using painstaking mapping methods involving the integration of single profiles of magnetics and seafloor bathymetry data. Plate tectonics, among the greatest revolutions in 20th century science, followed directly from such efforts. During the past decade, fostered by earlier classified programs within he U.S. Navy, oceanographic research vessels have begun to map seafloor bathymetry over large swaths directly.

Prior to the advent of GPS, the mapping relied upon infrequent Transit satellite fixes and dead reckoning. Data collection efforts were generally followed by months of painstaking processing involving track readjustments and rubber sheet distortions of data to remove inconsistencies in the data collected. Repositioning a ship on the otherwise highly accurate topography to install a station, to repeat a depth measurement, or for reoccupation in general, was essentially impossible.

GPS has revolutionized mapping in the oceans. The resolution of the swath mapping systems, given the size of the acoustic footprint, is approximately 100 m, sometimes a bit better. In order to position these footprints on the seafloor in a regional or global reference frame, accuracies better than 100 m are needed (C/A code). Through efforts within the Navy, the installation of high-value GPS receivers on all Navy-owned ships in the oceanographic community is planned.

A trial with an installation on a single ship has been a great success. It is anticipated that when this experiment with Navy-owned ships (e.g., Melville, Knorr, and Thompson) proves successful, similar receivers will be deployed on other university-operated oceanographic ships (e.g., Ewing and Atlantis II) where accurate positioning is important.

4.6.5 Other Shipboard Applications

The measurement of gravity from a moving ship has been a challenge since the 1920s. The first measurements were made in submarines using a pendulum. Technology has advanced considerably and inertial tables are now used to maintain a standard gravimeter in a vertical position. However, one of the greatest sources of error in seaborne gravimetry involves corrections of ship's speed and heading, the *Eotvos Correction*. While crossover errors of 1–2 mgal are routine and probably indicative of measurement accuracy, the use of precise positioning at sea to determine velocity and heading could improve upon these standards considerably. Furthermore, GPS precise positioning allows the proper registration of the gravity data with the underlying topography.

One of primary economic drivers in the development of differential GPS techniques near continents was petroleum exploration involving 3-D migration of multichannel data. In this experiment, the ship, sources, and receiving array is navigated with an accuracy on the order of 2 m. The data is collected in this precise grid and then migrated downward in three dimensions to reveal extraordinary details in the subsurface structure. While oceanographers have used this 3-D technique in important surveys near continental margins and trenches near land, the lack of a similar reference frame in the open ocean precludes similar experiments on, say, mid-ocean ridges. Perhaps GPS with greatly improved orbits could be used to post-process position data to facilitate such experiments.

While centimeter-level positioning on land has become routine using GPS, the same is not true for the oceans. While long-term averaging is possible on land, the dynamics of a moving platform at sea preclude the use of these methods. However, differential GPS measurements to a float with attached acoustic transponders to fixed monuments on the seafloor, have been successfully used to obtain centimeter-level accuracy. Such seafloor geodetic measurements will allow, for the first time, the determination of ocean ridge spreading rates and the nature of the episodicity of spreading. A pilot experiment on the Juan de Fuca Ridge has been underway for several years. The technique depends entirely upon the use of differential GPS so that open ocean measurements appear to be precluded by current technology.

4.7 Atmospheric Sensing

Water, by virtue of its unique physical properties, plays an important role in atmospheric processes that act over a wide range of spatial and temporal scales. Water vapor is the most variable and inhomogeneous of the major constituents of the atmosphere. The distribution of water vapor is intimately coupled to the distribution of clouds and rainfall. Due to the large latent heats associated with the water's phase changes, the distribution of water vapor plays a critical role in the vertical stability of the atmosphere, and in the structure and evolution of storm systems.

The transport of water vapor and its latent heat by the general circulation of the atmosphere is an important component of the Earth's meridional energy balance. Water vapor contributes more than any other component of the atmosphere to the greenhouse effect. Conversely, the high albedo associated with clouds limits the solar radiation available to heat the Earth. In light of these considerations it is clear that atmospheric water vapor plays a crucial role in both weather and climate.

Atmospheric scientists have developed a variety of means to measure the vertical and horizontal distribution of water vapor. The radiosonde, a balloon-borne instrument that sends temperature, pressure, and humidity data to the ground by radio signal, is the cornerstone of the operational analysis and prediction system at the National Meteorological Center, and at similar operational weather forecast centers worldwide. Space-based water vapor radiometers (WVRs) are used to map integrated water vapor (IWV) over the oceans, and ground-based WVRs can provide similar data over land.

None of these systems provide adequate coverage of the water vapor distribution in both space and time. Accordingly there is considerable interest in the meteorological community in developing new approaches to the measurement of atmospheric water vapor that can complement the systems already in use. One of the most promising emerging technologies is GPS meteorology.

GPS meteorology refers to the use of the Global Positioning System for remote sensing of the atmosphere in general, and of water vapor in particular. Two major approaches to this goal have been identified.

1. Ground-based GPS meteorology. This technique uses ground-based networks of geodetic GPS receivers to measure integrated water vapor (IWV) or, equivalently, precipitable water (PW) overlying each receiver in the network on a time continuous basis, with a temporal resolution of 10–30 minutes. In most cases the ground-based approach will provide no direct information on the vertical distribution of water vapor.

2. Space-based GPS meteorology. GPS receivers based in low-Earth orbit (LEO) satellites would be used to measure GPS signal delays for sub-horizontal signal paths through Earth's atmosphere during atmospheric occultation events. These data would be used to estimate vertical refractivity profiles through the atmosphere. Given prior knowledge of atmospheric temperature the refractivity could be used to infer atmospheric humidity, or vice-versa. The spaced-based approach will provide relatively little information on the lateral variation of atmospheric conditions.

The ground-based and space-based concepts were developed independently. While the ground-based approach exploits techniques developed by GPS and VLBI geodesists, the space-based approach has it origins in the radio occultation technique developed by planetary astronomers to study the atmospheres of Mars, Venus, and the outer planets. The ground- and space-based approaches are complementary rather than competing techniques, and ideally both will be implemented as operational systems that will support improved weather predictions, better regional water vapor climatologies, and basic research into atmospheric storm systems and global climate change.

4.7.1 Ground-Based GPS Meteorology

An important task in the geodetic analysis of GPS or VLBI observations is estimating atmospheric propagation delays affecting the microwave signals recorded by a GPS or VLBI receiver. These delays are caused both by the ionosphere and the neutral atmosphere. Ionospheric delays are dispersive and are estimated by acquiring observations at two frequencies. The delay due to the neutral atmosphere can be partitioned into a hydrostatic delay and a wet delay. The hydrostatic delay can be predicted given accurate surface pressure measurements.

The possibility of using continuously operating geodetic GPS networks for remote sensing of atmospheric water vapor is based upon the development of "deterministic" least squares and Kalman filtering techniques in which the zenith wet delay (ZWD) affecting a GPS receiver is estimated from the observations recorded by that receiver. The physical basis for this measurement is the simultaneous observation of the signal delays at a given receiver from multiple radio sources which differ in their angles of elevation.

Using these techniques it is now possible to estimate, on a routine basis, the ZWD at each station in a continuously operating GPS network with less than 10 mm of long-term bias in equivalent excess path lengths, and less than 10 mm (rms) of random noise. Since the ZWD at a radio receiver is nearly proportional to the vertically integrated water vapor overlying the receiver, the possibility arises of using emerging networks of geodetic GPS receivers for remote sensing of atmospheric water vapor.

If the vertically integrated water vapor overlying a receiver is stated in terms of precipitable water (PW), that is as the length of an equivalent column of liquid water, then this quantity can be related to the ZWD at the receiver. Thus, in the following equation, ZWD is given in units of length, and the dimensionless constant of proportionality, K, is a function of various physical and chemical constants and a parameter, Tm, rather misleadingly known as the "mean temperature," which is a function of the vertical temperature and water vapor distribution.

$$PW = K \bullet ZWD \quad (1)$$

As a rule-of-thumb K ≈ 0.15, but its dependence on Tm, which changes with site, season and weather, causes the value of K to vary by as much as 10%.

Given access to surface temperature observations at a GPS receiver it is possible to predict K with a relative rms error of about 2%, and numerical weather models can used to predict K with a relative rms error of about 1%. The significance of these results is that when equation (1) is used to transform an estimate of ZWD into an estimate of PW, very little noise is introduced by the transformation. The error in the resulting PW estimate would derive almost entirely from the error in the earlier estimate of ZWD.

For GPS networks with apertures smaller than about 500 km both the determinstic (least squares) and Kalman filtering techniques used to estimate zenith delay are more sensitive to relative rather than absolute delays. This situation comes about because a GPS satellite observed using two or more receivers is viewed at almost identical elevation angles, causing the delay estimates to be highly correlated. The estimates of ZWD and hence PW derived from a small network are subject to an unknown bias at each epoch. The value of the bias is constant across the whole network (i.e. the bias varies in time but not in space).

There are several possible approaches to estimating this bias, a task known as "levering" (one levers the group of biased ZWD estimates up the ZWD axis until they all have the correct absolute value). One is to measure PW with a WVR at a single site, then solve for the bias in the GPS-determined ZWD and apply this correction across the network (this is known as "WVR levering"). Other approaches have been conceived but are not discussed here. The most attractive approach to eliminating the need for an independent measurement of PW somewhere within the network is to incorporate a few GPS stations that introduce baselines in excess of 500 km. Provided that sufficiently good orbit information is available it will then be possible to estimate absolute ZWD and therefore absolute PW using the GPS observations alone.

In a recent experiment, a GPS receiver and a WVR were operated at either end of a 50 km baseline in Colorado and it was demonstrated that the GPS-derived and WVR-derived time series for the difference in PW at either end of the baseline usually agreed to better than 1 mm.

A much larger demonstration experiment called GPS/STORM involved collecting GPS observations at five Wind Profiler sites in Oklahoma and Kansas, and at a site in Platteville, Colorado. A WVR at Platteville was used to lever the ZWD values so as to deliver absolute estimates of PW at the five remaining sites. At three of these sites PW was measured independently using WVRs. Thirty days of GPS- and WVR-derived estimates of PW were then compared (Figure 22). The difference between the WVR and GPS solutions for PW had an rms value of 1.6 mm. Part of this error derives from errors introduced by the WVRs.

Even at this early stage in its development ground-based GPS meteorology has already proved capable of delivering PW measurements of practical utility to meteorology.

4.7.2 Future Opportunities in Ground-Based GPS Meteorology

It should soon be possible to develop and demonstrate a nearly real-time GPS meteorology capability using a continuously operating GPS

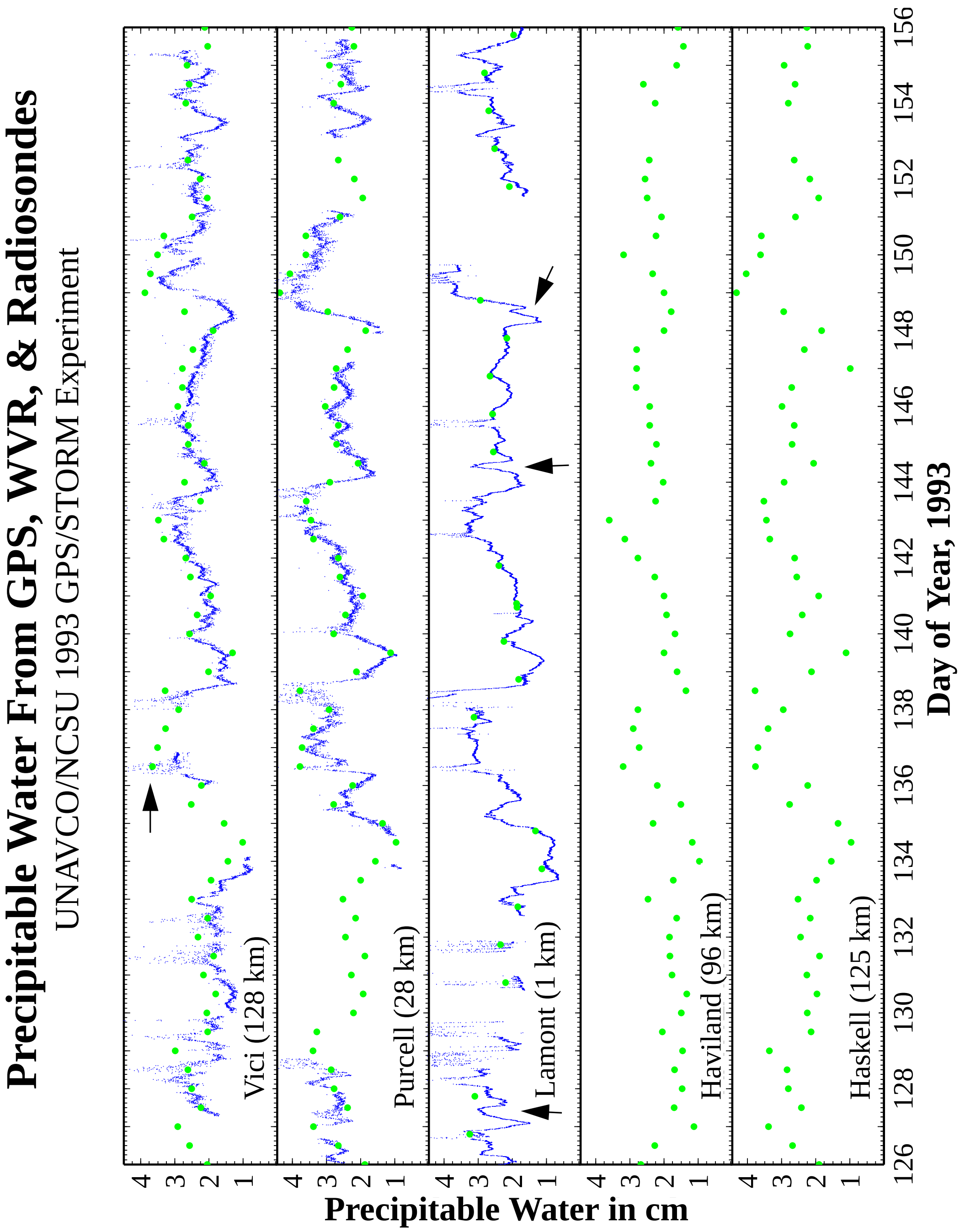

Figure 22. Precipitable water (PW) is shown for 30 days and five stations (Rocken et al., 1994). Each panel shows the station name and distance from nearest ROAB release site in the lower left corner. The small blue dots in the top three traces of each panel are WVR measurements, small red lines are 30-minute GPS estimates, and the isolated green points, separated by many hours, are determined from RAOBS. WVRs at VICI and Purcell were pointed at the GPS satellites and the measurements were scaled to zenith. The Lamont WVR observed in the zenith direction only, thus the reduced scatter of the WVR measurements. The arrows in the Lamont panel point at examples of faulty WVR data—in these cases caused by dew on the WVR window. Other WVR outliers in the top three panels are typically caused by rain.

network being constructed in the central U.S. under the auspices of the NOAA Wind Profiler group, and possibly using other testbeds in addition. Once a real-time capability has been demonstrated it is likely that the meteorology community will push ground-based GPS meteorology as a major operational initiative.

There are major potential synergies between this activity and GPS networks presently planned by a variety of government agencies. The FAA is planning to install continuously operating GPS receivers at more than 300 airports in the U.S. to support precision landings during the next few years. The Coast Guard is planning to install 30–50 continuously operating systems at coastal sites in order to support DGPS navigation. Many state geodetic surveys and highway departments are constructing or have already constructed small continuous GPS networks.

If these efforts could be coordinated, it should be possible to construct a national multipurpose GPS network capable of supporting a wide range of scientific, governmental, and commercial applications. GPS meteorology could act as the catalyst in forging such an alliance. The National Weather Service already has stations in most of the airports at which the FAA plans to install GPS, and has many years of experience in nearly real-time data gathering. The major problem in organizing a national GPS network will be political ones—it requires several disparate government agencies to work in a timely fashion towards a common goal.

4.7.3 Space-Based Meteorology with GPS

Preliminary studies indicate that accurate, high-resolution atmospheric soundings can be retrieved from the observations obtained when the radio path between a low Earth orbiting (LEO) GPS receiver and one GPS satellite traverses the Earth's atmosphere. When the path of the GPS signal begins to transect the mesopause at about 85 km altitude, it is sufficiently retarded that a detectable (1 mm) delay in the dual-frequency carrier phase observations is obtained by the LEO GPS receiver. As the signal path descends through successively more dense layers of the atmosphere, the delay increases to approximately 1 km at the Earth's surface.

Thus, the atmosphere creates a unique signal with over 6 orders of magnitude in dynamic range. A single LEO GPS receiver could observe more than 500 total occultations per day (~250 rising and ~250 setting), with roughly uniform global coverage.

The delay is caused primarily by increased bending as the ray path descends through increasingly dense layers of the atmosphere, and to a lessor degree by the reduction in propagation velocity. GPS can be used to measure the precise positions of the satellites involved, just as the system is used on Earth. In addition, the LEO receiver can be used to record precise phase measurements on the occulted GPS signals. Combined with the precise positions, these phase measurements provide a time series of "excess Doppler" (i.e., Doppler in excess of that explained by the motion of the spacecraft), which can be inverted to a refractivity profile of the atmosphere.

Measurements of this type could provide new data for at least two key global change variables: atmospheric temperature and moisture distribution. For dry air (typically, measurements above 7 km), the refractivity profile can be converted to a temperature profile with an accuracy of ~1° C up to an altitude of about 45 km. For regions with significant moisture in the atmosphere, the refractivity profile can be converted to a moisture profile with an accuracy of roughly 10% RH, provided ancillary temperature data, or a model of temperature is available.

An operational system that meets its full potential could significantly improve weather forecasts, particularly over ocean areas, where meteorological data is sparse today. A long record could provide valuable new climate data. Such a system could be implemented using a constellation of 50–100 very small (<20 kg/20 W) dedicated satellites. These satellites could be mass produced and launched 8–16 at a time on small, inexpensive launch vehicles. It is estimated that the average cost per operational satellite, delivered in orbit, would be less than $5 million in such a scenario.

To investigate the practical potential of the concept, UCAR/UNAVCO is developing a system to collect radio occultation data using a commercial spacecraft and a special GPS receiver. The project, known as GPS/MET, is being funded by NSF, FAA, and NOAA. Partners in the project include NCAR/MMM, Orbital Sciences Corporation, Allen Osborne Associates, the Jet Propulsion Laboratory, and the University of Arizona. Data will be collected and published on the Internet for approximately 6 months beginning shortly after launch.

4.7.4 Probing the Ionosphere

The non-neutral part of the Earth's atmosphere affects the GPS signals dispersively. Dual-frequency GPS receivers can therefore provide a direct measure of the integrated number of electrons between the receiver and the satellite and thus a direct measure of ionospheric activity. This very precise measurement of ionospheric activity can be used in ionospheric science.

Precise dual-frequency measurements by ground- and space-based GPS receivers will probe the ionosphere along many paths. Variations in signal phase will reveal ionospheric density waves caused by seismic, tsunami, massive explosions (as caused by nuclear tests), meteorological, and many other atmospheric and geophysical events. These data can be used to study the relationship between the source event and the atmospheric effect, and to trace the flow of energy within and across different Earth systems.

Measurement of total electron content along these paths will be assembled into high-resolution, 3-D electron distribution maps by computerized tomography to study irregular and transient mesoscale structures, such as the equatorial bubbles and the mid-latitude trough. Study of the ionosphere with GPS signals will lead to a better understanding of communication problems associated with ionospheric disturbances.

4.8 Instrument Arrays and Data Networks

UNAVCO scientists are interested in continuously operating GPS networks in a wide variety of contexts. Some new or emerging applications of GPS, especially GPS meteorology, actually require fixed and continuously operating networks in order to achieve useful results. Some of these applications will involve deploying fixed, continuously running networks for periods as short as a few months; others (for example water vapor climatology) will require very long-term deployments.

Other applications, like volcano monitoring, can be performed in a campaign mode but become far more powerful when implemented using permanent networks. Most crustal motion projects involving large numbers of stations in remote areas are likely to rely predominantly on field campaigns for the foreseeable future, on purely financial grounds, but nevertheless may benefit considerably by incorporating a small permanent subnetwork. Global tracking has much improved over the last few years, but even now there are some areas of the world (e.g. polar areas and the Pacific Ocean basin) where additional tracking stations would be very valuable.

The key concept for promoting continuously operating GPS stations is multipurpose justification. Another but related concept is building up these networks using multiple sources of funding. For example NOAA might be interested in funding permanent stations at some tide gauges in the Pacific. The rationale is only permanent tracking can average down vertical errors to the point that one can distinguish between absolute and relative sea level change. Meanwhile, DOE's ARM project might fund several other stations in the region for the purposes of water vapor climatology. The existence of these sites might enable a crustal motion researcher to write an NSF proposal to add a few more permanent stations nearby the DOE and NOAA sites, and end up with large network that could support crustal motion research. The crustal motion project might add barometers to its stations so that they could support water vapor studies. One of the tide gauge sites might send data out daily to SIO, JPL and CODE to support improved global tracking.

The point is that few applications can justify the construction of large numbers of continuously tracking GPS stations in a given region, but that such a network might come about by seeking multiple applications and multiple sources of funding and sharing the data. Each effort leverages the others! Small interdisciplinary groups of PIs can set up collaborations of this kind, but they will need to think about configuring each station so that it supports the broadest possible range of activity—even non-scientific activities such as DGPS navigation where local government support would be useful.

5 Accomplishments and Ideas

At the time of the workshop which formed the basis for this report, numerous individuals provided written summaries of their research based on the Global Positioning System. These summaries are reproduced here to provide a sample of the great variety of new GPS research programs spanning virtually the whole of the geosciences.

5.1 Subsurface Geodesy

Roger Bilham, *University of Colorado*

Several categories of geological process are not well monitored using surface geodesy. For example, the surface deformation fields of horizontal detachments are indistinguishable from buried vertical faults. Another complication can occur where several thrusts may be stacked and intermittently active. Another application where interpretation of surface geodesy is ambiguous occurs where several parallel faults are active within a plate boundary. An example is the widened velocity field found where the San Andreas, Calaveras, and Hayward faults overlap. It is not possible to distinguish the portion of the subsurface slip uniquely as a function of depth from the surface geodesy alone.

The inherent ambiguity in these measurements can be overcome by combining borehole metrology and GPS. Advances in borehole metrology permit horizontal deviations of a borehole to be measured to sub-mm accuracy. Random errors of inclinometer measurements grow as $k\sqrt{L}$ where L is the borehole length in km and k is a constant in the range of 0.5 to 1.4. Vertical measurements using fiber rods attached at different depths yield mm accuracy, and micron accuracy can be obtained using interferometric methods and optic fibers. A combination of vertical and horizontal measurements permit 3-D subsurface positions to 1.4 mm accuracy to depths of 2 km.

A corollary of the method is to use boreholes to provide exceptionally stable control points even in regions considered unsuited to precise GPS geodesy: hillslopes, permafrost, and sedimentary basins.

5.2 Measurement of Local Geoid Slope

Roger Bilham, *University of Colorado*

First-order spirit leveling delivers a relative elevation measurement accuracy of approximately 1 mm in 2 km. GPS over similar distances yields similar accuracies in relative ellipsoidal elevations. The difference in elevations measured by these two techniques provides a measure of the slope of a co-geoid at the local elevation of the Earth's surface. At sea-level, the measurement is of geoid slope.

A 2-km line of GPS and double-run leveling can be measured in a day by a three-person crew. Thus geoid slope data are relatively easy to acquire. The angular accuracy is in the order of 1 microradian, similar to quality measurements of the deviation of the vertical. Unlike deviation of the vertical measurements using stellar setting, GPS/leveling combined measurements yield a spatial densification of geoid undulations, and investigations of the vertical gradient of geoid slope.

Two applications are envisaged for geoid slope data: verification and spatial densification of geoid undulations, and investigations of the vertical gradient of geoid slope. The first application is important in regions where leveling lines are rare, for example, parts of the Himalaya. In these locations, spot verifications of geoid slope would be of great value, as would an investigation of geoid "granularity." The second application, useful in mountain ranges, is to measure the slope of co-geoids at different elevations. The gradient of the geoid slope provides an indication of gross mass distributions, hitherto accessible only to gravity measurements.

5.3 Precise Airborne Surface Altimetry Based on GPS Positioning

D.D. Blankenship, *Institute for Geophysics, University of Texas*

R.E. Bell and V.A. Childers, *Lamont-Doherty Earth Observatory*

J.M. Brozena, *Naval Research Laboratory*

Precise surface elevation measurements are crucial to understanding the dynamics and mass balance of major ice sheets as well as the form of vertical tectonics. As part of an interdisciplinary effort to understand the interaction of the West Antarctic ice sheet with the underlying lithosphere the CASERTZ project (Corridor Aerogeophysics of the Southern and Eastern Ross Transect Zone) has developed the capability to recover precise measurements of the ice surface. This capability is a component of a broad spectrum aerogeophysical platform which couples simultaneous airborne gravity, aeromagnetic, ice-penetrating radar, and laser ranging measurements with kinematic GPS positioning, UHF radio navigation, laser-gyro inertial navigation and high-resolution pressure altimetry. The program has focused on a 97,000 square kilometer region along the southern flank of the West Antarctic rift system which traverses critical boundaries both in the rift system and the ice sheet.

The CASERTZ aircraft includes a high-resolution surface imaging capability using a Holometrix laser altimeter. This laser altimeter has a ranging accuracy of 0.1 m, a footprint of about 0.9 m and is capable of up to 1,000 range observations per second. In general, an average of 64 ranges is recorded every 10 m along track. We have evaluated the quality of the ice surface measurements derived from the CASERTZ laser altimetry system including the corrections for aircraft attitude and full differential GPS positioning. The ice surface along coincident profiles flown in the same field season and approximately 70 m apart has a mean difference of 24 cm with an rms deviation of 35 cm. Preliminary results indicate that the full three-dimensional ice surface will have an absolute accuracy of approximately 0.5 m.

5.4 Airborne Geophysical Observations of Long Valley Caldera

C.R. Carrigan, *Lawrence Livermore National Laboratory*

J.B. Rundle, *University of Colorado*

The Long Valley Caldera is a 640 cubic kilometer basin formed from the collapse of the crust over a magma chamber that violently erupted its contents some 700,000 years before the present. Both seismic and geodetic data suggest that the chamber underlying the basin may currently be refilling with a fresh charge of magma. At the point of maximum uplift in the basin near Highway 395, the surface is rising at a rate of about 0.1 m per year. Because it is so active in terms of its seismicity and inflation, a number of detailed geodetic surveys have been carried out in this region in recent years. Thus, it represents an ideal location to employ a new, rapid surveying technique that can be validated against the results of earlier, but more standard surveys. By combining the elevation data from an ATLAS laser altimeter mounted beneath a T39 aircraft with the highly accurate airplane locations provided by two onboard commercial GPS receivers, extremely rapid surveys of topographic elevation can, in principle, be obtained over large areas. During September, 1993, such an aerial survey was conducted in a joint experiment with NASA, UC San Diego, the USGS and LLNL. The flight plan took the laser altimeter over the region of maximum uplift near Highway 395. It is hoped that accuracies in elevation of 5 cm can be ultimately achieved, besides validating a novel technique. The survey results will be used in constraining geodynamical models of an active volcanic region. Presently, Lawrence Livermore National Laboratory is using finite element models that can utilize this type of data to better understand the nature of magma injection beneath the caldera.

Possible future applications of this technique include rapid aerial survey of suspected underground nuclear test sites as part of an on-site inspection program intended to verify that the conditions of a nuclear treaty are being observed by its signators. Such a wide-area survey approach could be used to pre-select much smaller areas using topographic signatures associated with underground detonations. The candidate sites would then be subjected to detailed surface studies—e.g., seismic aftershock observations and detection of noble gas transport—by a ground team to determine both the occurrence and nature of a suspected underground event.

5.5 GPS Measurement of Relative Motion of the Cocos and Caribbean Plates and Strain Accumulation Across the Middle America Trench

Timothy H. Dixon, *University of Miami*

GPS measurements in 1988 and 1991 on Cocos Island (Cocos plate), San Andres Island (Caribbean plate), and Liberia (Caribbean plate, mainland Costa Rica) provide an estimate of relative motion between the Cocos and Caribbean plates. The data for Cocos and San Andres Islands, both located more than 400 km from the Middle America Trench, define a velocity that is equivalent within two standard errors (7 mm/yr rate, 5 degrees azimuth) to the NUVEL-l plate motion model. The data for Liberia, 120 km from the trench, define a velocity that is similar in azimuth but substantially different in rate from NUVEL-l. The discrepancy can be explained with a simple model of elastic strain accumulation with a subduction zone that is locked to a relatively shallow (20±5 km) depth.

5.6 Constraints on Deformation of the Resurgent Dome, Long Valley Caldera, California from Space Geodesy

Timothy H. Dixon, Frederic Farina, and Stefano Robaudo, *University of Miami*

Marcus Bursik, *State University of New York*

Susan Kornreich Wolf, Michael Heflin, and Frank Webb, *Jet Propulsion Laboratory*

Long Valley Caldera near Mammoth Lakes in east-central California has experienced increased levels of seismic activity and surface deformation associated with inflation of a shallow crustal magma chamber since 1978. Inflation is concentrated in the vicinity of a central resurgent dome. We use VLBI and SLR data from the western U.S. to constrain the regional tectonic setting of Long Valley, and VLBI and GPS between Owens Valley Radio Observatory (OVRO) and sites near (Mammoth) or on (CASA) the resurgent dome to investigate local volcanic strain.

OVRO has significant (10±0.5 mm/yr.) north-northwest motion with respect to stable North America, suggesting that OVRO, Mammoth, and CASA all lie west of the Eastern California Shear Zone. Vertical velocities defined by Mammoth VLBI data (1983–1986) and early CASA GPS data (1985–1988) have large uncertainties (1 errors are ±14.7 and ±5.3 mm/yr., respectively), but suggest no significant uplift relative to OVRO, consistent with other observations, suggesting this was a volcanically quiet period. In contrast, GPS data for CASA for the period 1988–1992 indicate uplift at of 24.4 mm/yr. ±2.8 mm/yr. and southward motion at 9.0±0.4 mm/yr. relative to OVRO, agreeing with the leveling and two-color laser geodimeter data within uncertainties. This motion is expected for a site on the south flank of an inflating dome. The GPS data are also consistent with the rate of deformation observed in geodimeter data after mid-1989, but are too sparse to define the strain event independently.

While available space geodetic data provide useful constraints on contemporary deformation in Long Valley, the number of sites is insufficient to define the regional tectonic or local volcanic strain fields, and the observation frequency of roughly once per year at CASA is too low to define the time-varying signal associated with volcanic deformation. The changing observation conditions characterizing these intermittent experiments have also contributed to systematic error. The advent of permanent GPS tracking networks, the declining costs of GPS receivers, and the need to improve accuracy and avoid temporal aliasing suggest that continuous monitoring of Long Valley with several GPS sites is both feasible and desirable.

5.7 GPS Monitoring of Crustal Strain in Southwest British Columbia with the Western Canada Deformation Array.

H. Dragert and X. Chen, *Geological Survey of Canada*

J. Kouba, *Geodetic Survey of Canada*

Contemporary crustal deformation has been monitored across the northern part of the Cascadia subduction zone since 1981. Measurements of accumulating horizontal strain have been obtained through repeated laser-ranging, GPS surveys, or both of five geodetic control networks established in various locations on Vancouver Island. Although shear-strain rates ranging from 0.05 to 0.23 ppm per year have been resolved, these estimates are spatially and temporally isolated since they lack a continuous common fiducial framework that has a precision commensurate with the internal survey precisions of the individual networks. To address this problem, the Geological Survey and the Geodetic Survey of Canada are cooperating in establishing a continuous automated network of four regional GPS tracking stations. A configuration of three Rogue receivers has now been operating continuously since August 1992. The fourth is scheduled to come on-line by October 1993. Dual-frequency pseudorange, and phase data, sampled at 30-second intervals, are collected daily by an automated process running on a Sun workstation. Quality checks are performed automatically by programs which generate statistical summaries and plots of the past day's data for each site. Baseline analysis is carried out using precise ephemerides provided by the Geodetic Survey of Canada. Results from the past year of data show a repeatability of 3 to 5 mm for baseline lengths of 300 and 600 km respectively. This order of precision will allow comprehensive monitoring of crustal strain on Canada's west coast.

5.8 GPS Used to Monitor Ground Movements at Augustine Volcano, Alaska

Daniel Dzurisin, *U.S. Geological Survey*

In June 1992, the USGS Volcano Hazards Program installed a permanent, radio-telemetered GPS network to monitor ground deformation associated with future eruptions of Augustine Volcano, Cook Inlet, Alaska. Augustine is the most active volcano in Cook Inlet, as exemplified by eruptions in 1935, 1963, 1976, and 1986. The island volcano has no permanent residents, but airborne ash from future eruptions could threaten air traffic and a landslide-generated sea wave could threaten the coastal city of Homer. The Augustine GPS project is a cooperative effort between the Cascades Volcano Observatory (Vancouver, Washington) and the Alaska Volcano Observatory (Anchorage/Fairbanks, Alaska).

The current USGS network consists of three Ashtech LD-XII dual-frequency, carrier-phase GPS receivers: one at the base of the volcano near the eastern shore of the island, one on the upper north flank, and one on the 1986 lava dome near the 1250 m summit. The near-shore station is held fixed for data processing; distances to the other stations are approximately 4.5 km and 4.8 km. Thirty-second epoch data are transmitted at 300 baud via VHF radio to an IBM compatible PC in Homer, 80 km away. A second PC in Homer is networked to the first, enabling users to download data via standard dial-up telephone lines.

Five 18-watt solar panels charging eight 12-volt 90 amp-hour batteries provide power at each field site. Because this is not sufficient power to operate the GPS receivers continuously (power consumption ≈ 20 watts), we control their duty cycle by issuing commands from the Cascades Volcano Observatory through the dial-in computer in Homer. These commands are radio-transmitted to the field sites, where a low-power controller receives and executes the commands to turn the receivers on and off. During the first year of operation, the receivers were turned on for 2-hour sessions once per week. Ice accumulation on solar panels and fiberglass antenna housings resulted in data loss for several months during the winter. Modifications to the stations were made in July 1993 in an attempt to mitigate this problem.

The Augustine GPS data are processed at the Cascades Volcano Observatory by an IBM compatible 486 PC using Ashtech software. Processing requires only minimal user-intervention. The time required to download and process 2 hours of data is approximately 45 minutes. Repeatability during the first year of operation (excluding data affected by antenna icing) was ±5 mm north, ±8 mm east, and ±35 mm up.

In a related effort, we are exploring the possibility of monitoring restless volcanoes using relatively inexpensive, single-frequency receivers such as the Motorola SixGun (approximate price = $3000). During preliminary tests, we processed SixGun data with Ashtech software and obtained several centimeter repeatability over baselines of 3 km and 8 km. Our goal is to design a field-ready, portable, telemetered station capable of ±1 cm horizontal repeatability and ±3 cm vertical repeatability over baselines up to 5 km, for a hardware cost of about $5000/station. Such instruments could be rapidly deployed during volcano emergencies together with portable seismic stations and electronic tiltmeters to provide real-time monitoring data in support of hazards assessments and eruption forecasts. Additional tests are planned for 1994.

5.9 Use of Airborne Kinematic GPS and Laser Altimetry for Determining Volume Changes of Mountain Glaciers

K. Echelmeyer, W. Harrison and C. Larsen,
University of Alaska

Mountain glaciers are sensitive indicators of climate change. In addition, it is believed that the mountain glaciers of Alaska and Canada play an important role in changes of sea level. The key parameter characterizing the effects of the glaciers on sea level and their response to a changing climate is glacier volume.

In the past, changes in glacier volume have been measured using repeat aerial photogrammetry or terrestrial surveying. Both of these methods were expensive and time consuming, and therefore existing data on volume changes of glaciers throughout the world is very limited. With the advent of compact laser systems and GPS positioning it has become possible to monitor changes in glaciers from small aircraft.

We have developed a lightweight, compact laser profiling system which can be mounted in a small single engine aircraft which is capable of flying at low speed over the winding surface of a mountain glacier. This system provides highly accurate elevation profiles of glaciers in mountainous terrain. Aircraft positioning at the decimeter level is provided by continuous kinematic GPS. Dual-frequency data is recorded for the entire flight, plus static initialization periods at the beginning and end of each flight. Post processing of the GPS data then gives the position of the aircraft relative to a fixed base station as a function of time. During the flight the laser range above the ice surface and the gyro-determined attitude (pointing angles) of the laser are measured continuously. Both of these data sets are given GPS time tags. All the data are then combined to give a profile of surface elevation for the glacier along a given transect. Comparison with previous profiles or with existing topographic maps then gives an estimate of volume change.

Results to date indicate that the profiles are accurate to 10 to 50 cm, depending on baseline length, ionospheric activity, altitude above the ice surface, and surface slope. This is an order of magnitude or more better than aerial photogrammetry. The major source of error, and the most time consuming aspect of the final profile, is the kinematic GPS data processing. Improvements in on-the-fly ambiguity resolution and receiver tracking abilities will lead to a reduction in both the overall error budget and the time involved in producing a final profile.

In order to repeat profiles in the future using the laser system, say on a yearly or 5-year basis, the aircraft must have the capability of real-time navigation which allows the given ground track to be repeated within ±5 to 10 meters. For such navigation we have utilized real-time differentially corrected GPS in which the correction factors are broadcast from a fixed base station over a radio modem. The airborne receiver then uses these correction factors to guide the pilot through a series of waypoints along the transect.

To date, several profiles have been done on glaciers in various climatic regions of Alaska. Preliminary results indicate that there has been substantial thinning of the measured glaciers in Arctic and interior Alaska, while the signature of volume change is variable in the coastal regions.

5.10 Use of GPS Technology in Glaciology

Keith Echelmeyer, *University of Alaska*

The study of the dynamics of ice sheets and mountain glaciers requires the determination of ice velocity, strain rates, thickening or thinning (mass balance), and ice thickness. Since 1989 we have been applying GPS surveying methods to these measurements. Examples of this work include:

l) Velocity and strain rate determination using static dual-frequency GPS positioning over relatively long baselines (50 to 500 km) in Greenland, Alaska, and Antarctica. Speeds we have determined range from 2 m/yr on the West Antarctic ice sheet, to 20 to 500 m/yr in Alaska (e.g., Ruth, West Fork, Black Rapids, Gulkana, and McCall glaciers) and West Antarctic ice streams (ice stream B), and up to 7000 m/yr on

Jakobshavns Isbrae in Greenland. The length of the baselines to fixed bedrock requires dual-frequency processing at the 1 to 10 ppm level.

2) Stop-and-go and continuous kinematic GPS measurement of surface elevation and mapping of terminus position. A GPS receiver is transported on foot, skis, or snow machine along the surface of a glacier or around the terminus. Comparison with existing topographic maps and optically surveyed transects then allows us to determine how glaciers in different regions have been changing over the past few decades. We have performed such studies on McCall Glacier in Arctic Alaska, Gulkana and Black Rapids glaciers in interior Alaska, and on glaciers flowing off of Mt. Wrangell, a south-central Alaskan volcano.

3) Differentially corrected GPS for positioning seismic and ice radar transects. In order to determine the depth of glaciers we employ both seismic and monopulse radar techniques. Positioning of the measurement systems and along-transect surface topography is needed to accurately determine ice depth, especially in a deep, narrow valley. We utilize post-processed differentially corrected GPS to obtain locations at the 2- to 5-meter level or stop-and-go kinematic to obtain positions at the centimeter level.

4) Control networks around glaciers for use in optical surveying. We routinely use static GPS to carry geodetic control into a glacier because high-order benchmarks do not usually exist in glaciated regions. One ppm accuracy is required.

5) Geoid determination in areas of high mountainous relief. Using concurrent GPS and optical surveying we have determined the height of the geoid in relation to the ellipsoid in Denali National Park. Accurate geoid information did not previously exist in this region, and departures from existing models were larger due to the large mass of Mt. McKinley which dominates the region.

5.11 Solar Hygrometer for GPS Field Use

Henry F. Fliegel, *The Aerospace Corporation*

Three methods are in common use by which to calibrate the effect of atmospheric water vapor delay on geodetic field measurements for GPS: (1) surface weather data models, based on temperature and relative humidity on the ground; (2) statistical modeling, in which the GPS data itself is used to provide an estimate of the delay as a stochastic variable, and (3) water vapor radiometry. These three methods are not suitable for all applications, since method (l) is not accurate, method (2) requires a long span of data under stable conditions, and method (3) is expensive. The solar hygrometer, which estimates total water vapor content in the line of sight from absorption bands in the visual or near infrared spectrum, is a logical candidate for a calibration instrument midway in cost and accuracy between methods (l) and (3). Until now, two strong objections to the solar hygrometer have been that (i) it must be pointed at the sun, and therefore cannot be used at night nor aimed toward a GPS satellite, and (ii) it cannot be used in cloudy weather. Two developments are worth exploring.

(I) There is a moderately strong water vapor absorption band at about 7000 Å, and also a complex of features in the blue visual spectrum (the so-called “rain bands”). Although these features are shallow and sloppy compared to the classic band at 9350 Å, they are accessible to standard photomultipliers, which have great sensitivity. Then a properly designed hygrometer can be aimed at stars by night and at the blue sky by day. Since the half height of the Rayleigh scattering component of the atmosphere is more than 5 kilometers, and that of water vapor 1 kilometer or less, the blue sky used with suitable corrections is almost as good a background for estimation of total water vapor content as the sun.

(II) A sufficiently sensitive instrument can be aimed at Polaris, which is now only about 0.7 degrees from the north celestial pole, and operated day and night. A diaphragm can screen out most of the skylight, and the rest can be filtered out. Using a clock drive, almost all background light can be excluded, since the diaphragm can be made very small, and since sky light 90 degrees from the sun is strongly polarized.

5.12 Non-Equilibrium Forces on GPS Satellites

Henry F. Fliegel, *The Aerospace Corporation*

Two anomalies in GPS space vehicle (SV) accelerations are manifested in the first few months of operation or during eclipse, especially during the first eclipse season after launch. (l) The initial acceleration away from the sun of an SV recently placed in orbit is about 6% higher than the final value, and then declines exponentially by a factor of e about every 18 weeks. It finally converges to within about 2% of the value predicted by the IERS adopted T20 model. (2) It then exhibits a residual acceleration history of about $\pm$2% around the mean value, roughly in phase with the eclipse seasons. I conjecture that the materials of the SV are outgassing. The integrated impulse for Block II SV's ranges from 20 to 75 kilogram meters/ second. Four contributors were examined as possible sources of outgassing: (A) the solar panels; (B) the SV body; (C) the apogee engine; and (D) the multilayered insulation (MLI) on the SV body. I conclude that water vapor from contributor D, the SV insulation, is the most likely primary source of the outgassing suspected to be responsible for the anomalous initial acceleration.

5.13 Sub-Daily Earth Rotation During Epoch'92 from GPS

A. P. Freedman, R. W. Ibanez-Meier, S. M. Lichten, and J. O. Dickey, *Jet Propulsion Laboratory*

Thomas Herring, *Massachusetts Institute of Technology*

Earth rotation data were obtained using GPS techniques during the Epoch'92 campaign in the summer of 1992. About 10 days of data were acquired during the last week of July and first week of August from 25 globally distributed stations and a constellation of 17 GPS satellites. These data were processed to estimate corrections to a nominal UT1 series at 30-minute intervals using several strategies. Earth orientation data during Epoch'92 were also obtained by several VLBI groups, and were processed together to yield VLBI estimates of UT1 at several time resolutions. One can see that the high-frequency behavior of both data sets is similar, although drifts between the two series of ~0.1 ms over 2–4 days are evident. The diurnal and semidiurnal variations of both series are largely attributable to changes in UT1 induced by non-equilibrium ocean tides, and are probably affected by diurnal atmospheric variations also. Tidally induced UT1 from both theoretical tide models and empirical (VLBI) measurements over many years were compared with the GPS and

VLBI series. In addition, estimates of atmospheric angular momentum (AAM) at 6-hour intervals generated by several meteorological centers have been compared with the geodetic data. These comparisons indicate that much of the GPS signal in the diurnal and semidiurnal bands can be attributed to known physical processes. At both longer and shorter periods, the GPS results may be affected by systematic effects such as unmodeled orbit or other errors.

5.14 Atmospheric Excitation of Rapid Polar Motions Measured by GPS

Richard S. Gross and Ulf J. Lindqwister, *Jet Propulsion Laboratory*

Daily polar motion values determined from observations taken during the GIG'91 GPS measurement campaign conducted during January 22, 1991 to February 13, 1991 are compared to twice-a-day polar motions induced by atmospheric angular momentum (AAM) excitation functions from the Japan Meteorological Agency (JMA). AAM-induced polar motion series are formed from just the wind term, just the pressure term (with and without assuming the inverted barometer approximation for the response of the oceans to surface atmospheric pressure changes), as well as from their sum in order to study the relative importance of these terms in exciting polar motions. It is found that the wind and pressure terms are of comparable importance to exciting the observed polar motions during this period, and that somewhat greater agreement with the observations are obtained when using the pressure term computed under the inverted barometer approximation. Treating the polar motion series as complex valued, correlations as high as 0.88 are obtained between the observed and AAM-induced series, and as much as 74% of the variance of the observed series can be explained by the AAM-induced series. It is therefore concluded that atmospheric wind and pressure fluctuations are largely responsible for the polar motions observed to have occurred during the GIG'91 measurement campaign.

5.15 Large Scale Combination of GPS and VLBI Data

Thomas Herring, *Massachusetts Institute of Technology*

In recent years large volumes of both GPS and VLBI data have been collected and analyzed. In our research we have been developing methods for combining these two data sets together to produce velocity fields and to study the non-steady state motions of the sites observed using these two systems. The formulation we use for these combinations is based on the Kalman filter. The basic inputs for these combinations are solutions from GPS and VLBI data analyses in which all of the site positions, satellite orbital elements, extragalatic radio source positions and a variety of tidal and Earth rotation parameters (currently only the VLBI analyses) are loosely constrained. These loose constrained solutions can be combined with additional constraints applied using the Kalman filter formulation.

The unique aspects of our implementation of these combination analyses are several fold. Within the GPS data analysis, we have the ability to "bias fix" using a constrained GPS solution and then to remove the constraints while maintaining the fixed biases. This procedure overcomes the problems of instabilities in the bias fixing algorithms if the solution is unconstrained when biases are fixed. Some other features of the combination system that we use include:

(1) The ability to combine all station information to produce position and velocity solutions while not heavily constraining any parameters in the analysis. In a post processing step, we are then able to constrain the adjustments so selected parameters are the same, to force specified parameters to their a priori values, or both. The former of these steps allows specification of survey ties between monuments without constraining the location of the ensemble of sites and to ensure that monuments in the same area move with the same velocity without constraining the value of the velocity. More importantly, as each constraint is applied we evaluate the change in χ^2 due to the imposition of the constraint and thus we are able to test the consistency between the parameter estimates and the constraints.

(2) As the Kalman filter is incremented with each new set of data, the change in χ^2 due to the addition of the new set is evaluated and can be checked for consistency between the current data set and the accumulated results from all previous data sets. The χ^2 increments are rigorously computed using the complete covariance matrix and thus fully account for correlations and possible rank deficiencies in the analysis. By selection of parameters to be estimated, and the methods used to eliminate unwanted parameters in the data sets, we can partition the increments in χ^2 between satellite orbits, regional stations, and global tracking stations, thus allowing the origin of large χ^2 increments to be isolated.

(3) The full solution and covariance matrix from an analysis can be saved and then later combined other data sets which themselves may be combinations. The advantage of this capability is that it reduces considerably the time required to combine all data set together. The typical fashion in which these features are used is to first combined the results from individual sessions within a GPS campaign lasting for several days to weeks. In this combination, satellite orbits may be integrated for several days and treated as either deterministic or stochastic parameters. Each of the field experiments are combined in this fashion, and then in later processing only the combined analyses are used. We often will then combine multi-year GPS data into a single analysis. In this case, station velocities will be estimated and often variations in Earth rotation parameters are also included. A similar combination can made for the VLBI data set and GPS data sets such as the global tracking network.

A resultant velocity field in California was obtained. This analysis uses 1,452 VLBl experiments with 738,470 group delay measurements included and 263 GPS days of data with 5,437,265 double difference ionospheric-delay free carrier-phase measurements. In all, the positions and velocities of 252 stations were estimated. One of the interesting features is that only the VLBI velocity field information was needed to obtain an accurate GPS velocity field in California. In the standard velocity analysis, no VLBI positional information was needed, and thus possible problems with tying between the VLBI and GPS reference points avoided.

5.16 Antarctic Search for Meteorites (ANSMET) Project

Ralph Harvey, Bill Cassidy, and John Schutt, *University of Pittsburgh*

ANSMET (the Antarctic Search for Meteorites) has conducted field research in Antarctica since 1976 on a yearly based. In general our work consists of detailed small-scale searches for meteorites on remote blue-ice areas of the East Antarctic ice sheet, which are recovered and returned to the U.S. for distribution to interested scientists throughout the world. One important facet of our research is our continuing efforts at understanding how meteorite concentrations develop in Antarctica. This involves detailed, fine scale mapping of the areas where the meteorites are found, and of longer term studies of regional ice movement and history. During the early years of the project, meteorite locations and surrounding bedrock and glacial features were surveyed using theodolite and EDM techniques. The slowness of these techniques and the harsh weather of Antarctica made these efforts laborious to set up and difficult to complete. In addition, it required that each meteorite be visited twice: once, when initially located, and again when surveyed in from an established base station.

During the past three seasons we have been experimenting with GPS as a way of replacing our antiquated methods for surveying meteorite locations. We are equipped with four Magellan 5000 handheld GPS receivers, which we use in differential mode from established base stations to survey meteorite locations. These instruments are limited to the use of carrier wave signal only, and cannot autonomously log all visible satellites. Thus our accuracy remains relatively limited (perhaps 10 meters at best), and we still must dedicate special days to surveying, when one field party member must remain in camp, logging a subset of the available satellites and relaying those satellite designations by radio to the remote units. To date, the use of GPS has improved our ability to survey meteorite locations by giving us all-weather capability and improving our range (to the limit of handheld radio communications). Our immediate goal for continued exploitation of GPS technology is to acquire (either on loan or by direct purchase) a low-end carrier phase GPS base station capable of autonomous satellite logging (something like an ASHTEC Ranger). Acquisition of such a unit would have a dramatic effect on our field work. With an autonomous data logger left running back in camp, we would have the ability to survey meteorite locations immediately when they are found and collected, eliminating a second trip to the meteorite and reducing the amount of time currently required for each meteorite in half. Ultimately we hope to use more sensitive base stations to directly measure small-scale movement of the meteorite icefields.

5.17 Landslide Hazard and GPS

M.E. Jackson, P. Bodin, and E. Nel, *University of Colorado*

W. Savage, *U.S. Geological Survey*

GPS has been used to map the horizontal velocity field of a rapidly moving earthflow to a greater spatial and temporal resolution than available with conventional survey methods. Our work suggests that the most active portion of the Slumgullion slide is moving at 1.5 cm/day and a portion of the slide assumed to be inactive may be moving at 3 mm/day.

The Slumgullion earthflow in the San Juan Mountains of southwestern Colorado, has been moving almost continuously for the last 300 years. The slide consists of an inner, active flow nestled within an inactive older slide. The old slide dammed the Lake Fork of the Gunnison River approximately 700 yrs b.p. resulting in the ponding of Lake San Cristobal. Traditional control surveys initiated over the last 20 years suggest that the upper portion of the active slide is moving at average velocities of ~0.5 cm/day, the middle or most active portion is moving at

1.6 cm/day, while the lower toe of the slide is moving at 0.4 cm/day. The Slumgullion landslide poses a significant risk to a small resort community along the shore of Lake San Cristobal because houses are built on old slide material and the town is directly downslope from the rapidly moving younger slide.

The GPS survey was initiated in June, 1993 to determine (1) if satellite geodesy could be used to rapidly map the slide velocity field, (2) the spatial and temporal distribution of velocity, and (3) if the inactive slide is moving relative to a stable benchmark well off the slide. A total of 7 GPS stations (baselines <5 km) were installed, 5 on the active slide, 1 on the inactive slide, and 1 on the stable portion of the slide headscarp. Station benchmarks consist of 1 m sections of capped steel pipe driven flush with the surface. These benchmarks probably have a long term stability of 3 cm which is negligible given the rapid velocities encountered on the slide. Relative coordinates for the network were carried from the Pietown fiducial tracking site in northern New Mexico to a precision of 3, 3.5, and 10 cm in the north, east, and up components, respectively. Each station was measured for at least two 4–6 hr sessions with most stations being occupied for four 4p6 hr sessions. The baseline between station SEI1 and GP01, located on the fastest moving portion of the active slide, was measured for nine consecutive 4–6 hour sessions.

The 1.5–1.2 cm/day velocities measured by GPS relative to a station on the inactive slide are similar to those estimated from traditional survey techniques and long-term creep studies but were acquired in a fraction of the time. Moreover, on short time scales the GPS data suggest the station velocities are constant. Although the spatial and temporal distribution of measurements are limited, it appears the inactive slide may be moving at ~2.5 mm/day relative to a stable station on the slide headscarp. If the older slide is indeed moving, the community built on slide material down valley may be at greater risk than was once thought.

5.18 Crustal Deformation at Convergent Plate Boundaries

James Kellogg, *University of South Carolina*

Global plate motion models describe the relative motion of the major tectonic plates averaged over the last few million years. These models are based primarily on data from divergent and transcurrent margins, as the orientations of trench slip vectors tend to be systematically biased whenever the plate convergence is oblique. The direction of slip in trench earthquakes tends to be between the direction of plate motion and the normal to the trench, suggesting active deformation within the overriding plate. The convergent boundary zone between the Nazca, Caribbean, and South American plates is particularly complex with active seismicity and deformation occurring over a broad area.

In January 1988, scientists from over 25 organizations in 13 countries established the CASA (Central and South America) network, the first major GPS network to measure crustal deformations in the northern Andes and the western Caribbean. The CASA 1988 experiment was the first civilian effort implementing a global GPS satellite tracking network. The repeatability of long baselines (400–1000 km) was improved by up to a factor of two on the horizontal vector baseline components by using tracking stations in the Pacific and Europe to supplement stations in North America. The results encouraged the establishment of a permanent civilian global tracking network in 1991.

Repeat measurements of the CASA network in 1990 and 1991 have confirmed global plate motion model predictions of rapid subduction at the middle America (76 mm/yr), Ecuador (71 mm/yr), and Columbia (54 mm/yr) trenches. However, intriguing differences occur between the measurements and the global models at the 95% confidence level. The northern Andean margin appears to be shearing northeastward relative to stable South America. Preliminary results also suggest Caribbean–North Andean convergence and an independent North Nazca oceanic plate. Perhaps the most surprising of all, the CASA results suggest the existence of a rigid Panama–Costa Rican Microplate that is moving northward relative to the stable Caribbean plate and colliding with the northern Andes. Planned additional occupations of the CASA GPS network will help resolve questions of active slip positioning at complex convergent margins.

5.19 The GPS Flight Experiment on Topex/ Poseidon

William G. Melbourne, *Jet Propulsion Laboratory*

TOPEX/Poseidon, a joint NASA/CNES mission to study ocean circulation by measurement of sea surface topography, was launched on 10 August 1992. After a decade of preparation, the GPS precise orbit determination (POD) experiment on TOPEX/ Poseidon is now yielding definite results. A wide range of orbit consistency and accuracy tests indicate that GPS is routinely providing satellite altitude with an rms accuracy of about 3 cm. Recent tests indicate better than 5 cm accuracy in the along-track and cross-track components.

Scientific Rationale. The principal limitation of past satellite altimetry missions to study ocean circulation has been the error in determining the geocentric radial position of the altimeter, which was provided by POD with tracking data from ground-based Doppler or laser ranging systems (SLR). The best SeaSat orbits, for example, had a radial accuracy of about 40 cm rms. Although that can suffice for regional and ocean variability studies, for global circulation a radial accuracy of 10 cm or better is needed. To reach 10 cm, the TOPEX/Poseidon Project raised its planned orbit altitude from 800 to 1336 km, reducing drag and gravity perturbations, and selected two operational precise tracking instruments—SLR and the CNES-sponsored DORIS Doppler system. It also supported extensive development of the ground segments of those tracking systems, and of spacecraft dynamic models. The project also chose to carry a GPS flight receiver as an experiment and to support the implementation of a global tracking network.

The GPS Tracking System. The GPS experiment on TOPEX/Poseidon was conceived in the early 1980s by a group at JPL seeking alternatives to conventional Doppler and SLR tracking. The motivation was simple: with the high precision of altimetry, ocean science would benefit from centimeter level orbit accuracies. But traditional POD techniques, which depend on precise models of satellite forces to recover the orbit, are limited by imperfections in the models, and these effects are exacerbated at lower altitudes. JPL turned to geometrical techniques, which are less sensitive to dynamical limitations, and soon realized that the enveloping coverage given by GPS offered an almost ideal solution. By the mid-1980s, a strategy known as reduced dynamic tracking emerged that sought to combine the best elements of dynamical and geometrical positioning to minimize overall orbit error. This technique has been applied to

TOPEX/Poseidon to yield the above cited POD performances.

The GPS tracking system consists of four segments: the GPS constellation, the flight receiver, a global network of GPS ground receivers, and a central monitor, control and processing facility. The POD strategy requires continuous tracking of the visible GPS satellites by ground and flight receivers. Data from all receivers are brought together and processed in a grand solution in which the TOPEX/Poseidon orbit, all GPS orbits, receiver and transmitter clock offsets, and other parameters are estimated. Simultaneous sampling at all receivers (which may be achieved by later interpolation) eliminates common errors, such as clock dithering from GPS selective availability. In the end, TOPEX/ Poseidon position and velocity are determined in a reference frame established by key sites in the global GPS tracking network, known to about 2 cm in the International Terrestrial Reference Frame. The accuracy of the GPS satellite ephemerides and terrestrial reference frame transformation parameters are also significantly improved over current results from the ground network by using TOPEX/ Poseidon flight data.

The Future. Innovations in data processing strategies and modeling that are planned for implementation over the next year should improve TOPEX/Poseidon POD accuracies by a factor of two or three. Although the GPS flight receiver on TOPEX/Poseidon has a few limitations (it only tracks six satellites concurrently and with a limited field of view), it is not unreasonable to expect that a GPS tracking system on future remote sensing platforms will provide 1 cm orbital accuracies. It is important to note that this accuracy is largely insensitive to orbital altitude over the range of 200 to 3000 km; thus, the orbital altitude of future altimetry missions may be drastically lowered to save mission costs without incurring POD penalties.

5.20 Use of GPS for Tethered Satellite Position Determination

Bjorn Johns and George W. Morgenthaler,
University of Colorado

In the late 1990s, tethered satellites may provide an effective tool for probing the Earth's upper atmosphere. Recently, Martin Marietta, Alenia, the Italian Space Agency (ASI), and NASA completed the design and fabrication of the first Tethered Satellite System (TSS-l). A proposed future Atmospheric Verification Mission (AVM) could follow TSS-l. While in an Earth orbit, the space shuttle would reel out the sub-satellite up to 120 km toward the Earth into a 90 km x 260 km elliptical orbit. In situ data collected at these altitudes would be very valuable in characterizing the lower thermosphere and also for determining sub-satellite aerothermodynamics.

GPS is considered to be the best system to determine the position of a tethered satellite with respect to the space shuttle. A relative positioning simulation was performed applying the position correction method to post-processed experiments, using only C/A code correlating receivers. The simulation provided simultaneous GPS data over a 118 km baseline, designed to simulate the space shuttle–tethered satellite separation. After performing differential corrections, the data was passed through a low-pass filter which suppresses the higher frequency components of the data. Since the tethered satellite dynamics are expected to be of a low frequency, higher frequency data is primarily from receiver noise.

The following 2σ errors were obtained:

	Un-Filtered	Filtered
Azimuth (deg)	0.00203	0.000463
Elevation (deg)	0.00577	0.00124
Range (m)	4.48	1.48

The above results were obtained using Trimble TANS C/A code correlating receivers. The data exceeds by a large margin the minimum accuracy requirements provided by Martin Marietta. Future work is proposed to determine the specific receiver type and hardware best suited for an actual space based application, and develop a real-time system to determine both position and velocity accuracies. Proper filtering schemes need to be evaluated, and the environmental effects on both the receiver and communication link operating at orbital velocities in the upper atmosphere must be addressed.

5.21 Status of GPS/Acoustic Measurements of Seafloor Strain Accumulation Across the Cascadia Subduction Zone

G. H. Purcell, Jr. and L. E. Young, *Jet Propulsion Laboratory*

F. N. Spiess, D E Boegeman and R. M. Lawhead, *Scripps Institution of Oceanography*

H. Dragert, M. Schmidt, G. Jewsbury, *Geological Survey of Canada*

M. Lisowski, *U. S. Geological Survey*

D. C. DeMets, *University of Wisconsin*

A long-term experiment was conducted using a hybrid GPS/acoustic system to determine strain rates across the Cascadia subduction zone. In May–June of 1991, long-lived acoustic transponders were installed on the sea floor on both sides of the Cascadia subduction zone. Measurements from a surface buoy, equipped with three GPS antennas and a precision acoustic transducer, located seafloor reference points in the coordinate frame of land-based GPS receivers. These measurements were repeated in September, 1993, and two additional transponders were set in place. Periodic measurements over five to ten years are expected to yield site velocities with sub-cm/year accuracy, sufficient to improve estimates of fault locking depth and net convergence velocity. Currently, determinations of these parameters rely on onshore geodetic measurements and plate motion models. This experiment also serves as an engineering test of the new GPS/acoustic system, and is expected to lead to substantial improvements in experiment design and analysis techniques.

5.22 GPS in Volcanology: Monitoring of Icelandic Volcanoes

Freysteinn Sigmundsson, *University of Iceland*

Volcanoes in Iceland deform at a rate of up to several cm per year during repose periods and crustal movements on the meter scale occur during eruptions. The deformation reflects pressure changes in the roots of the volcanoes that can be caused by a number of processes such as: magma movements, heating of magma from below, partial melting of country rock, and focusing of regional strain near magma chambers. Deformation monitoring provides important constraints on these and other processes occurring at volcanoes. The advantages of GPS over conventional geodetic techniques are of great importance in volcano monitoring. The simultaneous horizontal and vertical control from GPS is important, as both type of motion are prominent at volcanoes. Adverse weather conditions prevail at many volcanoes in Iceland and the almost weather independence of GPS facilitates measurements greatly. Rugged topography at volcanoes prevents line-of-sight between many control points that can be measured with GPS but not with a geodimeter. Regional GPS measurements have been conducted in Iceland since 1986 as an international collaborative project. In addition to providing important constraints on plate boundary deformation, these measurements have also provided information on deformation of volcanoes, including a recording of magma chamber deflation associated with the 1991 Hekla eruption in South Iceland. The small number of GPS points near the Hekla volcano limited the information about the deformation. Recognizing the need for dense local networks on volcanoes, the Nordic Volcanological Institute has now initiated a program to monitor dense GPS networks on volcanoes in Iceland. In 1993 five such networks have been measured, each consisting of 20–30 control points with a typical spacing of a few km. The networks will be partly or wholly remeasured periodically of intervals 1–2 years. Some goals of the measurements are to: (1) monitor inflation and deflation of magma chambers and to observe possible precursors to eruptions, (2) search for anomalies for Mogi point source displacement fields at volcanoes, e.g., displacement anomalies associated with caldera faults or extension across fissure swarms transecting volcanoes, and (3) be able to use GPS data to resolve possible simultaneous magma chamber deflation and dike injection associated with future eruptions in Iceland. The local networks are connected to the regional GPS network in Iceland, allowing the monitoring of the interplay between local (volcanic, seismic) and regional (plate boundary) deformation.

5.23 GPS Geodesy and Seismology

Bob Smalley, *Memphis State University*

An application of combined GPS and seismology is the study of short- to medium-term (days to years), post-seismic deformation. One area to investigate is any relationship between aftershock activity and a) co-seismic slip on the fault (obtained from seismic data and, if it exists, geodetic, especially GPS data) or b) postseismic deformation in the near field (principally from GPS geodetic data). A great earthquake on a strike slip fault (length of rupture zone is typically much larger than width) where slip information is available from surface rupture and seismology would provide the simplest and most well-constrained “experiment” of this type.

As modern VBB seismometer response (100–300 seconds) and GPS response, the time necessary to obtain mm accuracy over relatively short baselines (now at 300-600 seconds) converge, one can combine a VBB seismometer with a GPS receiver, resulting in an instrument for installation in the near field with an effective frequency response of fractions of a second to years, at least in the horizontal. A combined network of seismometer-GPS instruments could obtain long records of spatially dense post-seismic deformation. Practically, development of a formal relationship with the IRIS program to combine GPS and seismic aftershock monitoring efforts would be beneficial to both groups, both scientifically and logistically (for example, the PASSCAL program is presently acquiring GPS receivers to provide a time base at each site).

Two applications that would benefit from real-time continuous deformation monitoring are volcanology, specifically assisting in prediction of eruptions based on the active deformation immediately preceding an eruption, and real-time earthquake warning systems. Both of these applications would depend on a new form of real-time differential that would provide the positions of all the receivers in the network in real time. This real-time differential operation would operate in a manner similar to a real-time seismic network in that the GPS data would be collected in a central location and processed sufficiently rapidly to be useful for real-time response. This depends on certain components beyond what is usually meant by real-time differential. First it will require the use of phase-plus-code receivers and a high-quality, inexpensive communication method to collect the pseudo-range and phase data in real time at a central location where network solutions can be automatically processed rapidly enough that they are useful for the short-term prediction. The technical question is: How fast could one unequivocally determine that a movement of x cm has occurred on a fault, where x is a threshold for declaring an event has occurred. For this to work, we would have to be able to detect a position change of say 20 cm for a magnitude 6.5 event within one or two seconds. Larger events would produce larger slips, but the time for detection, determined by the time for the seismic waves to arrive at the threatened population center, would remain the same. Incorporation of such a GPS component into the early warning seismic networks being built in several places (SCEC, Japan, and Taiwan) would add significant robustness to the event declaration process. This technology could also be applied to the study of deformation of volcanoes before eruptions, landslides, slumps, glacier surges, and other geologic phenomena where there is motion on the order of mm to m per day. The volcano application is interesting because the surface deformation can be used to estimate that rate at which magma is moving within a volcano. Combining this data with seismic data, which can be used to delimit the magma chamber, one can obtain a better understanding of the plumbing of volcanoes. These applications depend on a significant decrease in the price of GPS receivers. As GPS technology enters the consumer market, prices should fall significantly, making networks of large numbers of continuously operating receivers possible.

5.24 Microplate Versus Continuum Descriptions of Active Tectonic Deformation

Wayne Thatcher, *U.S. Geological Survey*

Whether deformation on continents is more accurately described by the motions of a few small rigid plates or by quasi-continuous flow has important implications for lithospheric dynamics, fault mechanics, and earthquake hazard assessment. Actively deforming regions of the western U.S., central Asia, Japan, and New Zealand show features that agree for both styles of movement, but new observations are necessary to determine which is most appropriate.

Geologic, geodetic, seismic and paleomagnetic measurements tend to sample complementary aspects of the deformation field, so an integrated observation program can utilize the strengths of each method and overcome their separate spatial or temporal biases. Provided the total relative motion across each region is known and the distribution of active faults is well mapped, determination of fault slip rates can provide potentially decisive constraints.

Reconnaissance geological studies supply useful estimates but precise values depend upon detailed intensive investigation of individual sites. Geodetic survey measurements can determine the spatial pattern of contemporary movements and extract slip rate information, but the sometimes elusive effects of cyclic elastic strain buildup and relief must be accounted for in relating current movements to the long-term deformation pattern. Earthquake catalogues can be applied to determine seismic strain rates and relative velocities, but must be averaged over large regions and are usually limited by the inadequate duration of historical or instrumental seismicity catalogues. Paleomagnetic determinations of vertical axis rotations provide estimates of block rotation rates, but are often locally variable and averaged over many Ma.

Which of the two descriptions of continental tectonics is more nearly correct depends on the local rheological stratification of the lithosphere, especially the strength and thickness of the elastic crust relative to the ductile lithosphere, and dynamical models can provide contrasting forecasts of observable features with testable consequences. Within a given region, earthquake hazard assessment methodology should differ considerably depending on whether deformation is concentrated on a few major faults or distributed widely on many equally important structures.

5.25 GPS Detects Vertical Surface Displacements Caused by Atmospheric Pressure Loading

Tonie vanDam, *NASA/Goddard Space Flight Center*

Geoffrey Blewitt and Michael B. Heflin, *Jet Propulsion Laboratory*

Tide gauge measurements only give sea-level variations relative to the crust, whereas the crust itself may be deforming vertically due to various factors. If vertical crustal deformation is ignored, then erroneous conclusions may be drawn with regard to the causes and predictions of global sea-level change. However, if tide gauge measurements were sufficiently well tied to a stable Earth-centered reference frame using space geodetic techniques, sea-level change would be observed in an absolute sense. We demonstrate that GPS is an excellent candidate for addressing the geodetic aspects of global sea-level studies by looking at a physical phenomenon that should have a detectable and calculable effect on station heights. Temporal variations on the geographic distribution of atmospheric surface pressure deforms the surface of the Earth at the several millimeter level. Starting with daily no-fiducial solutions of the global GPS network, we show a new method of deriving a time series of individual station heights (an improvement over the more usual geodetic baseline analysis). Atmospheric loading is modeled using Farrell's Greens Functions, and using pressure values from the NCAR database on 2.5 grid. A sample plot taken from Yellowknife, Canada, shows vertical displacement where both the modeled and GPS-estimated station heights are smoothed using a seven-day sliding window. Out of the seven stations investigated so far, six have decreased rms height distribution after calibrating for modeled atmospheric height loading. One of the questions currently under investigation is how to model the height variations of coastal sites (which are important for tide-gauge measurements). For coastal sites, the crustal response is a function of the extent of the inverted barometer effect, in which the ocean tends to act as a high-pass filter (t = several days) in transmitting atmospheric pressure to the crust.

5.26 Ionospheric Monitoring Using GPS

Anonymous, *Universitat Hannover*

GPS satellites provide signals on two frequencies in order to enable the user to correct for signal delays due to ionospheric refraction. The difference in propagation time between the L1 and L2 GPS signal's code or phase contains information on the electron content integrated along the signal path. This information cannot only be used to observe the total ionospheric electron content, but also to detect and study ionospheric disturbances—e.g., phase scintillations caused by small-scale irregularities in the electron content of the ionosphere. These small-scale irregularities may have severe effects on radio propagation. Precise GPS applications are affected in such a way that the continuous satellite tracking is frequently interrupted. The resulting carrier phase cycle slips need to be fixed in the post-processing. Under disturbed conditions, each fixing of a cycle slip requires an increased effort due to the present irregularities. Therefore, ionospheric scintillation should be avoided for precise GPS applications. In order to be able to predict and avoid scintillation occurrence, detailed observation and long-term studies have to be performed on small-scale irregularities in the ionosphere. Here, GPS plays an important role. Dual-frequency GPS phase measurements allow a detailed description of the occurrence of phase scintillation. At the Institut fur Erdmessung (Institute of Geodesy) of the Universitat Hannover in Hannover, Germany, we have developed algorithms which enable us to detect phase scintillations in GPS phase data.

5.27 Atmospheric Noise in Airborne Gravimetry

Jim Johnson, Christian Rocken, Fred Solheim, Teresa Van Hove, and Randolph Ware, *University Navstar Consortium*

DGPS measurements are being widely used in airborne gravimetry to correct for aircraft vertical acceleration errors. Accurate airborne gravimetry has scientific as well as mineral and petroleum exploration applications. However, variations in GPS signal delay resulting from atmospheric water vapor, or wet delay, introduces apparent accelerations that limit the accuracy of airborne gravimetry. In order to evaluate GPS wet delay error, we observed wet delay using a water vapor radiometer (WVR) and compared apparent vertical accelerations resulting from GPS wet delay to GPS multipath and receiver noise.

We operated Trimble 4000 SSE 8-channel dual-frequency C/A and P-code receivers at both ends of a 10-meter baseline on the roof of a laboratory in Boulder, Colorado. Data were recorded at 1-second intervals. Each GPS antenna was mounted in a dished, l-meter diameter slab of microwave absorber, 0.5-meter thick. The absorber reduced observed carrier multipath amplitude by a factor of two. For GPS data analysis we used the Kinematic and Rapid Static Software (KARS) developed by G. L. Mader at the National Geodetic Survey. One-second vertical GPS solutions were calculated. Fifty-second filter solutions and apparent vertical accelerations calculated as the second time derivative of the filtered solutions were also obtained. The apparent vertical acceleration resulting from GPS multipath and receiver noise is 1.5 mgal rms. Multipath clearly dominates. We anticipate that the multipath signal can be further reduced by a factor of three or more through the use of choke ring antennas, internal suppression in the receiver, or through mapping and subsequent removal in processing.

We measured zenith wet delay with a Radiometrics WVR (manufactured by Radiometrics Inc., Boulder, CO). The WVR observed sky brightness temperatures at 23.8 and 31.4 GHz and converted them into wet delay. The WVR is calibrated using an ambient blackbody target, a noise diode, and a tipping curve. The sampling interval was one minute. Wind speed during the WVR observations was typically several m/sec. In order to approximate observations from a fixed-wing aircraft, we compressed the time scale by a factor of 24. Assuming a wind speed of 2 m/sec at the WVR sites this approximates an airspeed of 100 mph. Fifty-second filter solutions and apparent vertical accelerations calculated as the second time derivative of the filtered solutions were obtained. The apparent vertical acceleration resulting from variations in WVR-measured GPS wet delay is 0.5 mgal rms.

The climate in Colorado is relatively dry, with a typical zenith wet delay of 5 to 15 cm. In more humid regions zenith wet delay may be as large as 40 cm, and the resulting apparent vertical accelerations resulting from wet delay variability may be larger than the 0.5 mgal seen in Colorado. If the GPS multipath noise is significantly reduced, GPS wet delay will become the dominant error source. To correct for GPS wet delay, WVRs could be operated at the GPS ground station and on the airborne platform. In order to avoid errors resulting from changes in WVR observation angle aboard the aircraft, attitude correction would be required. With a combination of multipath reduction and wet delay correction, fixed-wing airborne gravimetry may be able to achieve 1 mgal resolution over distances of 1 km. This capability would be valuable for scientific research applications, and also for rapid, cost-effective exploration for minerals and petroleum.

5.28 Improved GPS Vertical Surveying

Chris Alber, Jim Johnson, Christian Rocken, Fred Solheim, Teresa Van Hove, and Randolph Ware, *University Navstar Consortium*

GPS signal delay caused by atmospheric water vapor, or wet delay, is a major source of error in high-accuracy vertical GPS surveying. Scientists at UNAVCO have been working to improve vertical GPS surveying accuracy. This work has been supported by grants from the National Science Foundation and the U.S. Geological Survey. UNAVCO scientists recently reported results from a GPS survey using water vapor radiometers (WVRs) pointed toward GPS satellites. The WVRs measure integrated water vapor which can be converted to wet delay for correction of GPS observations. Agreement of wet delays measured by two WVRs separated by 30 m is 3 mm rms, indicating the ability to correct for GPS wet delay at this level of accuracy. The tripod-mounted WVRs were designed for use in GPS surveying, and were loaned by Radiometrics, Inc., of Boulder, Colorado. GPS receivers and WVRs collected data at both ends of a 50-km baseline from Boulder to Platteville, Colorado. Vertical repeatability was 2.6 mm with pointed WVR corrections. Precision was degraded by a factor of two using Kalman filter or least squares methods commonly used to correct for wet delay. The pointed WVR results are more than a factor of three better than previous results. and a factor of two better than Kalman or least squares results. Improved vertical GPS surveying has applications in geodesy, earthquake studies, volcanology, sea level measurements, airborne and ground-based gravimetry, atmospheric sensing, and GPS orbit determination.

5.29 Sensing the Atmosphere with an Orbiting GPS Receiver

Mike Exner, Christian Rocken, Bill Schreiner, Fred Solheim, Chuck Spaur, and Randolph Ware, *University Navstar Consortium*

Mikhail Gorbunov and Sergei Sokolovsky, *Institute of Atmospheric Physics (Russia)*

Ken Hardy, *Lockheed*

Ben Herman, *University of Arizona*

Tom Meehan and Bill Melbourne, *Jet Propulsion Laboratory*

The National Science Foundation, the National Oceanic and Atmospheric Administration, and the Federal Aviation Administration are jointly sponsoring the $3 million proof-of concept GPS/MET program. It is being conducted by scientists at the University Corporation for Atmospheric Research (UCAR), UNAVCO, the National Center for Atmospheric Research (NCAR), JPL, and the University of Arizona. The goal of the program is to demonstrate active limb sounding of the atmosphere by an orbiting GPS receiver. The private sector is also participating in GPS/MET. Orbital Sciences Corporation is providing launch and spacecraft services under its innovative “data sale” contractual agreement with UCAR. Allen Osborne Associates, Inc. is supporting development of special receiver equipment needed for GPS sounding.

Phase shifts in GPS signals transecting the atmosphere will be detected by the orbiting GPS receiver. These data will be converted into vertical refractivity, temperature, and humidity profiles. One-km vertical resolution from 50 km to the surface, and sub-Kelvin temperature accuracy in the lower stratosphere are expected. The GPS/MET data set will be made available for weather, climate, and other research. Currently, weather forecasting relies heavily on radiosonde data obtained from 0:00 and 12:00 Z launches from 600 sites. Most of the sonde data are collected over land in the northern hemisphere. A single orbiting GPS receiver can observe 600 longitudinally distributed soundings per day (latitudinal distribution depends on orbit inclination). Most of the GPS soundings will be obtained over oceans where sonde data are sparse. Improved weather forecasts over oceans may have value for commercial aviation.

5.30 GPS Sensing of Atmospheric Water Vapor

Chris Alber, Jim Johnson, Christian Rocken, Teresa Van Hove, Fred Solheim, and Randolph Ware, *University Navstar Consortium*

GPS signals are delayed by atmospheric water vapor. This *wet delay* can be measured using GPS receivers and analysis software developed for high accuracy geodetic surveying. Wet delay converts easily into perceptible water vapor (PWV). More widespread PWV data could be used to improve precipitation forecasts. Currently, weather forecasts are based on radiosonde data collected twice daily from 600 sites worldwide. Soon, GPS-sensed PWV measured by permanent GPS arrays may be used to improve weather forecasts.

GPS sensing of PWV was recently reported by scientists at UNAVCO in Boulder, Colorado. UNAVCO is a national facility that assists university investigators using GPS technology for geosciences research. UNAVCO scientists were working to improve the vertical accuracy of GPS high-accuracy geodetic surveying.

They found that half-hour GPS and water vapor radiometer (WVR)-sensed PWV agreed to better than 1 mm for several weeks of observations. Portable high-accuracy WVRs were provided for this experiment by Radiometrics, Inc., Boulder, Colorado.

Scientists from UNAVCO and North Carolina State University are exploring the use of GPS technology in weather forecasting. In June 1993 they gathered GPS and WVR data from NOAA Wind Profiler sites and a Department of Energy Atmospheric Radiation Monitoring (ARM) site in Oklahoma and from sites in Colorado. Improvement in weather forecasting using GPS-sensed PWV from these sites will be explored. Scientists from NOAA's Forecast Systems Laboratory in Boulder, Colorado, plan to collect GPS-sensed PWV data and evaluate its use for weather forecasting. They will occupy Wind Profiler and ARM sites in Kansas and Oklahoma. UNAVCO scientists have agreed to cooperate during the implementation and help analyze the GPS data and convert it into PWV.

Large numbers of high-accuracy GPS receivers are now in continuous operation worldwide for geodesy, surveying, orbit determination, and other applications. Data from most of these sites could be accessed in near real time via the Internet or telephone. This presents a new, cost-effective opportunity to improve precipitation forecasts using GPS sensing of water vapor.

5.31 GPS in Antarctica

Ian Whillans, *Ohio State University*

The stop-and-go GPS technique was used to determine horizontal strains and relative vertical velocities of markers in the West Antarctic ice sheet with a precision and scope never achieved before. The strain rates were mathematically inverted into stresses and used in a force budget analysis to describe the stresses acting at depth, the objective being to understand the flow of the giant anomalous ice streams. The vertical velocities were used to demonstrate that most of the flow forms standing waves, presumably associated with basal disturbances. Other surface features are migrating against glacier flow, an astonishing and unexplained result.

GPS is also being used to determine the rate of thickening or thinning of selected sites on the Antarctic ice sheets. Special considerations must be taken to allow for snow compaction and ordinary glacier motion. The success of the method relies on both the long-distance capability and precision of GPS. The results will be "fiducial" sites for the calibration and interpretation of repeat satellite or aircraft radar or laser altimetry.

In the past ice velocities at remote sites were determined by repeat Doppler satellite tracking. A TRANSIT receiver would track for 24 hours at each site in each of two years. This entailed 2 aircraft visits each year to deploy and recover the receiver. Precision positions could not be determined after the field season ended. Now we have cut field costs to less than half. Sufficient data are acquired with 20 minutes of tracking, while the aircraft waits. Moreover, relative positions can be calculated at the tent camp later that day, and problems identified while there is still an opportunity to repeat the work.

The advent of low-noise receivers and full L1 and L2 capability will enable important new projects to be undertaken at reasonable cost. For example: (1) Quick determination of the point mass-balance of the ice sheets. It will enable the contribution of the current ice sheets to the present-day rise in sea level to be reliably assessed. (2) Determination of the crustal rebound rate toward isostasy to assess the size of the former ice sheets. This will bear on the role of various ice sheets and the cause of the great glaciations. (3) Airborne repeat GPS controlled laser altimetry to monitor ice sheet geometry. (4) Monitoring the inflation and deflation of volcanoes and other magma chambers (e.g. Rebus). (5) Intracontinental strain due to plate-tectonic action. (6) Intracontinental flexure due to changing ice load and mantle motion or phase changes. (7) Search for episodic seafloor spreading rates. (8) Refinement of techniques for ice strain and ice velocity determination.

5.32 Fast Technique for Computing Precise Aircraft Acceleration from GPS Phase

T. P. Eunuch and C. A. Raymond, *Jet Propulsion Laboratory*

R. E. Bell, *Lamont Doherty Earth Observatory*

D. D. Blankenship, *University of Texas*

Experience with GPS in aerogravity surveys has revealed two fundamental facts: (1) the aircraft vertical acceleration may be accurately extracted from differential GPS carrier phase measurements, and (2) the extraction of vertical acceleration by traditional GPS methods can be costly and time-consuming when it relies on algorithms devised for static positioning rather than airborne gravimetry. Here we present a simple and robust technique which avoids full phase connection and ambiguity resolution, which are not required for precise acceleration measurements.

GPS has been widely used in aerogeophysical surveys. Airborne gravimetry requires moderately accurate position and velocity and highly accurate vertical acceleration. For 1 mgal gravimetry tracking, requirements are: height above the geoid to <3 m; lateral velocity to 5-30 cm/s; and vertical acceleration to <1 mgal. Initially, GPS was used only to determine position and velocity, though more recently it has been adopted to recover vertical acceleration as well. Traditional phase-based GPS analysis techniques have required that phase lock be maintained throughout the flight and that all integer cycle phase ambiguities between flight and ground receivers be resolved.

While in principle that approach can achieve position accuracies of a few centimeters (far better than needed), in practice it has proven difficult to meet the conditions required for success. In the usual analysis technique, the entire flight, which may last 6-10 hours, must be processed as one continuous event. Ideally, the flight receiver would maintain continuous lock on all visible GPS satellites, with no cycle slips. In practice this is improbable since, during turns, satellite visibility may be blocked or large bursts of multipath may cause cycle slips. In addition, if a satellite rises and sets during the flight its ambiguities may be unresolvable. If the data set is processed independently in both directions (as if the flight had been flown forward and backward), unflawed processing would yield an identical trajectory both ways. This in fact is standard check. In reality, because of remaining phase breaks and faulty ambiguity resolution, toward and backward processing give typical altitude discrepancies of several meters. The irony is that data problems that cause those discrepancies almost invariably occur during turns or transits, when the data are of no interest.

The technique described here processes only the straight segments, each independently, in an automatic and almost foolproof procedure. The result is a vertical acceleration measurement that may actually be more accurate than that obtained with current techniques—and only a few tenths of milligal off the ideal.

Carrier phase is highly precise, but has an unknown phase bias. Pseudorange is about 100 times less precise, but is absolute—that is, it has no bias. Apart from the bias in carrier phase, the two data types measure the same quantity: the range plus the time offset between the GPS satellite and the receiver. This allows us to estimate the bias of the phase measurement by comparing phase and pseudorange measurements made at the same time. With phase and pseudorange measurements at one time point, our estimate of the phase bias is just the difference between the two and it will have the precision of 1-2 m. If we have phase and pseudorange at many time points, and phase continuity is maintained over the interval so that the bias is common to all phase points, then we can estimate the bias by averaging the phase-minus-pseudorange differences over the full interval. This effectively slides a phase curve to the mean of the phase of the unbiased pseudorange curve. Note that the phase biases are estimated separately as real-valued parameters for each receiver-satellite pair: No effort is made to determine the integer-cycle ambiguity in the differenced observables between flight and ground receivers.

The typical measurement interval for airborne surveys is 1 second, which yields 1200 measurements in 20 minutes. If the errors on all measurements were independent, a 20-minute average would reduce the error on the bias estimate by more than a factor of 30, to a few centimeters. In reality, because of the low frequency content of the multipath error, the typical error reduction for a 20-minute average is more like a factor of 5 or 10, giving a typical bias error of 20 cm. Taking into account observing geometry (PDOP, or position dilution of precision) this becomes a bias in the altitude measurement of typically 60-80 cm. which translates into a bias of about 0.2 mgal in accelerations computed over the interval. This has been confirmed in limited tests with GPS flight data collected in Antarctica.

This technique still requires phase continuity during the (comparatively short) straight line flight segments over which the averages are computed. Fortunately, phase breaks are extremely rare under such steady conditions with the highest quality GPS receivers. By avoiding the problematical turns, keeping the data segments relatively short, and dispensing with troublesome cycle ambiguity resolution, processing headaches are removed. A program to estimate the bias averages for a full 6-hour flight will execute in a few minutes or less, and the procedure can be easily automated with robust quality checks. Moreover, there are further computational gains that come from dealing with 20–30 minute data sets, rather than a full 6-hour set. This technique will work well with the data from any high-quality, dual-frequency GPS receiver that produces both phase and pseudorange data, and thus can be used to improve results from existing data sets.

6 Technology

This section provides some technical background on the Global Positioning System: how it works, the sources of error, and the accuracy requirements.

6.1 GPS Methodology

6.1.1 Introduction

In this section the various methods, the accuracy, and the applications of GPS techniques are discussed. The discussion ranges from the applications of static positioning, to dynamic positioning, to applications of the ancillary products that are produced in GPS analyses (such as estimates of water vapor delays). The types of GPS receivers available are also discussed although the discussion will concentrate on the high-accuracy applications of GPS. First, the basic applications of GPS and the types of receivers available are reviewed.

The basic observables of a GPS receiver are the pseudo-ranges (defined as the difference in time between the transmission and reception of a signal as determined by the clocks in the satellite and receiver) to the satellites visible, and optionally the phase of the GPS receiver signal relative to a local oscillator phase. This latter quantity is often referred to as the carrier beat phase. The signals from the GPS satellites are transmitted on two frequencies: L1 (1.57542 GHz, λ=190 mm) and L2 (1.2276 GHz, λ=244 mm). Two pseudo-random codes are written on the L1 signal using p phase changes. These two codes, the C/A (course acquisition) code and the P (precise) code, are modulated on the carrier signal with different amplitudes, with the C/A code being the strongest. The modulation rate for the C/A code is 1.023 MHz, i.e., the code may change phase at about 1 msec intervals; for the P-code the modulation rate is 10.23 MHz. The C/A code also repeats at about 1 msec intervals where as the P-code does not repeat for a full week. When the GPS satellites are in Anti-Spoofing (AS) mode, there is an additional modulation of the P-code by the so-called W-code. The W-code modulates the P-code at a rate of about 20 KHz. Either the C/A code or the P-code (with W-code modulation when AS is on), but not both, are written on the L2 carrier signal. Nearly always is the P-code written on the L2 channel.

In the simplest of the GPS receivers, only the pseudo-range on the L1 signal is measured by cross correlating the C/A generated in the receiver with the incoming signals. Because of the weaker modulation of the P-code on L1, the existence of P-code can be ignored during this correlation at the cost of a slight increase in the noise of the measurement. Within this class of receivers are navigation receivers and hand-held receivers. The accuracy of the pseudorange measurements obtained from this class of receiver varies greatly, but is on the order of 100 m. Whenever four or more satellites are visible, these pseudorange measurements can be used to determine the position of the receiver and the difference between the receiver clock time and GPS time. These time and position determinations are strongly affected by Selective Availability (SA), which primarily is implemented by “dithering” the fundamental oscillator on the satellite by amounts which introduce timing errors of up to about 0.2 msec (at the current level of SA). The effects of SA can be removed almost totally through the use of differential techniques, either by real-time transmission of range corrections or by postprocessing data and using the difference between stations of the range measurements.

The most accurate applications of GPS use measurements of the phase of the reconstructed carrier (i.e., the carrier signal after the p phase changes introduced by the codes are removed). In these accurate applications, the phase and possibly the range at the two frequencies transmitted by GPS are used. Instruments that measure phase come in several varieties. Early model geodetic quality GPS receivers (e.g., the TI4100 circa 1980) made phase and range measurements at both L1 and L2 assuming knowledge of both the C/A and P codes. However, uncertainty about civilian access to the codes in the future prompted the development of “code-less” receivers that could measure phase (or half-cycle phase) without any knowledge of the codes other than that the encoding scheme was bi-phase (e.g., Macrometer). These receivers had practical limitations because they could not decode the satellite ephemeris measurements and could not re-synchronize their clocks because they made no range measurements at all. By the mid-1980s it was clear that the access to the C/A code would not be denied and receivers were developed (e.g., MiniMac, Trimble SST, and Ashtech II) that used the C/A code to make L1 range and phase measurements and used one of the code-less schemes to make measurements of the phase. By the late 1980s it was clear that it would be some time before access to the P-code would be denied (effectively by superimposing on it the W-code) and a resurgence of instruments that would use the P-code to measure phase and range at L1 and L2 appeared. These latter generation instruments (e.g., the Rogue, Turbo Rogue, Trimble SSA, and Ashtech IIP) could revert to codeless tracking of L1 and L2 if AS was turned on. The techniques used to recover L2 phase and range were refined in this generation of instrument. Although not on the market yet, instruments that could take advantage of the low modulation rate of the W-code are now being developed, and these instruments offer a significant signal-to-noise (SNR) advantage for L2 measurements over those currently available. All modern geodetic quality GPS receivers appear to be able to measure phase with an rms error of < 1 mm under good SNR conditions and range with an rms error of between 0.05 and 1 m, with most instruments operating in the 0.1–0.2 m range.

6.1.2 Static Receiver

The most accurate applications of GPS to date have been those that have used GPS to monitor tectonic deformations and measure Earth rotation variations. There are several types of deployment of receivers used in static applications, with the choice depending primarily on accuracy requirements and logistics. The most accurate long-term GPS results are likely to be obtained from permanent deployment of GPS receivers such as those currently in operation associated with the International GPS Service (IGS), which became a permanent service in January, 1994. There are currently 45–50 stations around the world in continuous operation and these stations report their data to several data collection facilities around the world with a few day lag time. Averaged over a week or so, the positions of these stations are currently determined relative to each other with accuracies and precisions of about 10 mm in the horizontal components and 20-30 mm in the vertical component. The continuous collection of data will allow the models used in the GPS analyses to be improved and in all expectation much better results will be obtained in the future and from the existing data through reprocessing (see Error Budget below).

For many applications the permanent operation of stations is not possible and in these cases, campaign-style GPS occupations are made. In this scenario, receivers are located over geodetic monuments for a relatively short period of time (usually 8 hours to several days) and then moved to other locations so that a much greater density of points may be measured over a campaign lasting for several days to several weeks. A large number of such campaigns have been carried out with many of them being located in the western United States, but a large number also being carried out in various regions around the world. Similar accuracies are obtained in these campaigns as in the permanently deployed stations, although since the intersite distances are usually much smaller for campaign-style measurements, the relative accuracy can be very good and often as low as a few millimeters. For reasons to be discussed in the infrastructure section, these campaign-style measurements are becoming increasingly accurate.

6.1.3 GPS Ocean Applications

GPS oceanographic applications have been discussed in detail elsewhere in this report. In this section the accuracy of GPS solutions for these ocean applications will be discussed. These applications include ship navigation and heading, buoy location, monitoring of ice extent and location, and monitoring of the vertical position of tide gauges. Accuracy requirements for ship locations are dependent on the application. General navigation requirements can usually be satisfied by position accuracy of a few tens to a few hundred of meters. There are applications where a few meters or better ship position is desired. Examples of this are harbor and river navigation, positioning of a ship to determine seafloor baselines, and ship and buoy positioning to determine the position of an acoustically tracked probe as it descends through the water column. In this last example, the position history of the probe relative to a ship and buoy yields the velocity of ocean currents with depth.

Achievable position accuracy for ships can vary from a few tens of meters to a few hundred meters for direct application of GPS, depending on whether or not SA is activated. Differential GPS can provide ship positions to a few meters or better in a post-processing mode even if SA is activated. Differential GPS can be used in near real time if a system were available to solve for ephemeris and clock errors for each GPS satellite and broadcast this information to the user. Wide area differential GPS (WADGPS) is a scheme that would allow suitably equipped users to perform differential GPS solutions for their positions in real time over a much larger region.

The WADGPS network comprises a master station, a number of local monitor stations, and a communications link. The local monitor stations report data from all GPS spacecraft in view to the master station. The master station estimates ionospheric time delay parameters, plus the satellite ephemeris and clock errors. These corrections are then transmitted to the user via any convenient communications link. A test of this concept is scheduled by the FAA for the U.S., but the concept could be extended worldwide with a few master stations and a few hundred monitor stations. Such a network has the potential to provide real-time navigation capability for land, air, and marine applications of a few meters worldwide.

Ship heading can be determined to better than one degree by the use of two GPS receivers located on a few meter baseline. However, ship heading accuracy generally will be limited by the multipath environment which can vary significantly depending on antenna location on a given ship.

While for most applications vertical errors in ship location are not important, there are many buoy applications where the vertical is the major component of interest. This includes measurement of sea surface height for monitoring of sea level, measuring sea surface slope to yield gravity vertical deflections at sea for a more accurate marine geoid, or for calibration of satellite altimeter range measurements. Differential GPS can provide ocean buoy position accuracy of a few centimeters to a few meters depending on data type and the baseline length to the fiducial site. For baseline lengths less than 100 km, and in a post-processing mode, kinematic buoy position can be determined to about a centimeter in the horizontal and about two centimeters in the vertical using carrier phase data in a differential mode.

Major sources of error for the determination of the vertical are tropospheric refraction, multipath, and errors in the vertical position of the fiducial station. Path delay errors and errors in the vertical station location map almost one for one into vertical errors in the buoy position. Tropospheric delay can be handled by estimation, by the use of water vapor radiometers, or by using radiosonde data acquired in the vicinity of the GPS receiver sites. The most convenient method of handling troposphere refraction is by estimation of the path delay. This also is probably the most accurate method, although recent water vapor radiometer results have been encouraging.

The use of GPS buoys has been shown to yield excellent results for calibrating the altimeter range measurement on the TOPEX/Poseidon satellite. For an experiment off the California coast at the Texaco offshore platform, Harvest, agreement between a GPS buoy and tide gauges for ocean surface height above the reference ellipsoid was approximately one centimeter. The TOPEX/Poseidon project also has installed a GPS receiver on the Harvest platform. This receiver has been used to determined the vertical position of the Harvest platform to better than one centimeter rms. Knowledge of the vertical component of the platform location to better than a centimeter is crucial to the accurate calibration of the TOPEX/Poseidon altimeter height bias.

The above comments regarding accuracy capability for ship and buoy locations also apply to ice monitoring although some problems may be more difficult such as those associated with coverage of the GPS constellation—i. e. no high latitude satellites and the ionospheric correction. Accuracy capability of differential GPS for ice applications therefore should range in the neighborhood of a few centimeters to a few meters depending on atmospheric conditions, GPS data type, and receiver location relative to fiducial sites.

6.2 Ancillary Data Output

There are three primary outputs of GPS that can be used by others: (1) timing, (2) ionospheric delay calibrations and thus estimates of the Total Electron Content (TEC) of the ionosphere, and (3) atmospheric delays. Direct timing applications are severely compromised by SA which effectively limits the quality of real-time output to time to 0.2 msec. When SA is not on, time tags accurate to several nanoseconds can be obtained from GPS.

Accurate estimates of the ionospheric delay are difficult to obtain from GPS because of interchannel biases between the L1 and L2 frequency channels and the differential delay in the satellites between the L1 and L2 channels. The former can be obtained from careful ground receiver calibration but will always be difficult for precise phase measurements due to the unknown number of cycles. The latter is calibrated in the GPS satellites before they are launched but the exact values when the satellites are in orbit are not known. However, GPS does provide an excellent method for studying the time variable behavior of the ionosphere, with the largest complication here arising from the need to separate spatial and temporal variations because of the relatively slow motion of the GPS satellites across the sky. (This characteristic can be contrasted with TRANSIT system measurements in which the satellite would pass from horizon to horizon in about 20 minutes, thus providing a single slice through the ionosphere at effectively one time.)

The applications of GPS for meteorological measurements is in its infancy. It seems clear that obtaining estimates of perceptible water to 1 mm is possible and with this accuracy it will be a very useful product for meteorological models.

6.3 Infrastructure

Of critical importance to routine applications of GPS is the global tracking network established by the International GPS Service (IGS) which is sponsored by the International Association of Geodesy (IAG). The routine operation of a network of stations of between 20 and 50 receivers for the past two years has made the processing of regional GPS campaigns much easier because of the availability of accurate orbits a week or so after the data has been collected. In addition, this service also maintains quality checks on both the receivers within the network and the satellites. The existing data set is also extremely useful for testing model improvements to the analyses of GPS data.

Another important function which must be addressed now is the archiving of GPS data. Although most data is distributed in the RINEX format, in the long run this format (unless revised) has severe limitations for maintaining the integrity of GPS data. As discussed below, there is no means for storing amplitude information adequately in this format and, when “clean” data is distributed, there is no means for saving the changes made to the data. The error flagging of data is so limited in the format that most centers need to delete data totally from the clean RINEX file for data which was not used in their analysis (e.g., due to low elevation angle) even though these data are likely to be error-free and could prove useful in the future when models for the atmospheric delay and multipath are improved. The current situation is that the raw data files from the receiver, raw RINEX files, and cleaned RINEX files all will need to stored in an archive for future use.

6.4 Error Budget

The error budget for GPS can be broken down into a number of components some of which are reasonably well understood and others which are not so well understood. In nearly all cases the full error spectrum is not known and here we lay out and give examples of those parts of the error spectrum which are understood. We also attempt to bound that part which is not well understood. For each component of the error we will attempt to quantify its magnitude and the spectral character of the error (i.e., the magnitude of the error as a function of frequency).

6.4.1 Data Noise

Data noise from instrumental effects should be the most quantifiable of the GPS error sources, and is likely to be one of the smaller contributions to the total error budget. The data noise can be theoretically computed from the gain of the GPS antenna, the GPS signal strength, and the thermal noise characteristics of the receiver and its environment. Data noise is expected to be elevation angle dependent (due to both the gain of the GPS antenna and the loss of signal strength due to greater attenuation of the Earth’s atmosphere) and averaging time in the GPS receiver. For L1 observations that decode either the C/A code or the P-code, the integration time required to achieve data noise of about 1 mm is only about 1 msec. Similar integration times can be used at L2 if the P-code is known but the integration times need to be increased almost a thousand-fold (to about 1 second) if codeless techniques are used at L2. (This increase in integration time compensates for the loss of SNR in codeless tracking systems and therefore the noise level does not appear that much better for codeless tracking. In dynamic applications, the increased integration time can and often does cause frequent losses of the lock on the GPS signal.)

One common method for experimentally determining the noise in GPS receivers is to connect two receivers to the same antenna and look at the differences of the measured phase and range values. However, these types of experiments need to be performed very carefully because reflections from the receivers back through the splitter used to divide the signal from the antennas between the two receivers can affect the output of the receivers. As an example of the results obtained from a split signal experiment, we show the double differenced phase residuals from a Trimble SST and SSE connected to the same antenna in Figure 23. Examples of similar type experiments with a variety of receivers have been carried out. Generally tests of this type have shown that the noise in the L1 and L2 phase measurements varies between 1 and 5 mm and often show some systematic trends. Also large trends can develop from drifts between the L1 and L2 phase measurements that are common to all channels within a receiver, but differ from receiver to receiver. This type of error does not affect the double difference observable because it cancels in the differencing operation, but it does affect estimates of the ionospheric delay. Between different receiver types, the error in ionospheric delay can be affected by up to 400 mm. Thus while instrumental errors are small, these error sources should be better understood than they currently are.

6.4.2 Multipath

Multipath for GPS receivers is defined as the contribution to the phase and range measurements from reflected signals. One of the major compromises that exists in designing omni-directional antennas of the type used in GPS is maintaining relatively high gain at low elevation angles while minimizing the gain for elevation angles less than zero. Multipath is difficult to characterize in general since its amplitude and phase depend on many parameters, although many of these parameters are sufficiently constant that multipath can be seen to repeat day-to-day because of the repeating orbits of the GPS satellites. In general, an object near a GPS antenna that appears smooth to the 190- and 240-mm wavelength GPS signals will act as a source of multipath. The most common of these are nearby buildings, trees, and the ground itself. The ground is generally a strong source of multipath, and if the ground is treated as an infinite level plane, the difference in the phase of the signal and the reflected signal is given by $2h\sin e$, where h is the height of the antenna above the ground in wavelengths, and e is the elevation angle. We show in Figure 23 a typical example of multipath. Here the oscillatory behavior of the double difference phase residuals is most likely due to the full rotation of the (weaker) reflected signal affecting the phase determinations. In extreme cases the receiver can temporarily lock onto the reflected signal and this may explain the single cycle slips that some receivers in certain circumstances experience.

One of the best diagnostics of the presence of multipath is the amplitude of the received signals, which will also show an oscillatory behavior in the presence of multipath. Unfortunately, the current international standard for exchange of data (RINEX) does not allow the amplitude to be reported with sufficient significant digits to allow it to be useful in detected and correcting multipath corruption of a signal.

While the multipath shown in Figure 24 averages effectively over the long interval of observations shown, for short periods of time (up to 2030 mins depending on h and the rate of change of elevation angle) multipath does not average to zero, and this can seriously effect the

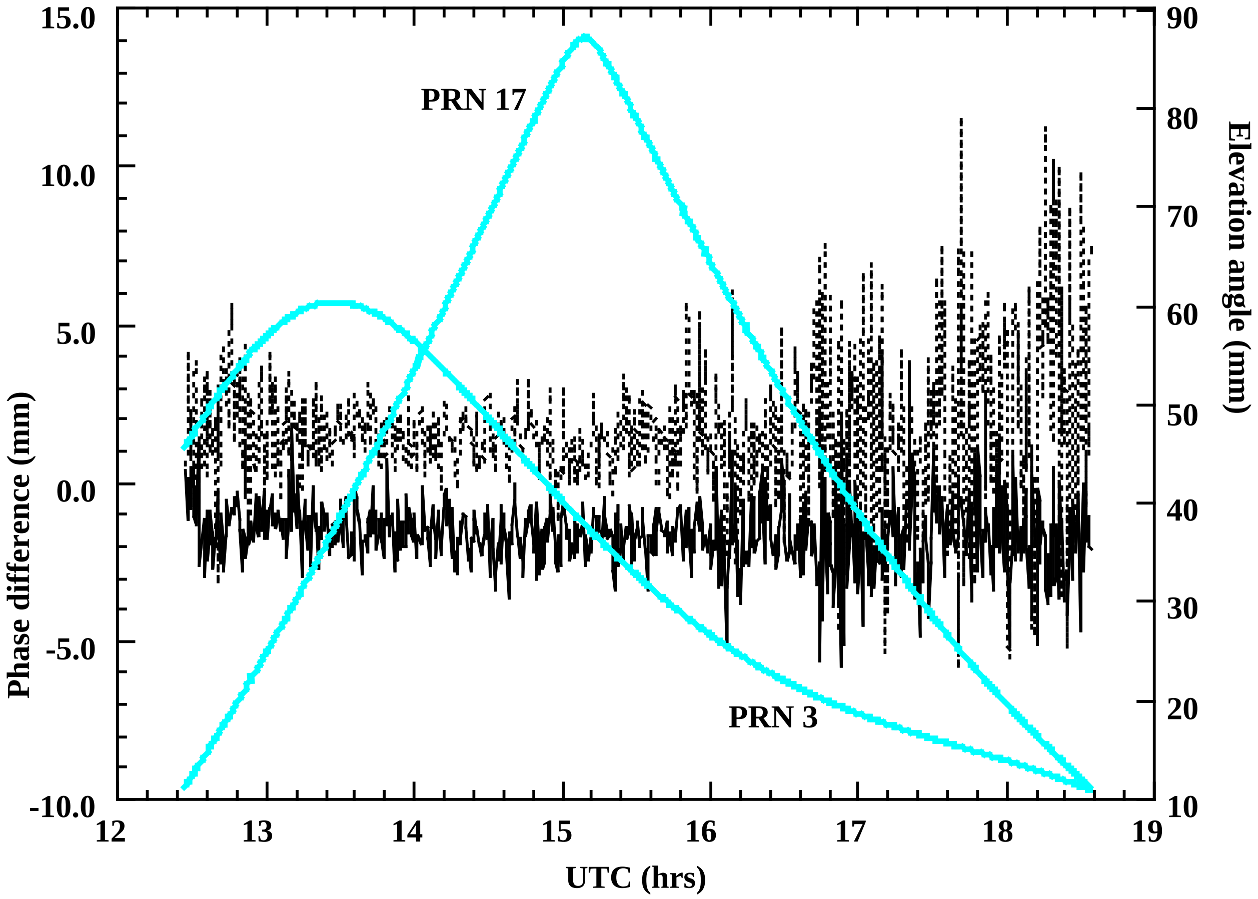

Figure 23. Double difference carrier phase noise obtained from a Trimble SSE and Trimble SST receiver connect to the same antenna (contributed by Herring). The solid line shows the differences between phase measurements to PRN 03 and PRN 07 at the L1 frequency; the dashed curve is for the L2 frequency. At L1 the mean and rms scatter (about the mean) of phase differences are -1.5 mm and 1.0 mm; at L2 the mean and rms are 1.6 mm and 2.1 mm. The stippled lines show the elevation angles of the satellites and clearly show that the noise is elevation angle dependent. The larger scatter at the L2 frequency is mostly likely due to the codeless tracking of the L2 signal in the SST. Although the means of these residuals are not zero; the differential position estimate from the two receivers was 0. x mm north, X m east and X mm in height.

results from kinematic and rapid static surveys where site occupation times can be as short as a few minutes. In these cases errors of tens of millimeters may occur because of multipath.

6.4.3 Receiver Timing

While the first-order effects of satellite and receiver clocks cancel during the double differencing operation or by estimating white-noise clock correction, there is a dependence of the geodetic results on the actual time at which measurements are made due to the non-linearity of the geodetic problem. The magnitude of the errors associated with incorrect timing of GPS signal sampling can be computed from the Doppler shift of the GPS signals, and it is typically 1 mm per microsecond of timing error. While such timing requirements should be easily met by a GPS receiver, examples can be found in data in

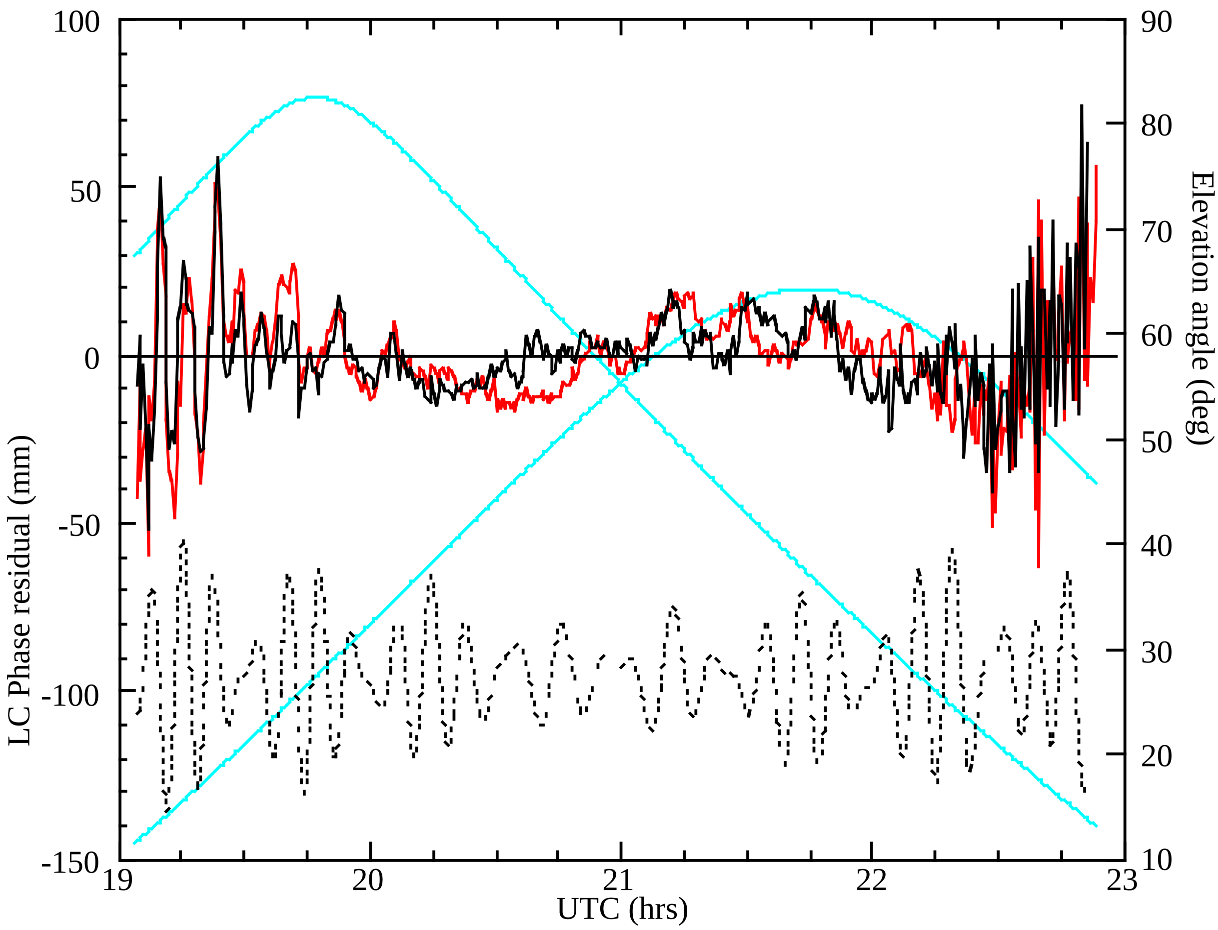

Figure 24. A typical example of multipath (contributed by Herring).

which this is not the case. These examples are reflected as single outliers in the double differenced LC observable, but with no perturbation to the ionospheric delay estimate of the wide-lane observable (computed using the range and phase measurements). Such behavior is consistent with the receiver making its measurements at a time different to that reported. The overall effect of this type of error is small except in those cases where the receiver does not correctly resolve the millisecond ambiguity in the C/A code range, in which case it becomes almost impossible to determine where the measurements were made. When this occurs, that data almost always need to be discarded. Ideally, this type of error should be detected in the field so that measurements can be repeated.

6.4.4 Atmosphere

Modeling the delay in the GPS signals due to the Earth's atmosphere is considered to be one of the limiting error sources in GPS primarily because of the natural variability of the delay and difficulty in developing a practical means for calibrating the delay other than through estimation techniques using the GPS data themselves. The full atmospheric delay can reach about 13 m at 10 degree elevation angle, but much of this is predictable from measurements of surface pressure. The remaining part of the delay primarily due to dipole component of water vapor refractivity and gradients in the atmosphere can not be so easily modeled. Recent attempts to calibrate the water vapor component using instruments such as water vapor radiometers have been encouraging. However, these newer results are very limited in location and time span.

Current analyses would indicate that residual errors in modeling the atmospheric delay could be tens of millimeters and may have annual signatures.

6.4.5 Second Order Ionospheric Delay

While the dual-frequency ionospheric delay calibration is likely to be accurate to a few millimeters in most cases there is theoretical evidence that the neglected contribution from the magnetic field in the dual-frequency correction could introduce errors of up to 30 mm. However, with some simplifying assumptions, this error appears to be reducible to a few millimeters in even the most extreme cases by modifying the method used to compute the effective frequencies of the GPS signals. The most serious consequence of the ionospheric delay may be the loss of lock on GPS satellites during periods of rapid ionospheric variations. This loss of lock is a serious problem for codeless receivers operating in polar and equatorial regions, and become a serious problem in these regions for full-coded receivers when AS is turned on.

6.4.6 Satellite Motions and Satellite Antenna Characteristics

The GPS constellation consists of 26 broadcasting satellites. The satellite orbits can be generally characterized by their Kepler orbit elements: semimajor axis = 26000 km (orbital period = 43082 sec, half of a sidereal day), eccentricity < 0.01, and inclination = 55 deg (Block II), plus three additional elements that depend on the specific satellite. The additional three orbit elements are: ascending node location (point where the satellite crosses the equator from Southern hemisphere to the Northern hemisphere, known as the "Right Ascension of the Ascending Node," with respect to a celestial reference frame), the perigee location (known as "argument of perigee"), and the time when the satellite was last at perigee. The orbital semimajor axis and eccentricity describe the shape of the orbit in terms of a conic section and the inclination describes the orientation of the orbit plane with respect to the Earth's equator. The GPS constellation consists of six orbit planes, with 4 or more satellites in each plane, evenly distributed within the plane. If the Earth were a sphere with constant, uniform mass density, the six orbit elements would be constant. Since the Earth rotates, the longitude of the location where the satellite crosses the equator changes with time even if the orbit elements are constant.

Various forces act on the satellites that produce changes in the orbit elements with time. These perturbing forces are dominated by the gravitational component associated with the Earth's oblateness, which produces a linear time variation in both the orbit plane ascending node location and the location of the perigee, with respect to an inertial reference frame. The node location makes one revolution in about 25 years in response to this perturbation; however, the time required for a complete revolution of perigee is about 50 years. These rates of change are much slower than the changes experienced by a low altitude satellite. Although the sun and moon produce a similar linear drift in these orbit elements, the effect is about a factor of five smaller than the oblateness effect.

In addition to the linear (or secular) variation in the node and perigee locations, the Earth gravity and luni-solar gravitational perturbations produce periodic variations in all orbit elements. The perturbation spectrum includes periodicities ranging from approximately one hour to 18.6 years. Over a one year interval of time, these periodic perturbations are dominated by the luni-solar forces that produce "long-period" changes in the orbit elements with periods of 14 days (lunar) and 183-days (solar semi-annual). At the GPS altitude, the gravitational forces on the satellite due to the Earth, moon, sun, and planets are well-modeled and understood. Furthermore, errors in the modeling of the mass variations in the Earth are diminished at GPS altitude compared to a much lower altitude. On the other hand, the non-gravitational forces experienced by the GPS satellites are complicated and prone to mis-modeling of the forces. The nongravitational forces are produced by solar radiation, Earth radiation, and thermal radiation from the satellites, to name the major contributors. These forces produce periodic variations in the orbit elements similar to gravitational forces. The mis-modeling of the nongravitational forces is one of the major contributors to GPS orbit error.

6.4.7 Impact of SA and AS

Selective Availability (SA) denies precise positioning by corruption of the GPS signal structure. It is composed of two components (1) corruption of broadcast navigation message and (2) rapid "dithering" or oscillations of the frequency standards in the satellites. The first component of SA is of little consequence to scientific users because in precise millimeter applications the orbits of the GPS satellites are computed from carrier measurements much more accurately than even the precise ephemeris available from the DoD. Also the dynamics of the GPS satellites are well enough understood that these orbits can be integrated forward in time by several days with accuracies better than the (uncorrupted) broadcast ephemeris except when there are thruster firings on the GPS satellites. The second component currently also has little effect when differential (either real-time or post-processing) techniques are used. We show in Figure 25 an example of the dithering of the GPS frequency standards obtained from the analysis of the data collected with the global GPS tracking network. In this particular example, SA is turned off the satellite at approximately 18:00 UTC. The results of dithering have been converted to meters of range error in this figure. Prior to SA being turned off, the rms error in the range measurements is 22 m; when SA is turned off, the range error rms drops to about 0.25 m. (These results are obtained from the analysis of carrier phase measurements, and therefore nearly all of the rms is due to dithering and the natural drifts in the satellite and ground station clocks.) While the effects of SA are almost totally eliminated in differential positioning, the rapid fluctuations in satellite clocks do complicate the process of removing slips in the number of carrier phase cycles accumulated by the receiver and SA makes it nearly impossible to use averaged phase measurements (normal points) with a much lower sampling rate. In real-time navigation problems, SA limits accuracy of navigation, although for aircraft this is not a major problem since the position of an aircraft can generally only be controlled to within about 100 m.

Anti-spoofing (AS) is meant to stop false signals from corrupting military receivers, but as a consequence of the system used, AS denies access to the P-code. AS is implemented by modulating the P-code with an additional code (the W-code), and because only the P-code (with the W-code modulation) is superimposed on the L2 frequency, some type of codeless tracking of L2 is required when AS is turned on. In Figures 26a and b we show the effect on two different receivers when AS is turned on at approximately 17:00 UTC. The degradation of the performance of the receiver in Figure 26a is immediately obvious, and severely limits the effectiveness of the automatic data processing systems. In Figure 26b, the degradation of the performance of the receiver is not so obvious

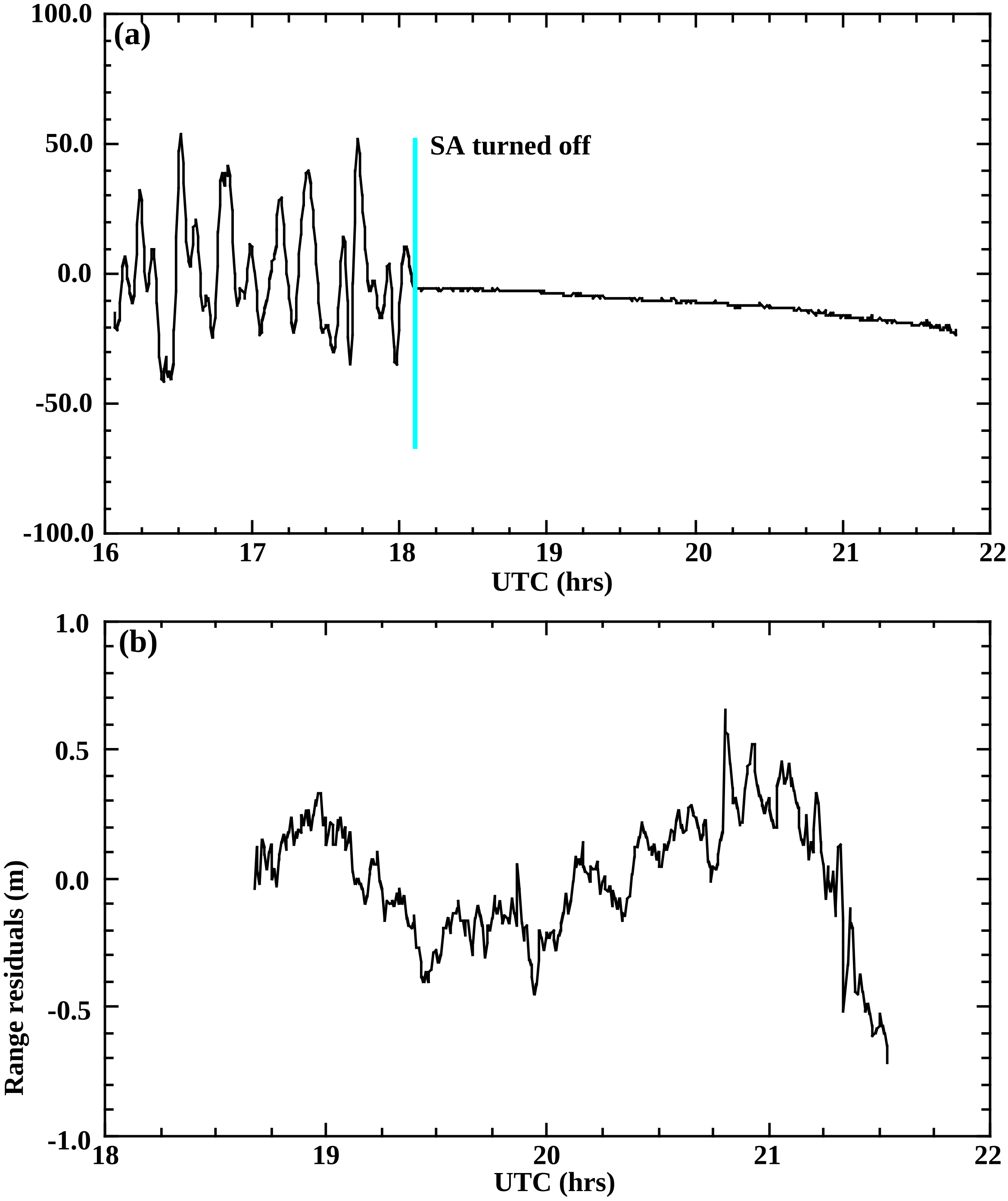

Figure 25. Example of Selective Availability (contributed by Herring). In this example, SA was turned off at about 18:00 UTC and impact of SA can be clearly seen. In (a), the range error to PRN 01 is shown. The rms error in the range errors when SA is on is 22 m, consistent with denying point positioning accuracies better than 100 m. In (b) an expanded view of the time interval when SA is not on is shown after a quadratic polynomial is removed. These results were obtained using carrier phase measurements. The rms range error for this interval is 0.25 m, and indicates that 1 meter accuracy point positioning would be possible with existing satellites and receivers if SA were not on.

although careful analysis of these data indicate that the effectiveness of automatic data processing systems is also compromised when AS is turned on. (It is also interesting to note the general stability of the receiver shown in Figure 26b is not as good as that for Figure 26a receiver when AS is off, possibly indicating the receiver manufacturer has put most of the efforts into handling AS rather than developing a stable receiver when AS is off.) The prime consequence of AS is loss of accuracy in both range measurements and phase measurements. For aircraft applications, this loss of accuracy (about 1000-fold for L2 tracking) is particularly severe because of the dynamics of the aircraft and the usually high multipath environment on the aircraft. In particular, results of the quality shown in Figure 26b can only be obtained by coherently averaging the L2 signal for about 1 second. This is an acceptable compromise for a static receiver, but in an aircraft leads to frequent loss of lock on the L2 signal.

7 References

Figure 1. Contributed by R. Ware, internal UNAVCO publication, 1994.

Figure 2. Feigl, K., D. Agnew, Y. Bock, D. Dong, A. Donnellan, B. Hager, T. Herring, D. Jackson, T. Jordan, R. King, S. Larsen, K. Larson, M. Murray, Z. Shen, and F. Webb, *Space Geodetic Measurement of Crustal Deformation in Central and Southern California, 1984–1992,* **J. Geophys. Res., 98**, 21,677–21,712, 1993.

Figure 3. Contributed by R. Ware, internal UNAVCO publication, 1994.

Figure 4. From K. Hudnut and M. Murray, U.S.G.S., January 25, 1994.

Figure 5. Donnellan, A., B. Hager, and R. King, *Discrepancy Between Geological and Geodetic Deformation Rates in the Ventura Basin,* **Nature, 366**, 333–336, 1993.

Figure 6. Contributed by Y. Bock, Scripps Institution of Oceanography, 1994.

Figure 7. Bock, Y., D. Agnew, P. Fang, J. Genrich, B. Hager, T. Herring, K. Hudnut, R. King, S. Larsen, B. Minster, K. Stark, S. Wdowinski, and F. Wyatt, *Detection of Crustal Deformation from the Landers Earthquake Sequence Using Continuous Geodetic Measurements,* **Nature, 361**, 337–340, 1993.

Figure 8. Yuan, L., R. Anthes, R. Ware, C. Rocken, W. Bonner, M. Bevis, and S. Businger, *Sensing Climate Change Using the Global Positioning System,* **J. Geophys. Res., 98**, 14,925–14,937, 1993.

Figure 9. Tapponnier P., G. Peltzer, A. Y. LeDain, R. Armijo, and P. Cobbold, *Propagating Extrusion Tectonics in Asia: New Insights from Simple Experiments with Plasticine,* **Geology, 10**, 611–616, 1982.

Figure 10. Dokka, R. K., and C. J. Travis, *Role of the Eastern California Shear Zone in Accommodating Pacific–North American Plate Motion,* **Geophys. Res. Lett., 17**, 1323–1326, 1990

Figure 11. Royden L., *Late Cenozoic Evolution of the Pannonian Basin,* **Am. Assoc. Petrol. Geol., Mem., 45**, 27–48, 1988.

Figure 12. Oral, B., *GPS Measurements in Turkey (1988-1992): Kinematics of the Africa-Arabia-Eurasia Plate Collision Zone,* doctoral thesis, MIT, 1994.

Figure 13. Calais, E., Y. Bock, et al., Scripps Institution of Oceanography, in preparation, 1994.

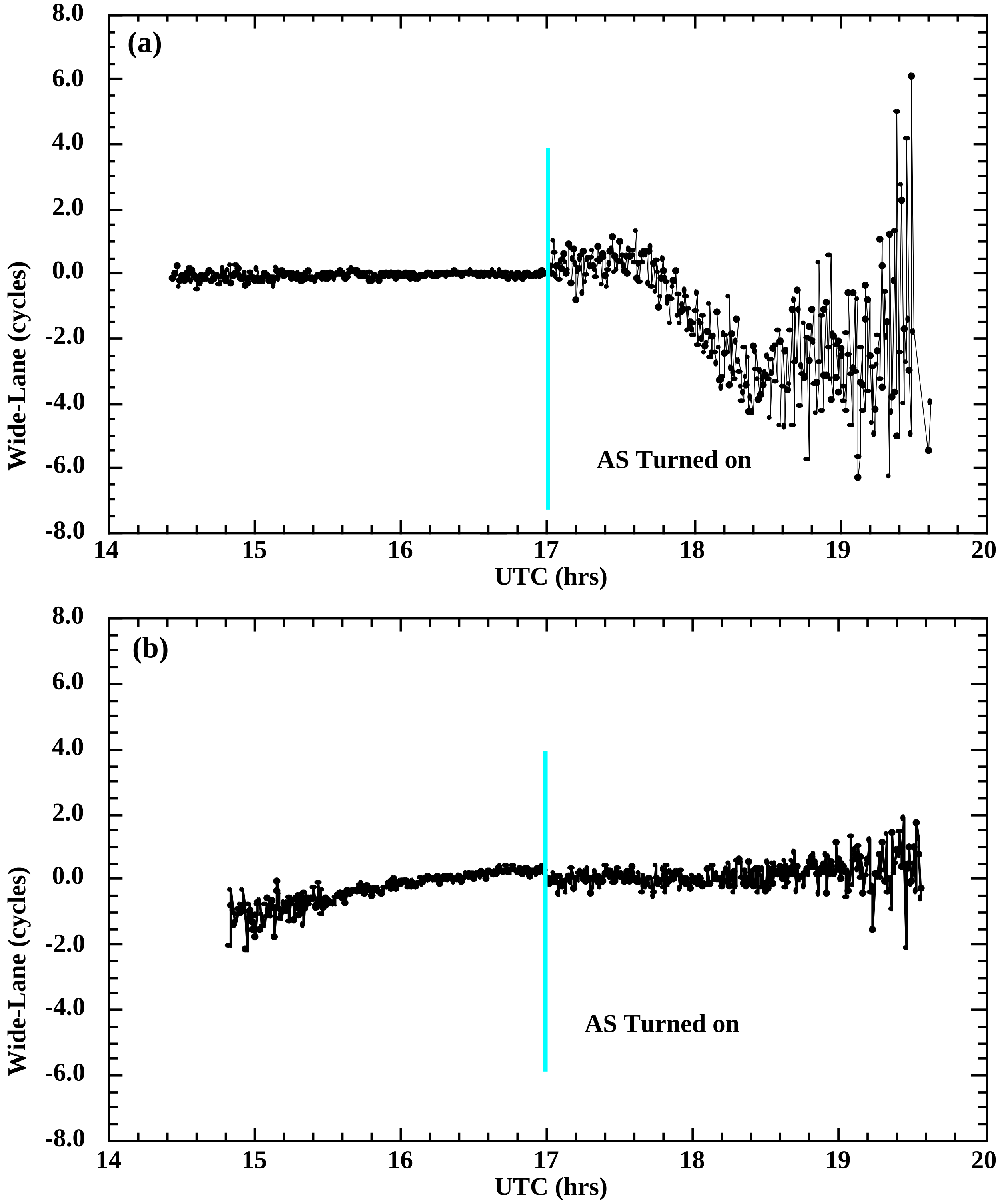

Figure 26. Example of the effects of Anti-spoofing (contributed by Herring).

Figure 14. Contributed by R. Smith, University of Utah, 1993.

Figure 15. Owen, S., P. Segall, J. Freymueller, A. Miklius, R. Denlinger, T. Arnadottir, M. Sako, and R. Bürgmann, *Rapid Deformation of the South Flank of Kilauea Volcano, Hawaii,* submitted to **Science**, 1994.

Figure 16. Contributed by C. Meertens and R. Smith, 1994.

Figure 17. Bürgmann, R., P. Segall, M. Lisowski, and J.L. Svarc, *Strain development subsequent to the 1989 Loma Prieta earthquake,* U.S.G.S. Professional Paper 1550D (in press), 1994.

Figure 18. Courtesy Herring, T., CSDEI Science Plan, 1993.

Figure 19. Waschbusch, P. and M. McNutt, *Yellowstone: A continental midplate (hot spot) swell,* **Geophys. Res. Lett., 21**, 1703–1706, 1994.

Figure 20. Baggeroer, A. and W. Munk, *The Heard Island Feasibility Test,* **Physics Today, 45**, 22–30, 1992.

Figure 21. Baggeroer, A. and W. Munk, *The Heard Island Feasibility Test,* **Physics Today, 45**, 22–30, 1992.

Figure 22. Rocken, C., T. Van Hove, J. Johnson, F. Solheim, R. Ware, M. Bevis, S. Businger, and S. Chiswell, *GPS/Storm—GPS Sensing of Atmospheric Water Vapor for Meteorology,* submitted to **J. Atmos. Oceanic Technol.**, 1994.

Figure 23. Contributed by T. Herring, MIT.

Figure 24. Contributed by T. Herring, MIT.

Figure 25. Contributed by T. Herring, MIT.

Figure 26. Contributed by T. Herring, MIT.